Title: Astrophysical constraints on dark matter annihilation with Sommerfeld enhancement

Date: May 10, 2011 03:30 PM

URL: http://pirsa.org/11050057

Abstract: In recent years, a number of observations have highlighted anomalies that might be explained by invoking dark matter annihilation. The excess of high energy positrons in cosmic rays reported by the PAMELA experiment is only one of the most prominent examples of such anomalies. Models where dark matter annihilates offer an attractive possibility to explain these
observations, provided that the annihilation rate is enhanced over the typical values given by conventional models of thermal relic dark matter annihilation. An elegant proposal to achieve this, is that of a Sommerfeld mechanism produced by a mutual interaction between the dark matter
particles prior to their annihilation. However, this enhancement can not be arbitrarily large without violating a number of astrophysical measurements. In this talk, I will discuss the degree to which these measurements can constrain Sommerfeld-enhanced models. In particular,
I will talk about constraints coming from the actual abundance of dark matter and the extragalactic background light measured at multiple wavelengths.

Astrophysical constraints on dark matter annihilation with Sommerfeld enhancement

Jesús Zavala Franco
(CITA National Fellow, University of Waterloo)

In collaboration with:

Mark Vogelsberger (CfA, Cambridge)
Simon White (MPA, Garching)
Volker Springel (HITS, Heidelberg)
Tracy Slatyer (IAS, Princeton)
Abraham Loeb (CfA, Cambridge)
Mike Boylan-Kolchin (University of California, Irvine)

Papers (arXiv): 0910.5221, 1103.0776

Perimeter Institute for Theoretical Physics, May 2011

Cosmic ray excesses and other anomalies

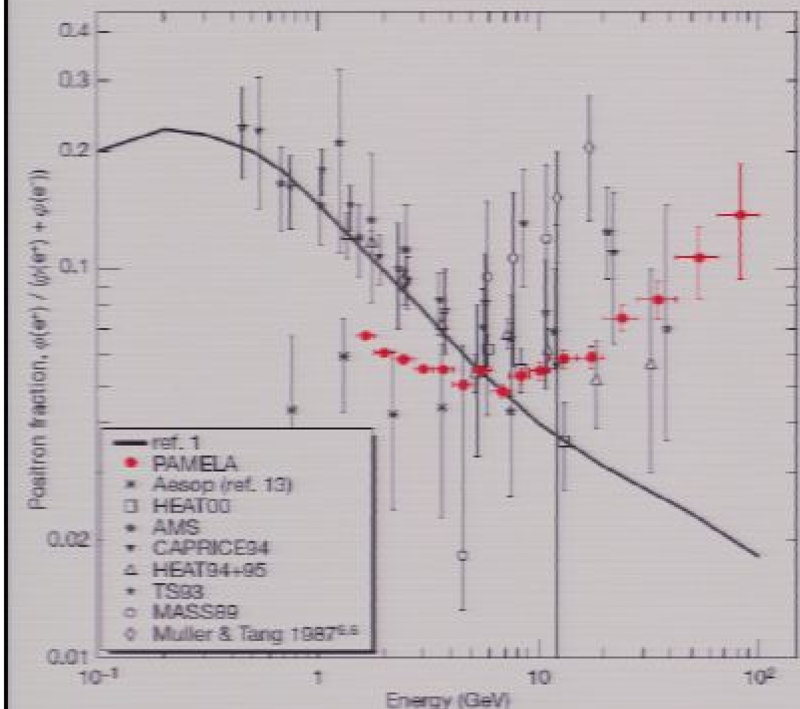

PAMELA, Adriani et al. 2009
excess of e+ for E>10GeV

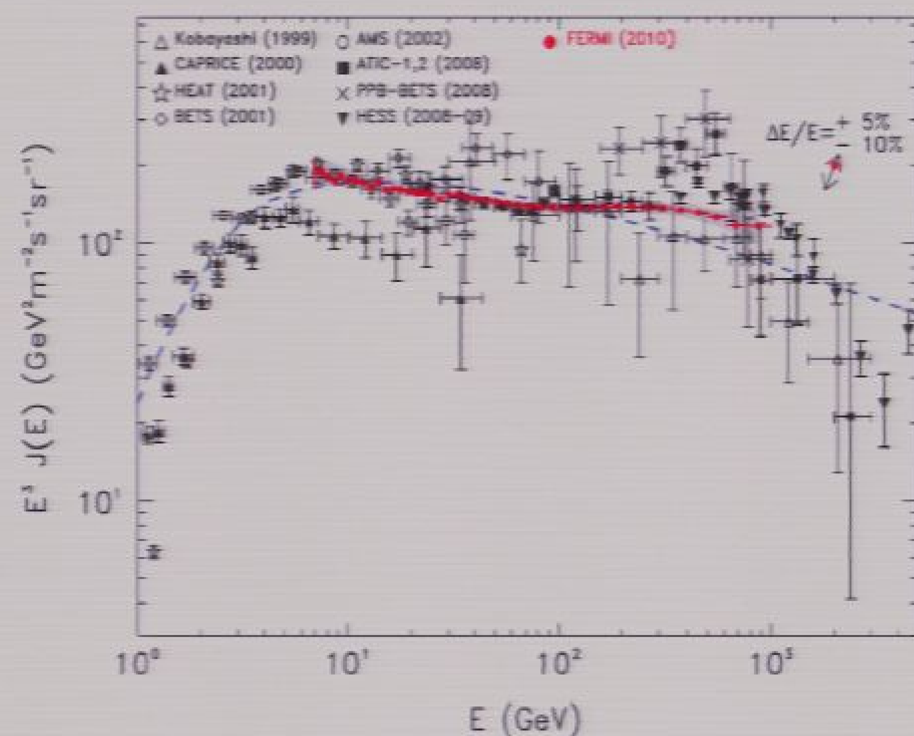

INTEGRAL/SPI, Weidenspointner et al. 2006
511 keV line, ~3x10^{42} e+e- pairs/s annihilating

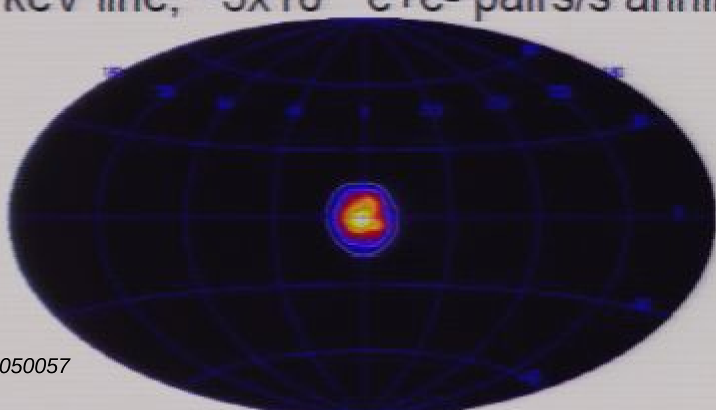

Fermi, Ackermann et al. 2010
e+e-, not a clear excess

Cosmic ray excesses and other anomalies

"WMAP Haze"
Dobler and Finkbeiner 2008

23 GHz WMAP residual

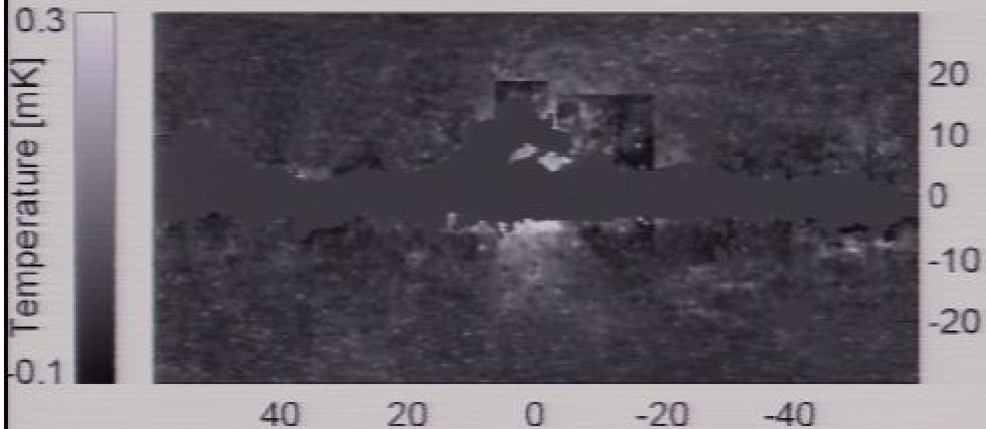

"Fermi Haze"
Dobler et al. 2010

5 < E < 10 GeV residual (1 < E < 2 GeV)

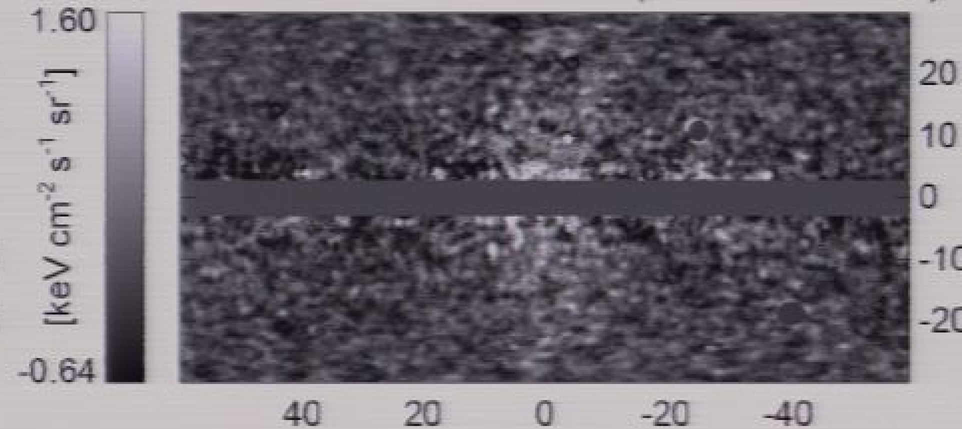

"Fermi Bubbles"
Su, Slatyer and Finkbeiner 2010

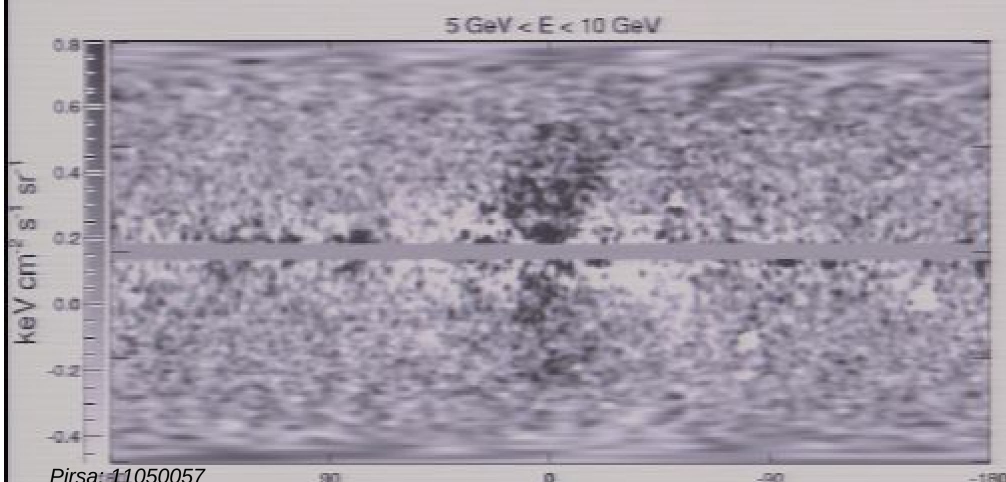

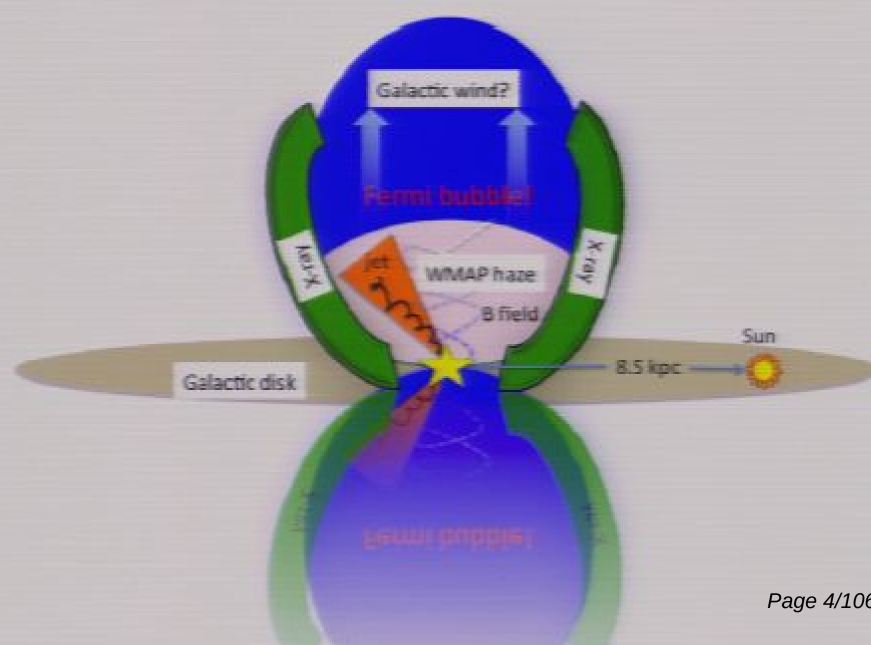

Cosmic ray excesses and other anomalies

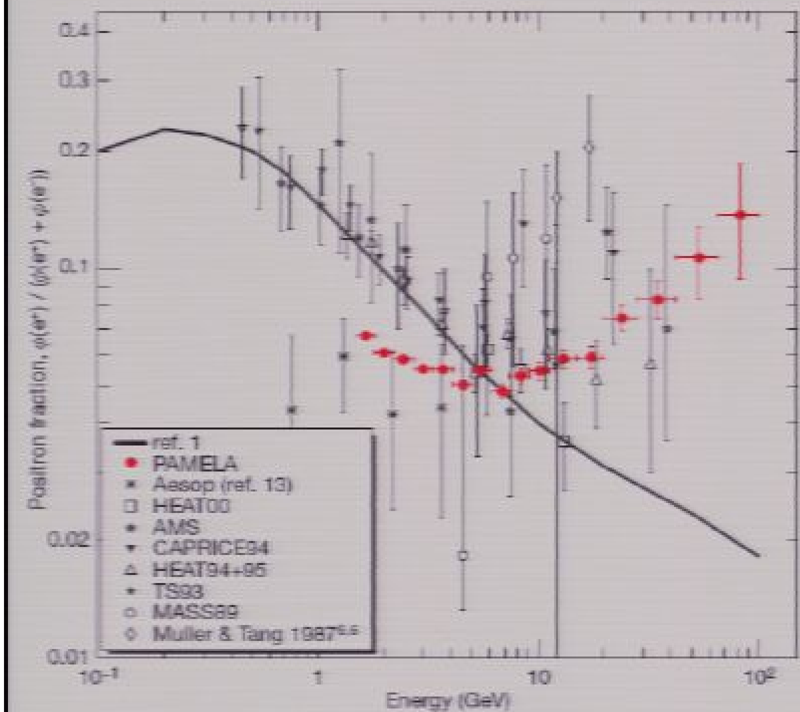

PAMELA, Adriani et al. 2009
excess of e+ for E>10GeV

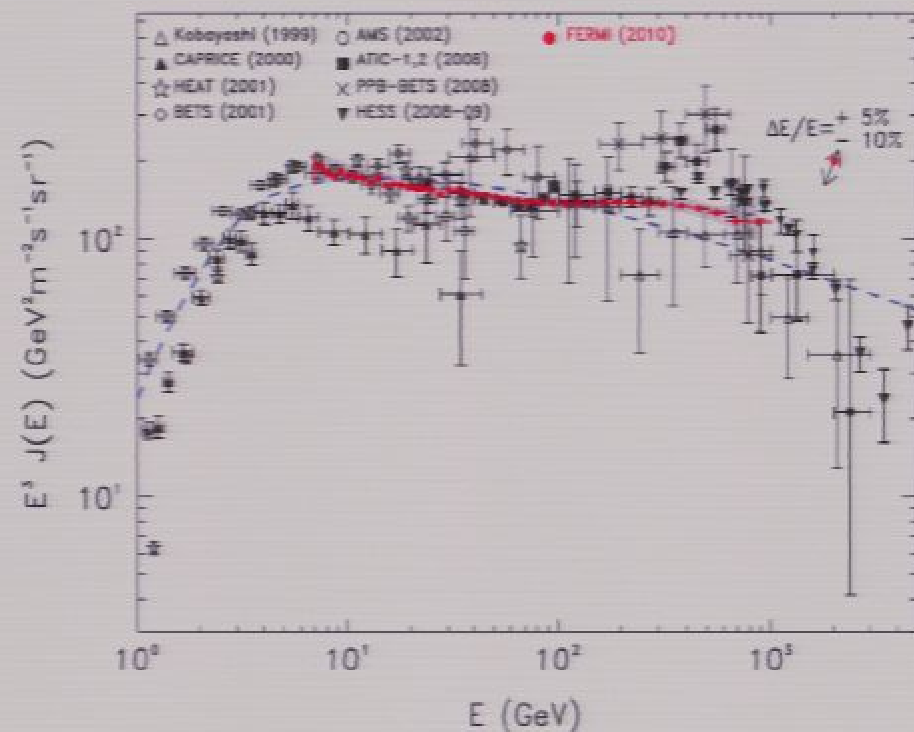

INTEGRAL/SPI, Weidenspointner et al. 2006
511 keV line, ~3x10^{42} e+e- pairs/s annihilating

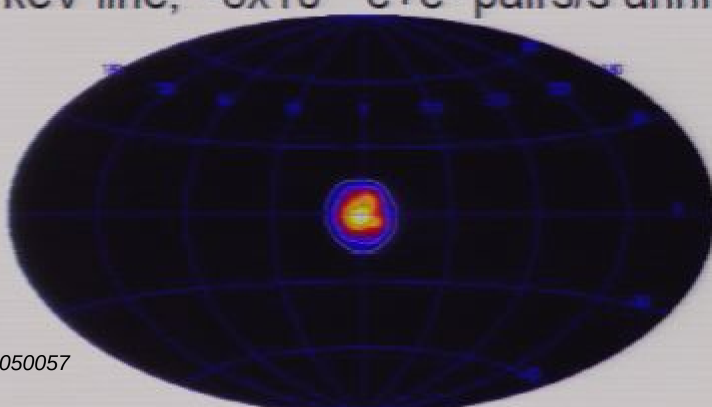

Fermi, Ackermann et al. 2010
e+e-, not a clear excess

Cosmic ray excesses and other anomalies

"WMAP Haze"
Dobler and Finkbeiner 2008

23 GHz WMAP residual

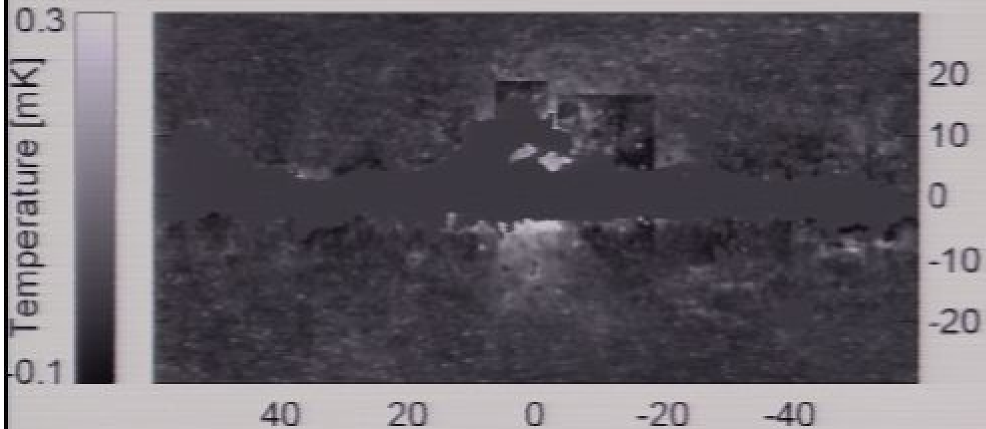

"Fermi Haze"
Dobler et al. 2010

5 < E < 10 GeV residual (1 < E < 2 GeV)

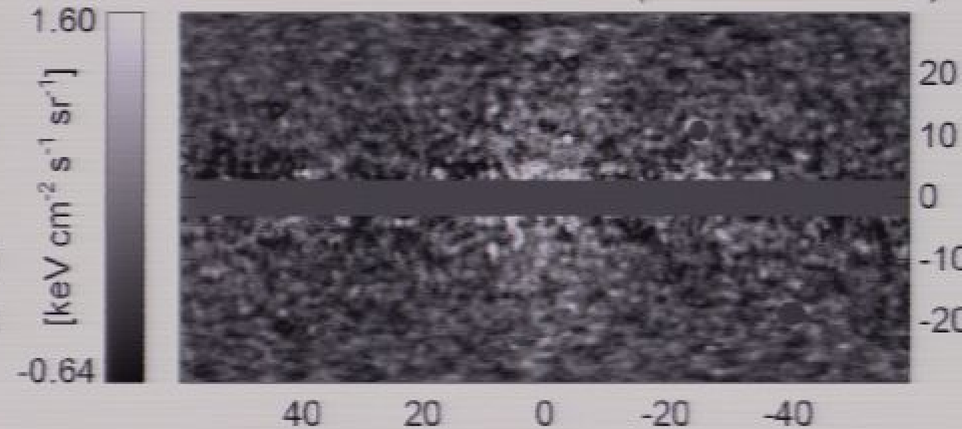

"Fermi Bubbles"
Su, Slatyer and Finkbeiner 2010

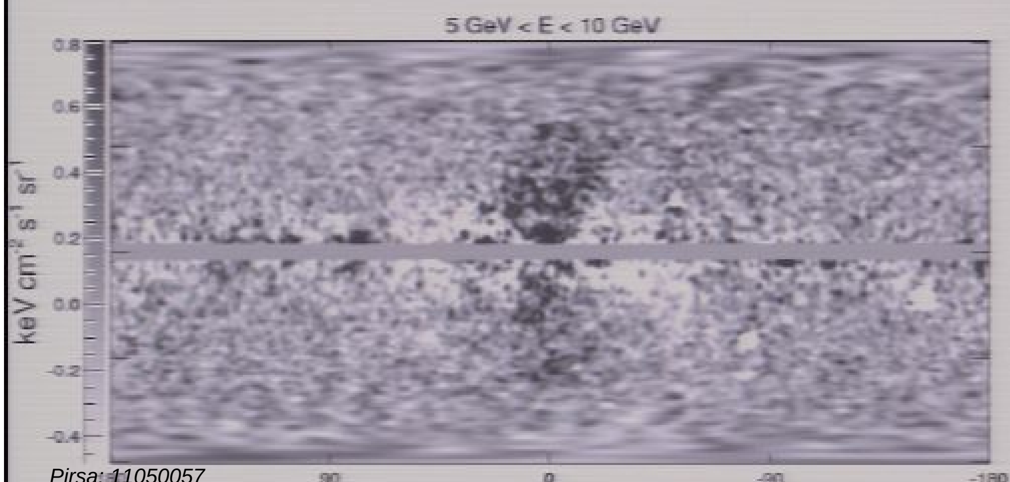

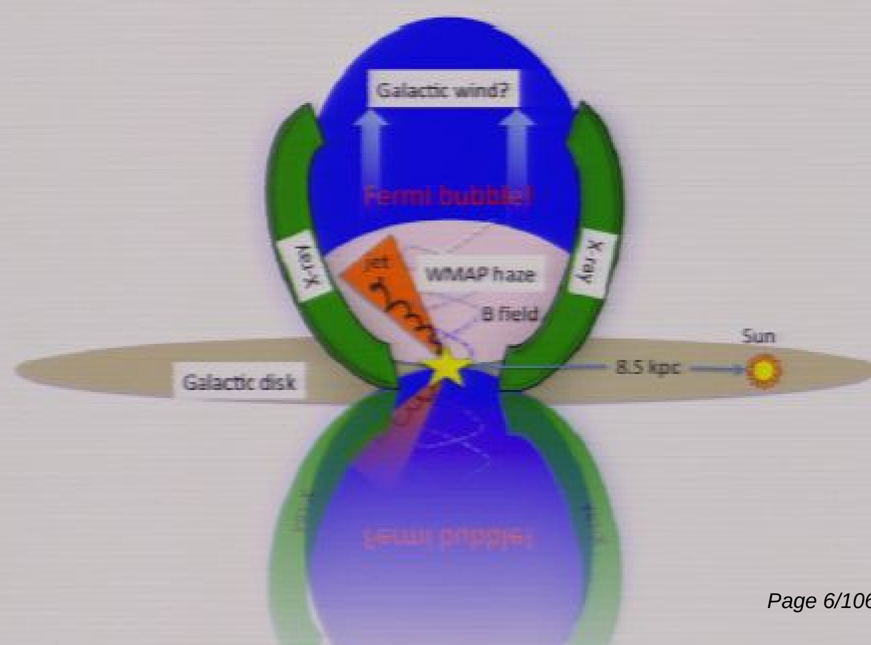

Dark matter annihilation?

- WIMPs naturally provide the appropriate relic abundance
- Interaction with ordinary matter and self-interaction offer attractive possibilities for detection
- WIMP annihilation can explain the anomalies but:

Large annihilation cross section mainly to leptons

Bergstrom et al. 2009, BF over "standard" value for correct cross section $<\sigma v>_0=3\times10^{-26}cm^3s^{-1}$

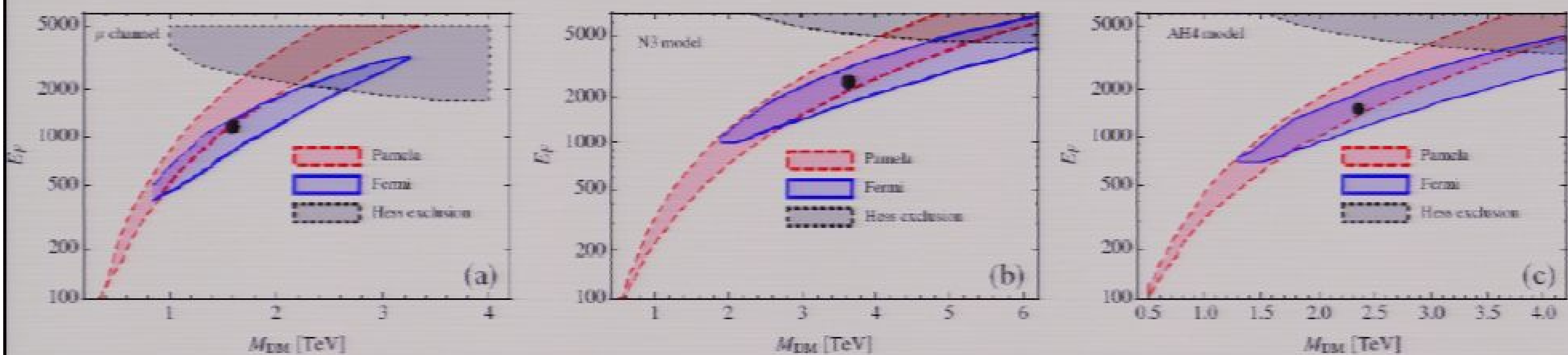

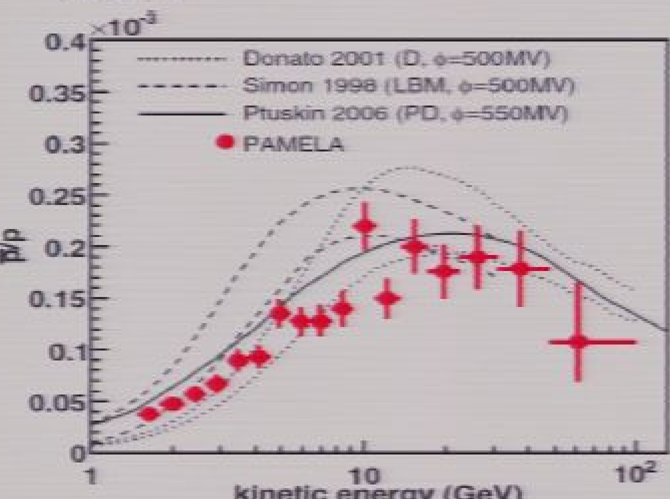

Low cross section into proton/antiproton

Adriani et al. 2009

Dark matter annihilation?

- WIMPs naturally provide the appropriate relic abundance
- Interaction with ordinary matter and self-interaction offer attractive possibilities for detection
- WIMP annihilation can explain the anomalies but:

Large annihilation cross section mainly to leptons

Bergstrom et al. 2009, BF over "standard" value for correct cross section $<\sigma v>_0=3\times10^{-26}cm^3s^{-1}$

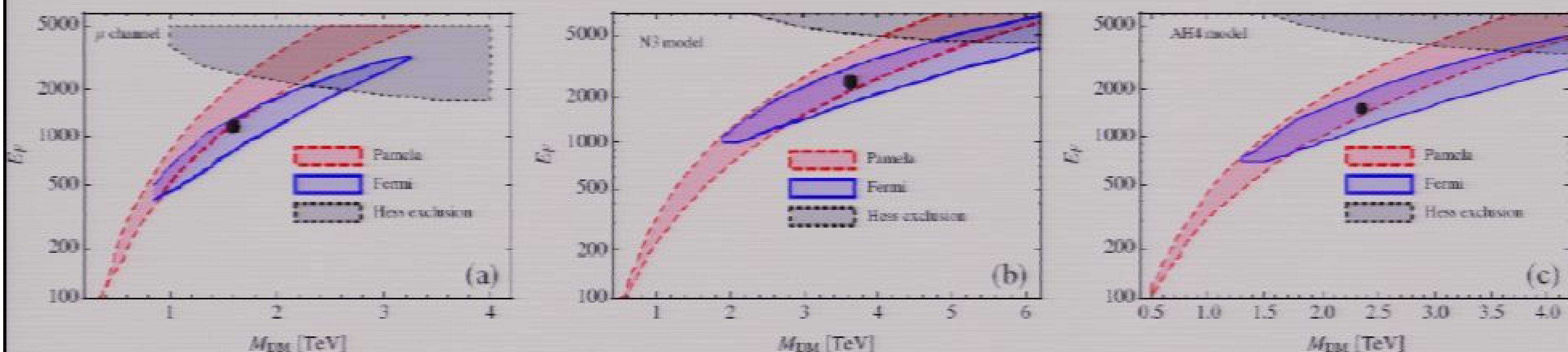

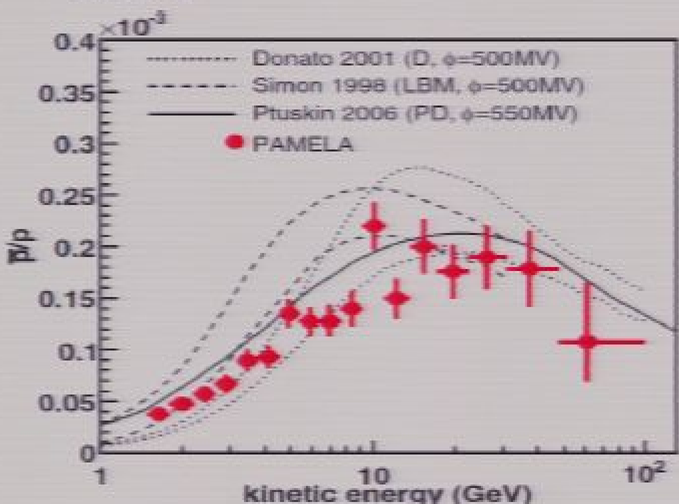

Low cross section into proton/antiproton

Adriani et al. 2009

Dark matter annihilation?

- WIMPs naturally provide the appropriate relic abundance
- Interaction with ordinary matter and self-interaction offer attractive possibilities for detection
- WIMP annihilation can explain the anomalies but:

Large annihilation cross section mainly to leptons

Bergstrom et al. 2009, BF over “standard” value for correct cross section $<\sigma v>_0=3\times10^{-26}cm^3s^{-1}$

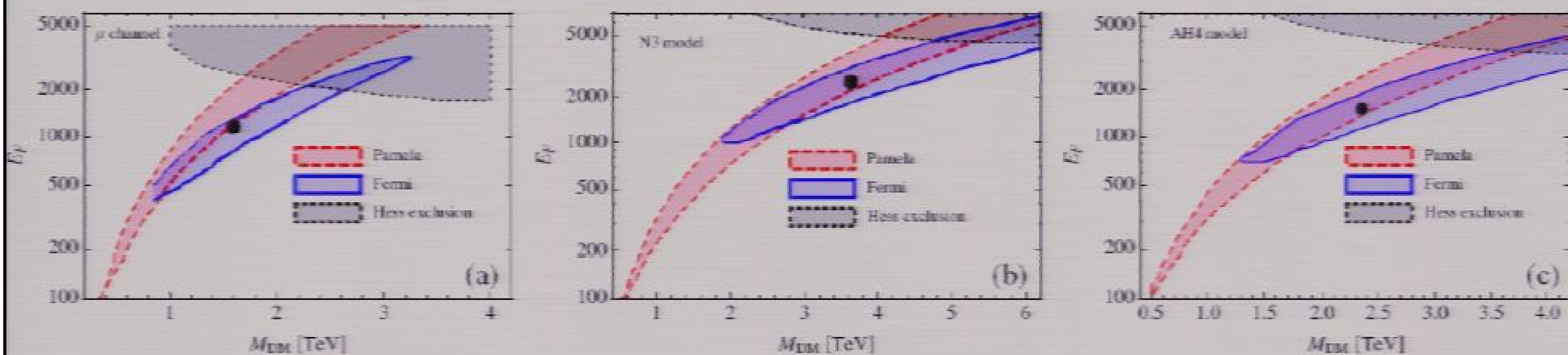

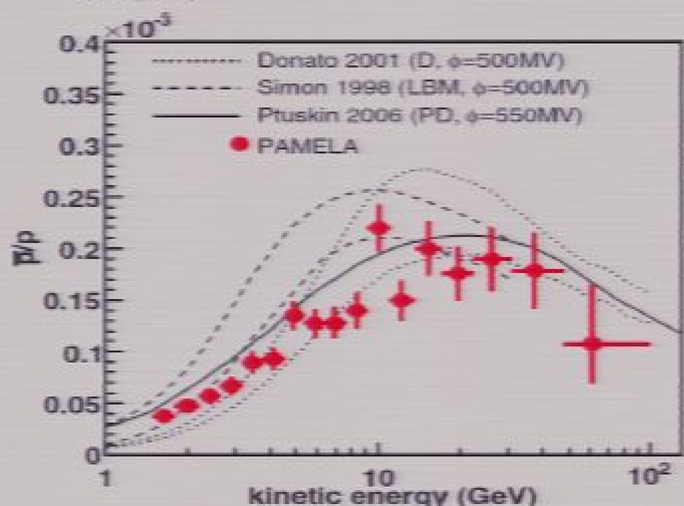

Low cross section into proton/antiproton

Adriani et al. 2009

Sommerfeld enhancement

- Classical analog:

Figs. from M. Cirelli, DMV, Cambridge 2011

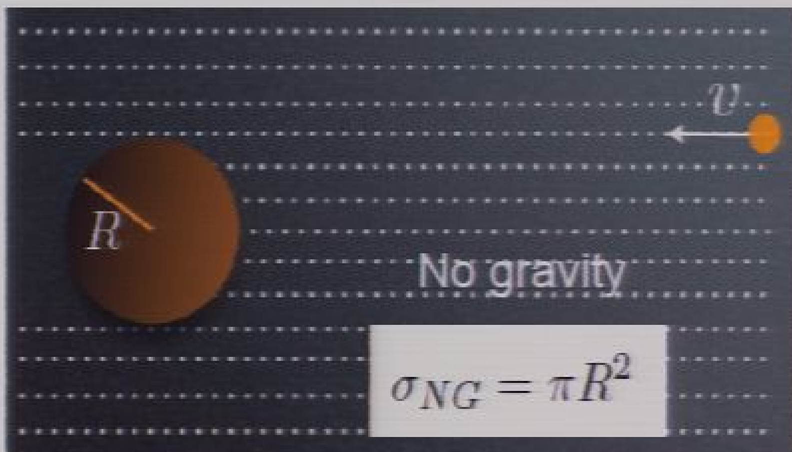

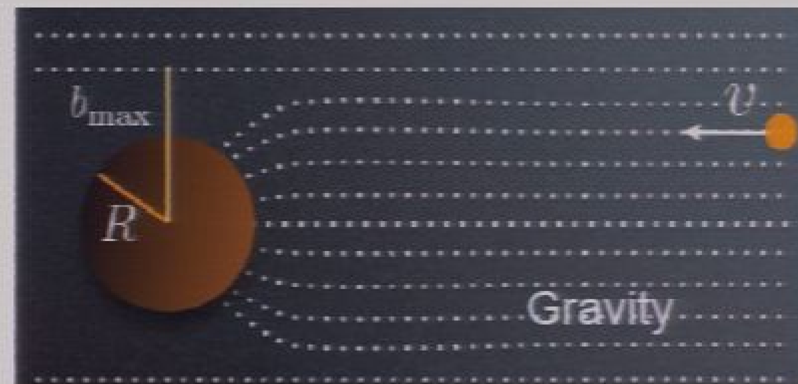

$$\sigma_N = \sigma_{NG}\left(1 + \frac{v_{esc}^2}{v^2}\right) = \pi b_{max}^2$$

- Annihilation enhancement (Hisano et al. 2004, Arkani-Hamed et al. 2009, ...)

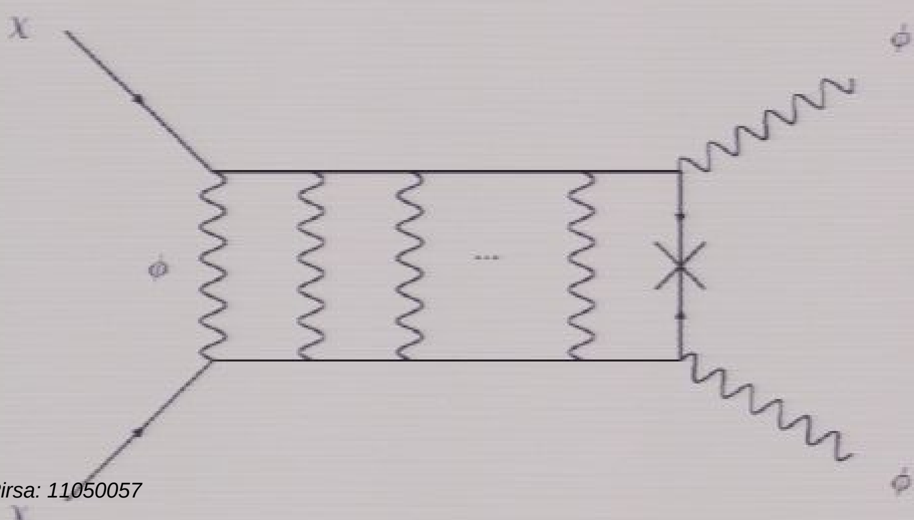

ϕ later decays into SM particles

$$\sigma = S\sigma_0, \qquad S = \frac{|\Psi(\infty)|^2}{|\Psi(0)|^2}$$

If mf<2mp -> decay into antiprotons kinematically forbidden

Sommerfeld enhancement

Simplified case, a scalar boson as a force carrier, Yukawa potential

$$\frac{1}{m_\chi}\frac{d^2\Psi(r)}{dr^2} + V(r)\Psi(r) = -m_\chi \beta^2 \Psi(r) \qquad V(r) = -\frac{\alpha_c}{r}e^{-m_\phi r}$$

Lattanzi and Silk 2009

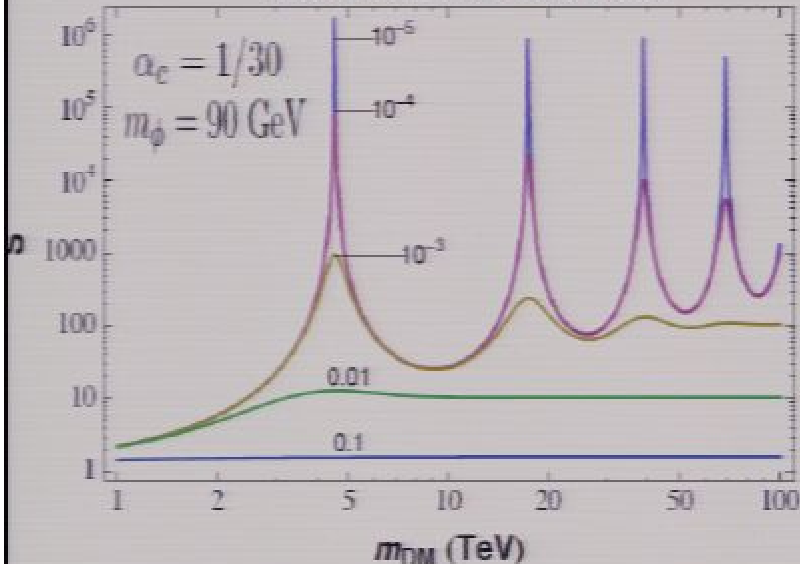

Coulomb approximation (m_ϕ -> 0):

$$S = \frac{\pi\alpha_c}{\beta}\left(1 - e^{-\pi\alpha_c/\beta}\right)^{-1}$$

$$S(\beta) \propto 1/\beta \quad \text{if} \quad \beta \ll \pi\alpha_c$$

General behaviour:

1) if $\beta^2 \gg m_\phi \alpha_c / m_\chi$ -> Coulomb case

2) if $\beta^2 \ll m_\phi \alpha_c / m_\chi$ -> bound states if $m_\chi = 4 m_\phi n^2/\alpha$

3) Close to "resonances" -> $S(\beta) \propto 1/\beta^2$

4) Saturation at very low velocities, finite life time of the bound states

Arkani-Hamed et al. 2009

$$S(\sigma_{\rm vel}) = \left(\frac{1}{2\sigma_{\rm vel}^3\sqrt{\pi}}\int_0^1 S(\beta)\beta^2 e^{-\beta^2/4\sigma_{\rm vel}^2}\, d\beta\right)$$

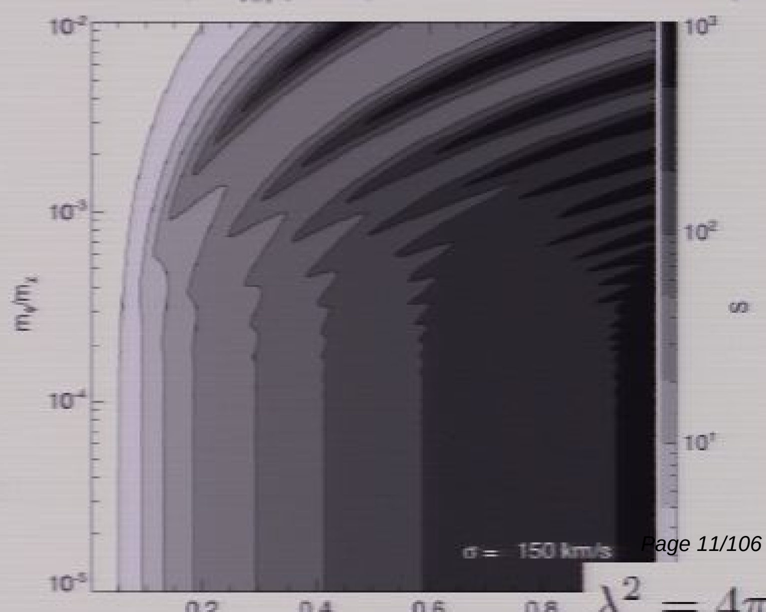

$\lambda^2 = 4\pi\alpha_c$

Relic density constraints

Boltzmann equation: $$\frac{\mathrm{d}n_\chi}{\mathrm{d}t} + 3Hn_\chi = -\langle \sigma v \rangle \left(n_\chi^2 - \left(n_\chi^{EQ}\right)^2 \right)$$

Change of variables: $x = m_\chi / T \qquad Y = n_\chi / s$

After freeze-out, the number density strongly departs from the equilibrium solution. For $t>t_F$:

$$\frac{1}{Y(x_0)} = \frac{1}{Y(x_f)} + \sqrt{\frac{\pi}{45}} m_\chi m_{Pl} \langle \sigma v \rangle_S \int_{x_f}^{x_0} \frac{g_*^{1/2}(x)\mathcal{S}(x_\chi)}{x^2} dx$$

$\langle \sigma v \rangle = \mathcal{S}(x) \langle \sigma v \rangle_S$

Note that:
$$S(\beta) \propto 1/\beta \quad \rightarrow \quad \mathcal{S}(x) \propto x^{1/2} \propto 1/\sigma_{vel}$$
$$S(\beta) \propto 1/\beta^2 \quad \rightarrow \quad \mathcal{S}(x) \propto x \propto 1/\sigma_{vel}^2$$

$\Omega_{\chi,0}h^2 \sim 2.757 \times 10^8 \left(\frac{m_\chi}{GeV}\right) Y(x_0)$ Dark matter abundance: $\Omega_{\mathrm{DM}}h^2 \sim 0.1143$

Kinetic decoupling: after freeze-out, scattering with SM particles keep T_χ=T, after kinetic decoupling T_χ drops as $1/a^2$ ("colder" than radiation):

$$x_\chi = x \quad \text{for} \quad t < t_{\mathrm{KD}}$$
$$x_\chi = x^2/x_{\mathrm{KD}} \quad \text{for} \quad t > t_{\mathrm{KD}}$$

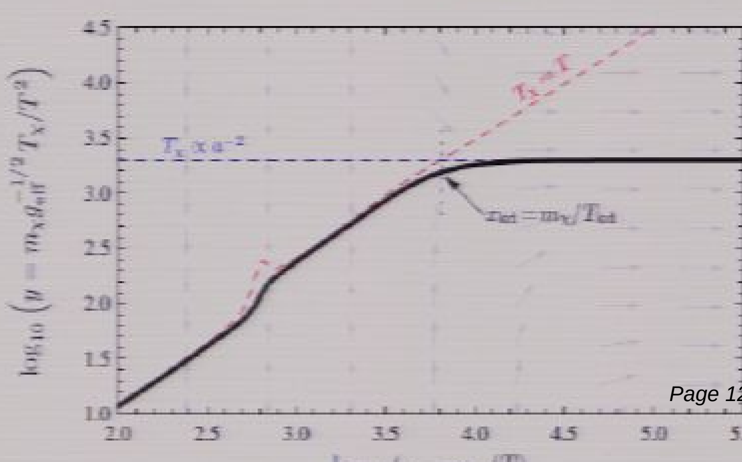

Bringmann 2009

Sommerfeld enhancement

Simplified case, a scalar boson as a force carrier, Yukawa potential

$$\frac{1}{m_\chi}\frac{d^2\Psi(r)}{dr^2} + V(r)\Psi(r) = -m_\chi \beta^2 \Psi(r) \qquad V(r) = -\frac{\alpha_c}{r}e^{-m_\phi r}$$

Lattanzi and Silk 2009

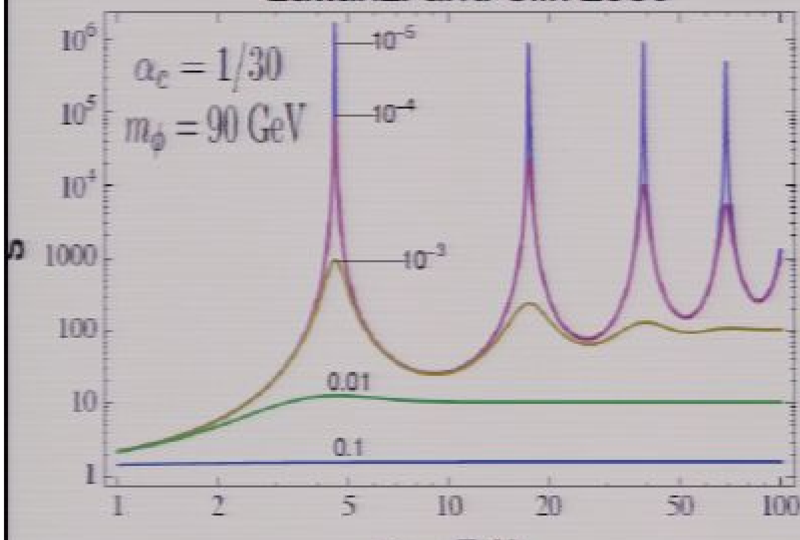

Coulomb approximation (m_ϕ -> 0):

$$S = \frac{\pi\alpha_c}{\beta}\left(1 - e^{-\pi\alpha_c/\beta}\right)^{-1}$$

$$S(\beta) \propto 1/\beta \quad \text{if} \quad \beta \ll \pi\alpha_c$$

Arkani-Hamed et al. 2009

$$S(\sigma_{\rm vel}) = \left(\frac{1}{2\sigma_{\rm vel}^3\sqrt{\pi}}\int_0^1 S(\beta)\beta^2 e^{-\beta^2/4\sigma_{\rm vel}^2}\, d\beta\right)$$

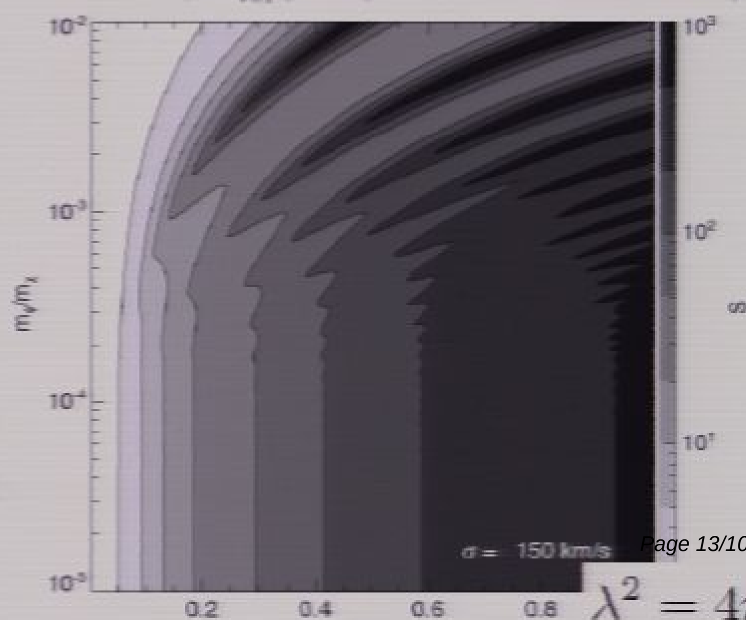

$\lambda^2 = 4\pi\alpha_c$

General behaviour:

1) if $\beta^2 \gg m_\phi\alpha_c/m_\chi$ -> Coulomb case

2) if $\beta^2 \ll m_\phi\alpha_c/m_\chi$ -> bound states if $m_\chi=4m_\phi n^2/\alpha$

3) Close to "resonances" -> $S(\beta) \propto 1/\beta^2$

4) Saturation at very low velocities, finite life time of the bound states

Relic density constraints

Boltzmann equation: $\frac{\mathrm{d}n_\chi}{\mathrm{d}t} + 3Hn_\chi = -\langle \sigma v \rangle \left(n_\chi^2 - \left(n_\chi^{EQ}\right)^2 \right)$

Change of variables: $x = m_\chi / T \quad Y = n_\chi / s$

After freeze-out, the number density strongly departs from the equilibrium solution. For $t>t_F$:

$$\frac{1}{Y(x_0)} = \frac{1}{Y(x_f)} + \sqrt{\frac{\pi}{45}} m_\chi m_{Pl} \langle \sigma v \rangle_S \int_{x_f}^{x_0} \frac{g_*^{1/2}(x) \mathcal{S}(x_\chi)}{x^2} dx$$

$\langle \sigma v \rangle = \mathcal{S}(x) \langle \sigma v \rangle_S$ Note that:

$$S(\beta) \propto 1/\beta \quad \rightarrow \quad \mathcal{S}(x) \propto x^{1/2} \propto 1/\sigma_{vel}$$
$$S(\beta) \propto 1/\beta^2 \quad \rightarrow \quad \mathcal{S}(x) \propto x \propto 1/\sigma_{vel}^2$$

$\Omega_{\chi,0} h^2 \sim 2.757 \times 10^8 \left(\frac{m_\chi}{GeV} \right) Y(x_0)$ Dark matter abundance: $\Omega_{\rm DM} h^2 \sim 0.1143$

Kinetic decoupling: after freeze-out, scattering with SM particles keep T_χ=T, after kinetic decoupling T_χ drops as $1/a^2$ ("colder" than radiation):

$$x_\chi = x \quad \text{for} \quad t < t_{\rm KD}$$
$$x_\chi = x^2 / x_{\rm KD} \quad \text{for} \quad t > t_{\rm KD}$$

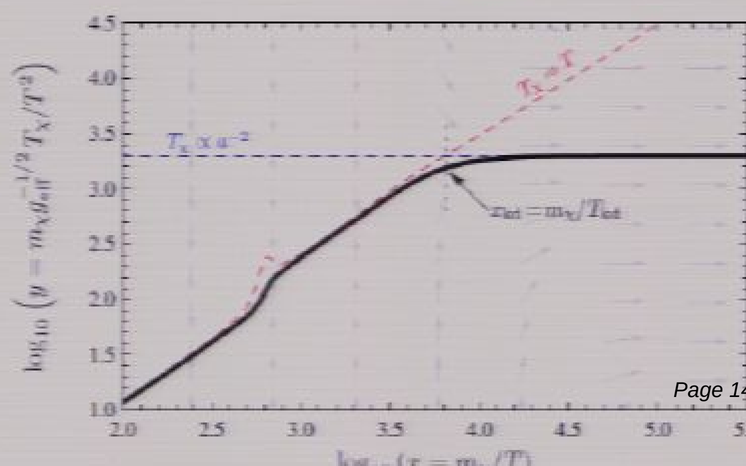

Bringmann 2009

Sommerfeld enhancement

Simplified case, a scalar boson as a force carrier, Yukawa potential

$$\frac{1}{m_\chi}\frac{d^2\Psi(r)}{dr^2} + V(r)\Psi(r) = -m_\chi\beta^2\Psi(r) \qquad V(r) = -\frac{\alpha_c}{r}e^{-m_\phi r}$$

Lattanzi and Silk 2009

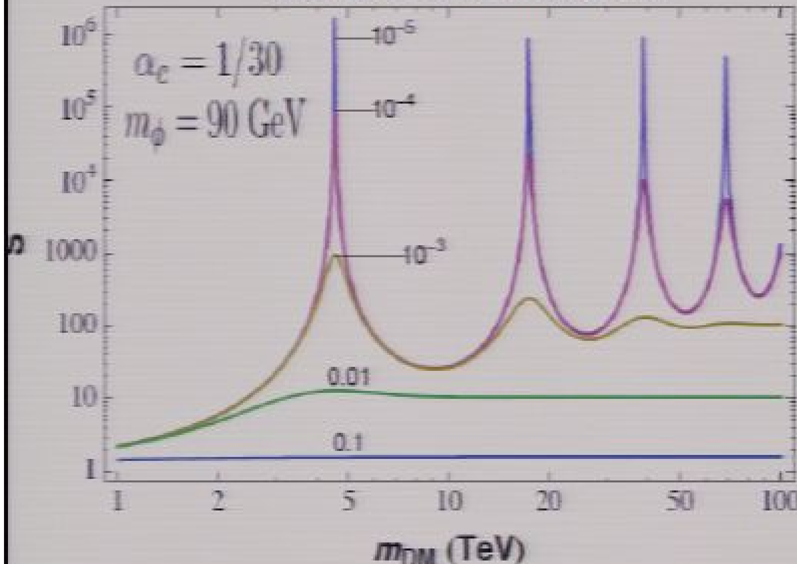

Coulomb approximation (m_ϕ -> 0):

$$S = \frac{\pi\alpha_c}{\beta}\left(1 - e^{-\pi\alpha_c/\beta}\right)^{-1}$$

$$\boxed{S(\beta) \propto 1/\beta \quad \text{if} \quad \beta \ll \pi\alpha_c}$$

Arkani-Hamed et al. 2009

$$S(\sigma_{\rm vel}) = \left(\frac{1}{2\sigma_{\rm vel}^3\sqrt{\pi}}\int_0^1 S(\beta)\beta^2 e^{-\beta^2/4\sigma_{\rm vel}^2}\,{\rm d}\beta\right)$$

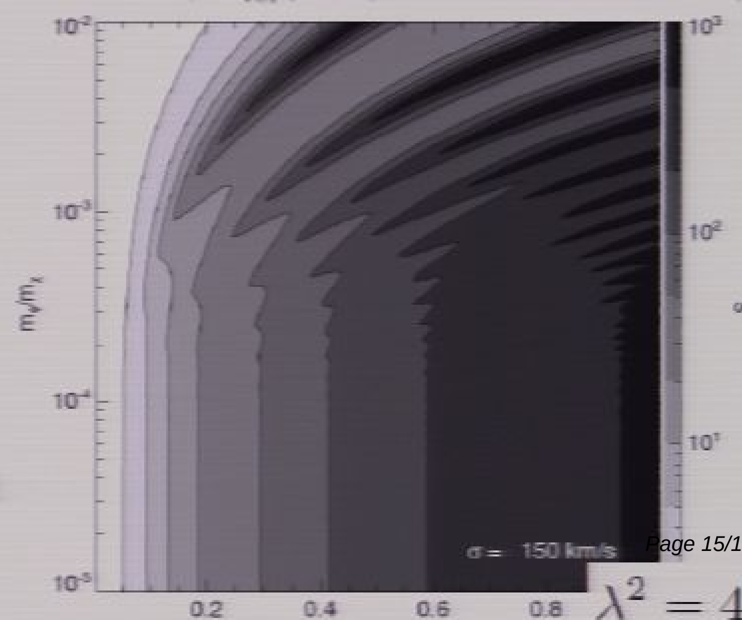

$\lambda^2 = 4\pi\alpha_c$

General behaviour:

1) if $\beta^2 \gg m_\phi\alpha_c/m_\chi$ -> Coulomb case

2) if $\beta^2 \ll m_\phi\alpha_c/m_\chi$ -> bound states if $m_\chi=4m_\phi n^2/\alpha$

3) Close to “resonances” -> $S(\beta) \propto 1/\beta^2$

4) Saturation at very low velocities, finite life time of the bound states

Relic density constraints

Boltzmann equation: $\frac{dn_\chi}{dt} + 3Hn_\chi = -\langle\sigma v\rangle \left(n_\chi^2 - (n_\chi^{EQ})^2\right)$

Change of variables: $x = m_\chi/T \quad Y = n_\chi/s$

After freeze-out, the number density strongly departs from the equilibrium solution. For $t>t_F$:

$$\frac{1}{Y(x_0)} = \frac{1}{Y(x_f)} + \sqrt{\frac{\pi}{45}} m_\chi m_{Pl} \langle\sigma v\rangle_S \int_{x_f}^{x_0} \frac{g_*^{1/2}(x)\mathcal{S}(x_\chi)}{x^2} dx$$

$\langle\sigma v\rangle = \mathcal{S}(x)\langle\sigma v\rangle_S$ Note that:

$$S(\beta) \propto 1/\beta \quad \rightarrow \quad \mathcal{S}(x) \propto x^{1/2} \propto 1/\sigma_{vel}$$
$$S(\beta) \propto 1/\beta^2 \quad \rightarrow \quad \mathcal{S}(x) \propto x \propto 1/\sigma_{vel}^2$$

$\Omega_{\chi,0}h^2 \sim 2.757 \times 10^8 \left(\frac{m_\chi}{GeV}\right) Y(x_0)$ Dark matter abundance: $\Omega_{\rm DM}h^2 \sim 0.1143$

Kinetic decoupling: after freeze-out, scattering with SM particles keep T_χ=T, after kinetic decoupling T_χ drops as 1/a[2] ("colder" than radiation):

$$x_\chi = x \quad \text{for} \quad t < t_{\rm KD}$$
$$x_\chi = x^2/x_{\rm KD} \quad \text{for} \quad t > t_{\rm KD}$$

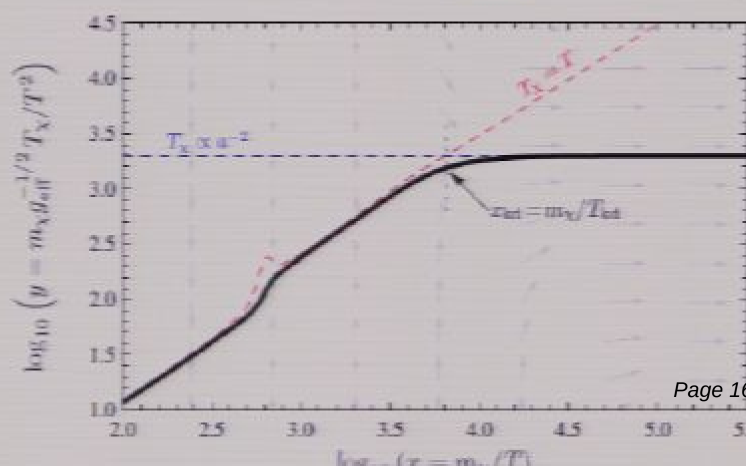

Bringmann 2009

Relic density constraints

Dent et al. 2010

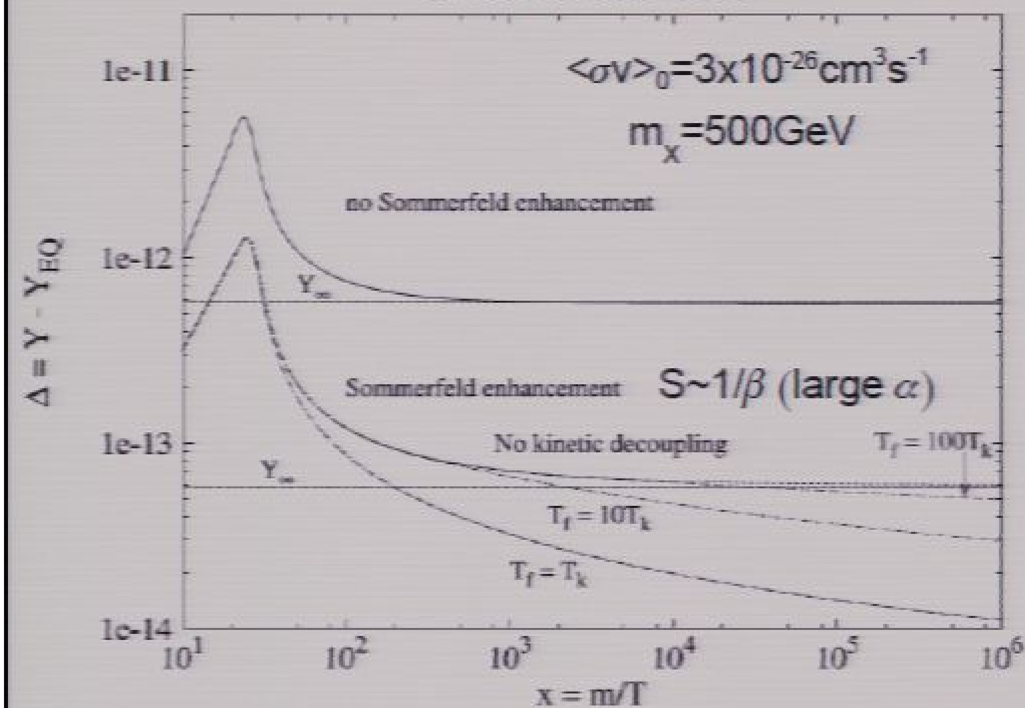

Zavala et al. 2010

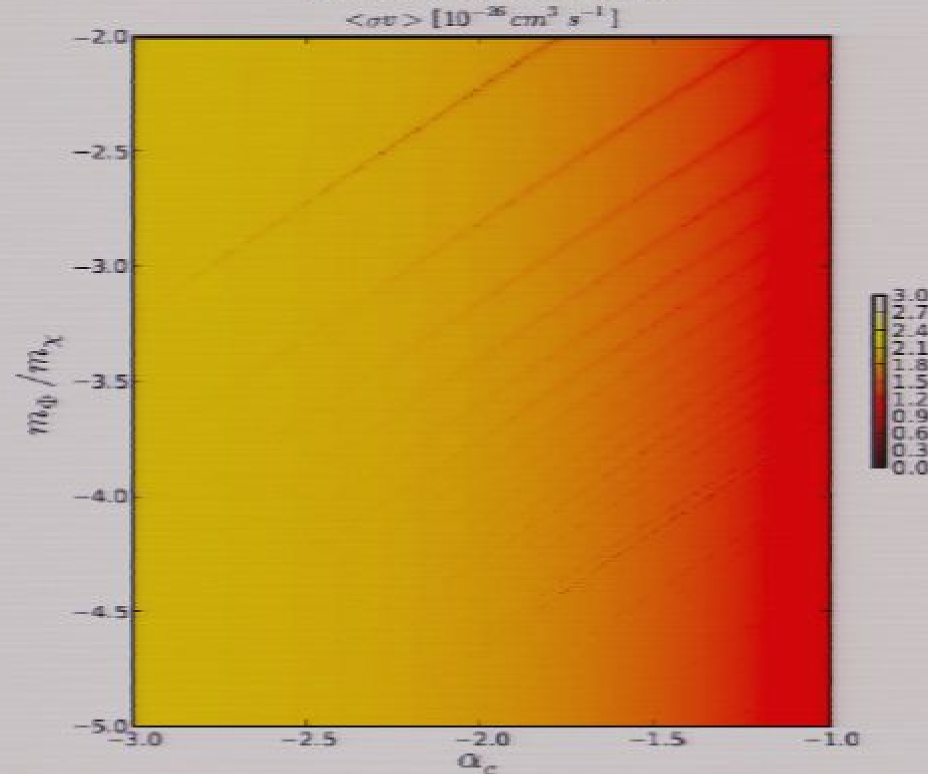

$\Omega_{DM}h^2 \sim 0.1143$

$<\sigma v>_0=2.4\times10^{-26}cm^3s^{-1}$ $m_X=100GeV$, $T_{kd}=8MeV$

Bringmann 2009

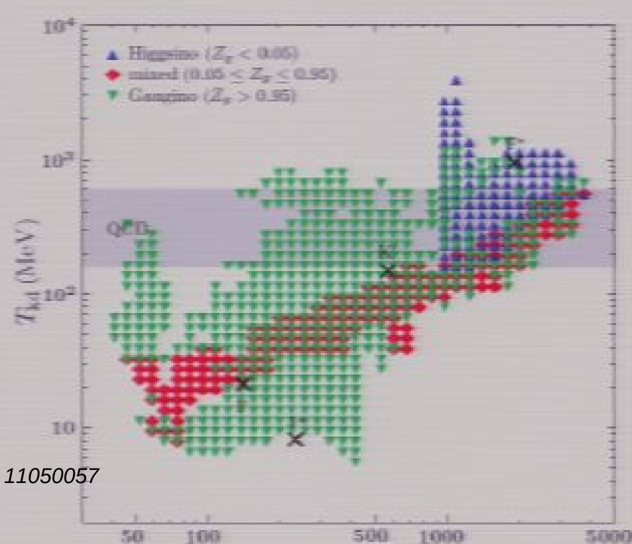

- If $S\sim1/\sigma$ then $Y\sim1/\ln x$ for $x>x_{kd}$
- If $S\sim1/\sigma^2$ then $Y\sim1/x$ for $x>x_{kd}$
- $<\sigma v>_0$ needs to be lower than the case without enhancement (a factor of a few) to give the correct relic density
- Kinetic decoupling temperature is a relevant parameter, the larger it is, the stronger the suppression on the relic density

Relic density constraints

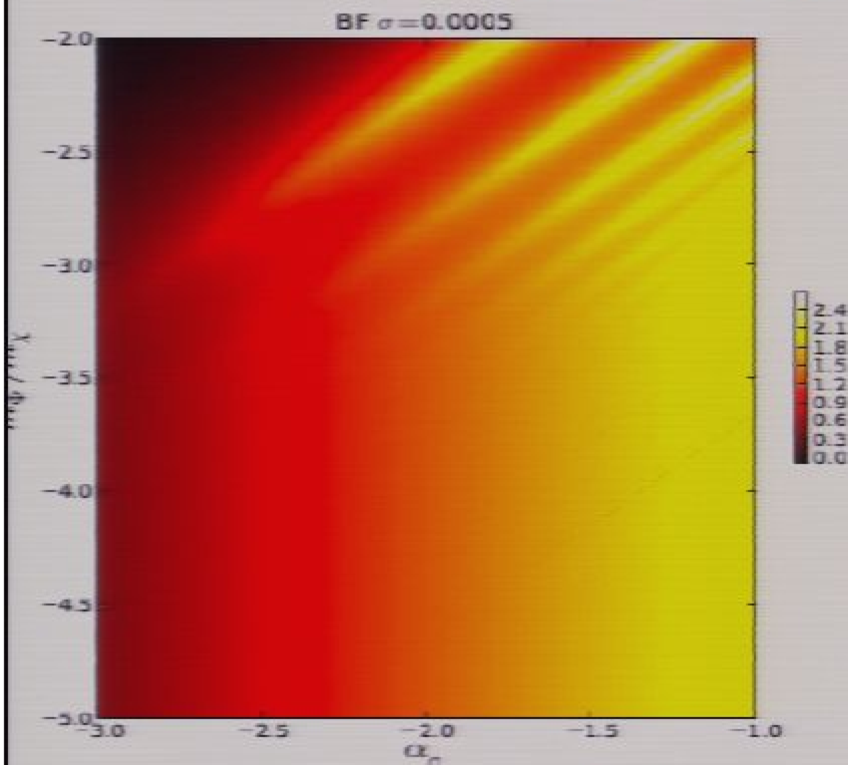

BF(relative to$<\sigma v>_0=3\times10^{-26}cm^3s^{-1}$) <100
for $\alpha<10^{-2}$, $m_\phi/m_X<10^{-3}$, m_X~100GeV

Feng et al. 2010
"maximal" BF

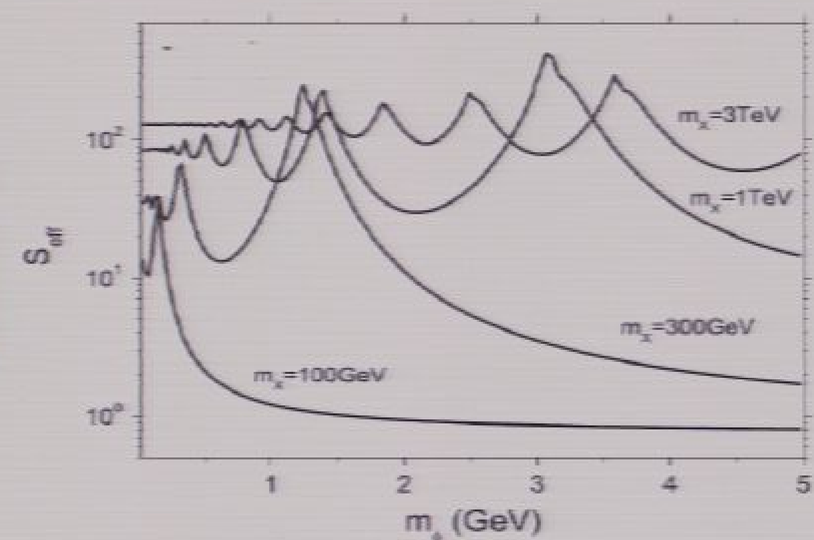

It is possible to have larger boosts in models with mass splitting

Finkbeiner et al. 2011

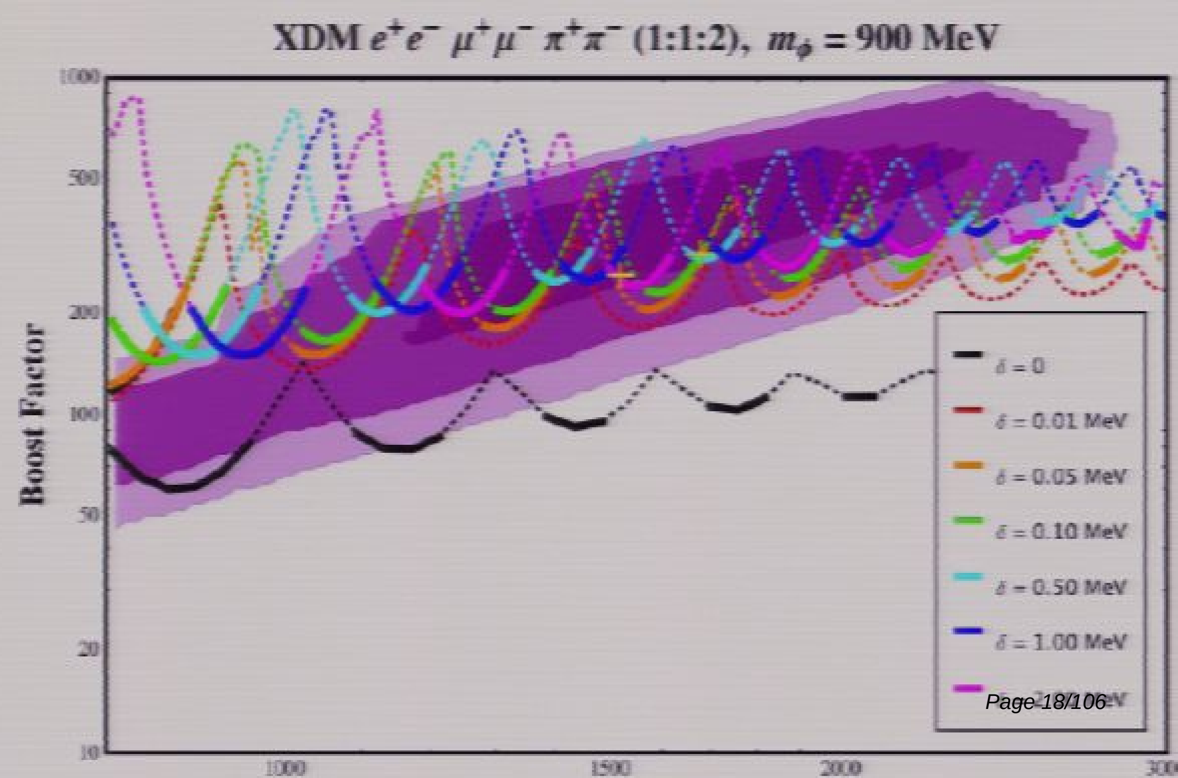

CMB constraints

Zavala et al. 2010

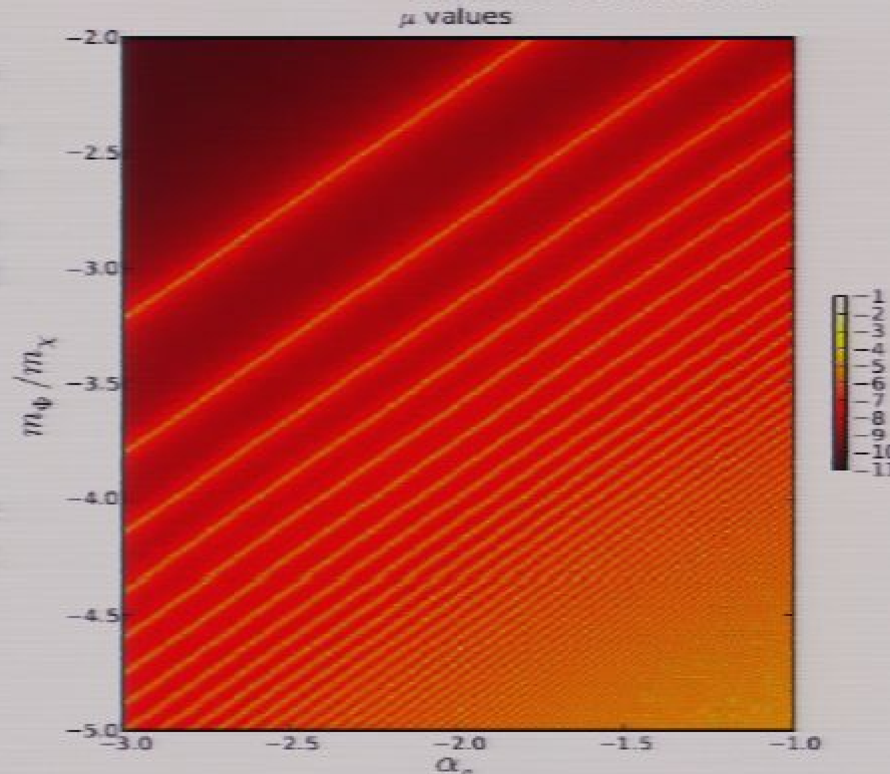

CMB energy spectrum: energy injection at $10^4<z<10^6$ effectively produces a Bose-Einstein energy spectrum with chemical potential μ instead of the pure black body spectrum (Illarionov and Sunyaev 1975). Limit by COBE/FIRAS $|\mu|<9\times10^{-5}$. "f" is the fraction that ionizes and heats the IGM.

$$\mu = 1.4\frac{\delta\rho_\gamma}{\rho_\gamma} = 1.4\int_{t_1}^{t_2}\frac{\dot\rho_\gamma}{\rho_\gamma}dt = 1.4\int_{t_1}^{t_2}\frac{f m_\chi\langle\sigma v\rangle n_\chi^2}{\rho_{\gamma,0}a^{-4}}dt,$$

Injection at $10^3<z<10^4$ produces a y-type distortion to the CMB (Hannestad and Tram 2011). Both are weak constraints.

Slatyer et al. 2009

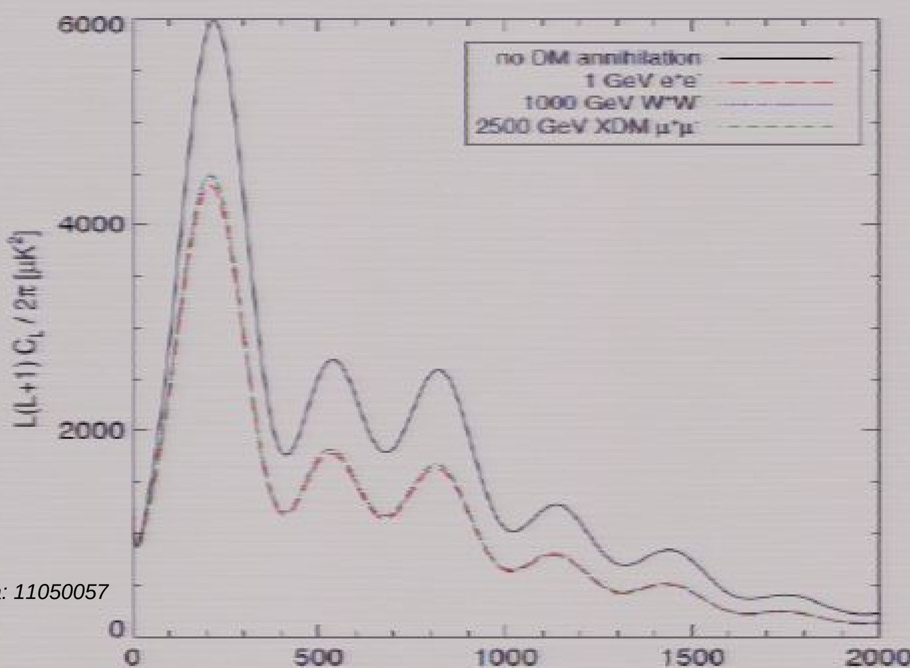

CMB power spectrum: e.g. Slatyer et al. 2009, limits based on WMAP5:

$$\frac{\lim_{v\to0}\langle\sigma v\rangle}{3\times10^{-26}\mathrm{cm}^3/\mathrm{s}} \lesssim \frac{120}{f}\left(\frac{m_\chi}{1\mathrm{TeV}}\right)$$

f~0.25 for annihilation into SM particles, except electrons (f~0.7) and neutrinos (f~0)

Finkbeiner et al. 2011, $m_0 \sim m_\phi$

$$BF_{\rm now} \lesssim (250/f)(m_0/1\mathrm{GeV})$$

Relic density constraints

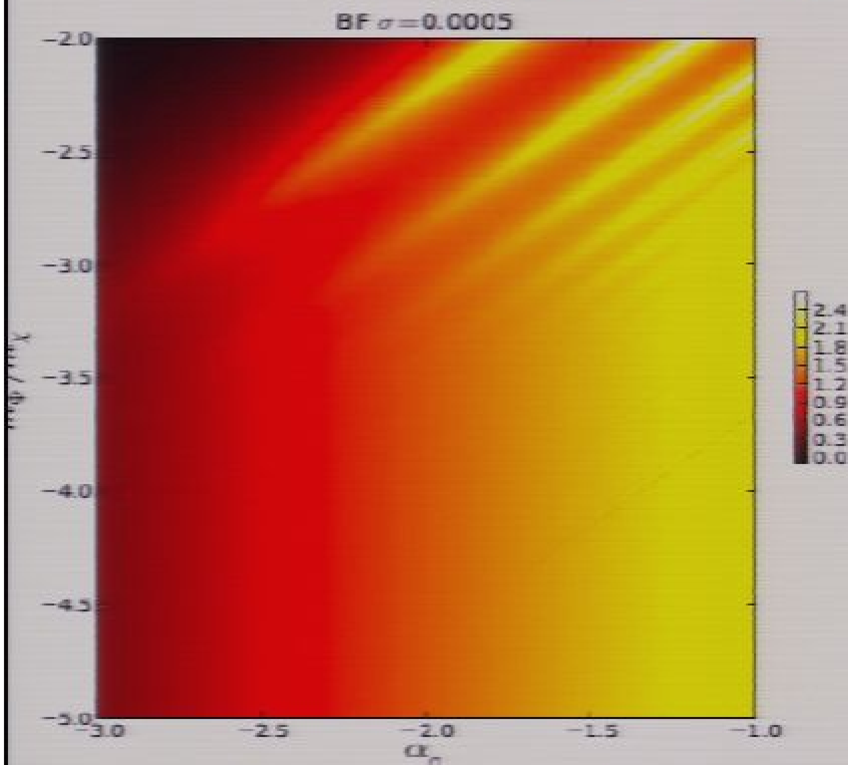

BF(relative to $\langle\sigma v\rangle_0=3\times10^{-26}cm^3s^{-1}$) <100
for $\alpha<10^{-2}$, $m_\phi/m_X<10^{-3}$, m_X~100GeV

Feng et al. 2010
"maximal" BF

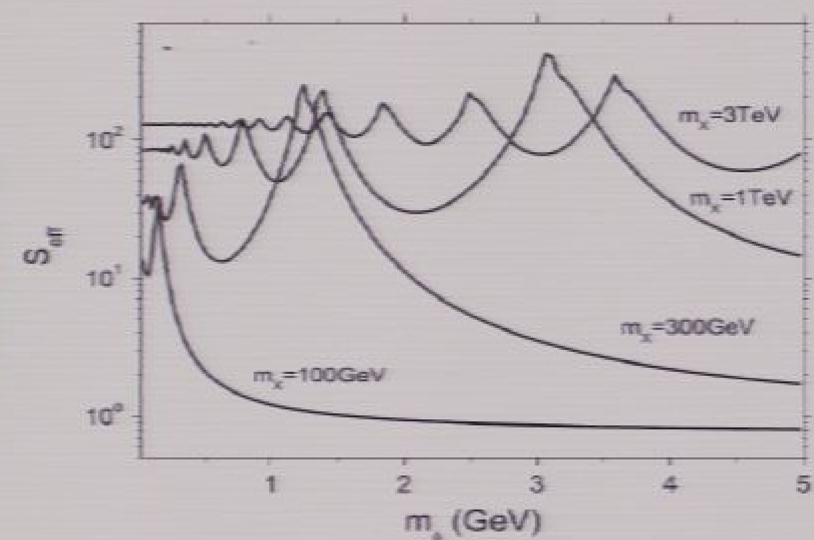

It is possible to have larger boosts
in models with mass splitting

Finkbeiner et al. 2011

XDM e^+e^- $\mu^+\mu^-$ $\pi^+\pi^-$ (1:1:2), m_ϕ = 900 MeV

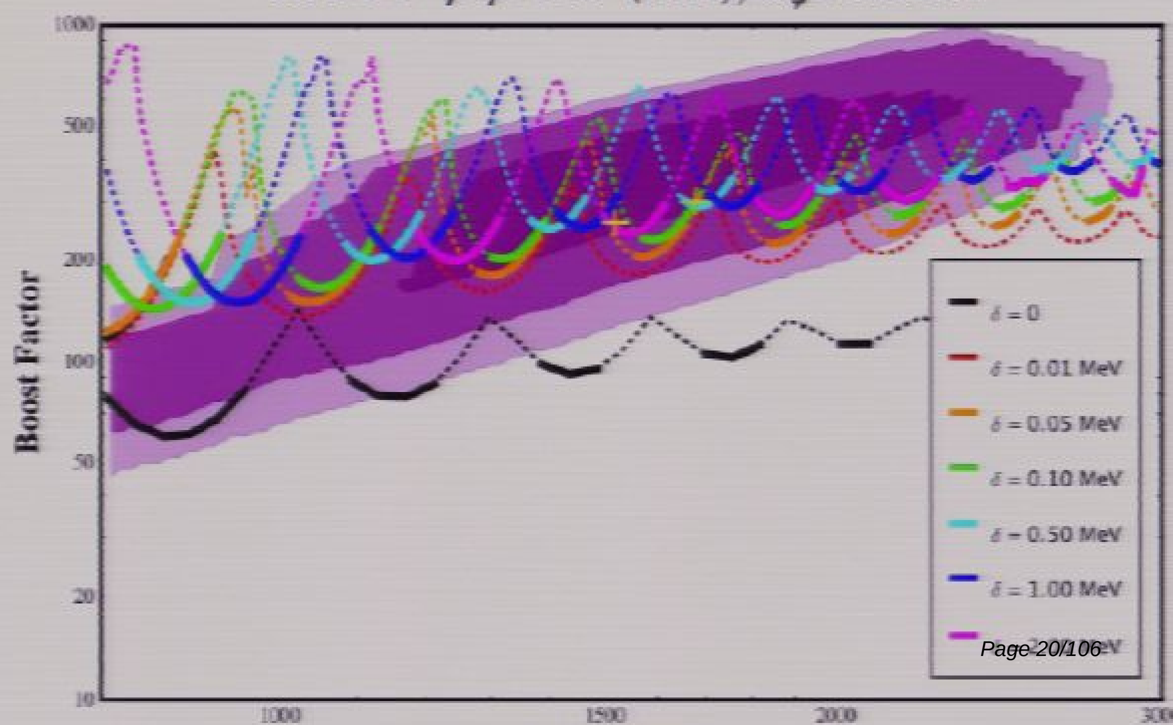

CMB constraints

Zavala et al. 2010

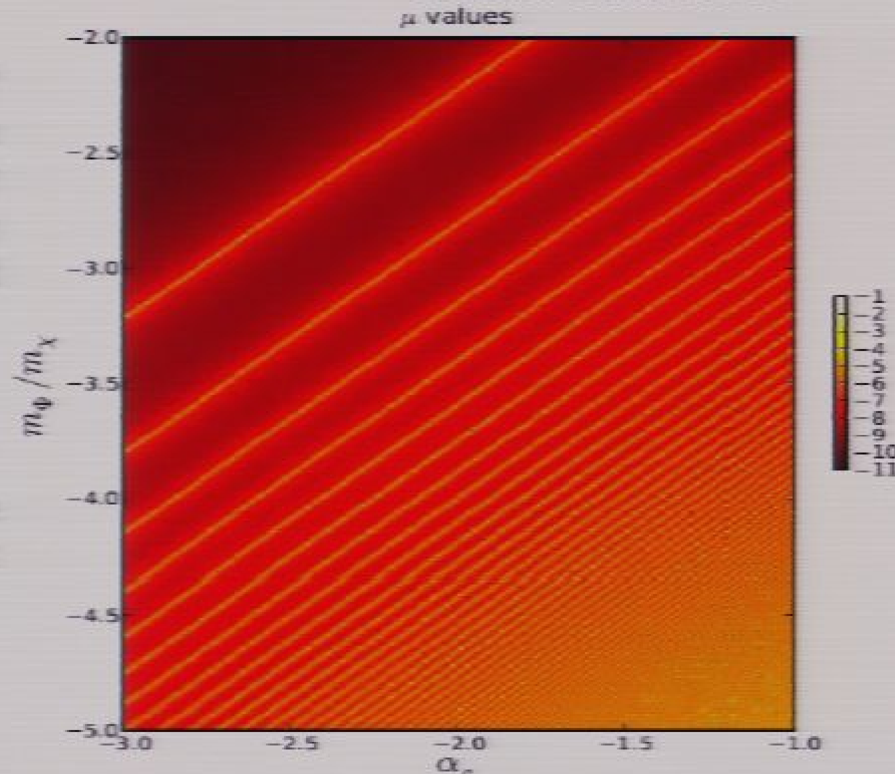

CMB energy spectrum: energy injection at $10^4<z<10^6$ effectively produces a Bose-Einstein energy spectrum with chemical potential μ instead of the pure black body spectrum (Illarionov and Sunyaev 1975). Limit by COBE/FIRAS $|\mu|<9\times10^{-5}$. "f" is the fraction that ionizes and heats the IGM.

$$\mu = 1.4\frac{\delta\rho_\gamma}{\rho_\gamma} = 1.4\int_{t_1}^{t_2}\frac{\dot{\rho}_\gamma}{\rho_\gamma}dt = 1.4\int_{t_1}^{t_2}\frac{f m_\chi\langle\sigma v\rangle n_\chi^2}{\rho_{\gamma,0}a^{-4}}dt,$$

Injection at $10^3<z<10^4$ produces a y-type distortion to the CMB (Hannestad and Tram 2011). Both are weak constraints.

Slatyer et al. 2009

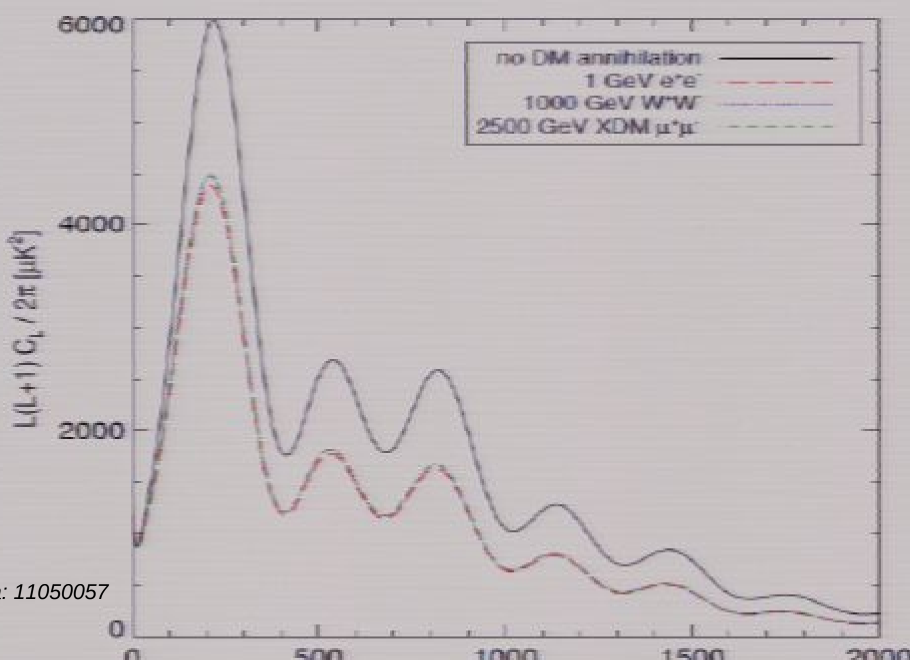

CMB power spectrum: e.g. Slatyer et al. 2009, limits based on WMAP5:

$$\frac{\lim_{v\to 0}\langle\sigma v\rangle}{3\times10^{-26}\mathrm{cm}^3/\mathrm{s}} \lesssim \frac{120}{f}\left(\frac{m_\chi}{1\mathrm{TeV}}\right)$$

f~0.25 for annihilation into SM particles, except electrons (f~0.7) and neutrinos (f~0)

Finkbeiner et al. 2011, $m_0 \sim m_\phi$

$$BF_{\mathrm{now}} \lesssim (250/f)(m_0/1\mathrm{GeV})$$

CMB constraints

Zavala et al. 2010

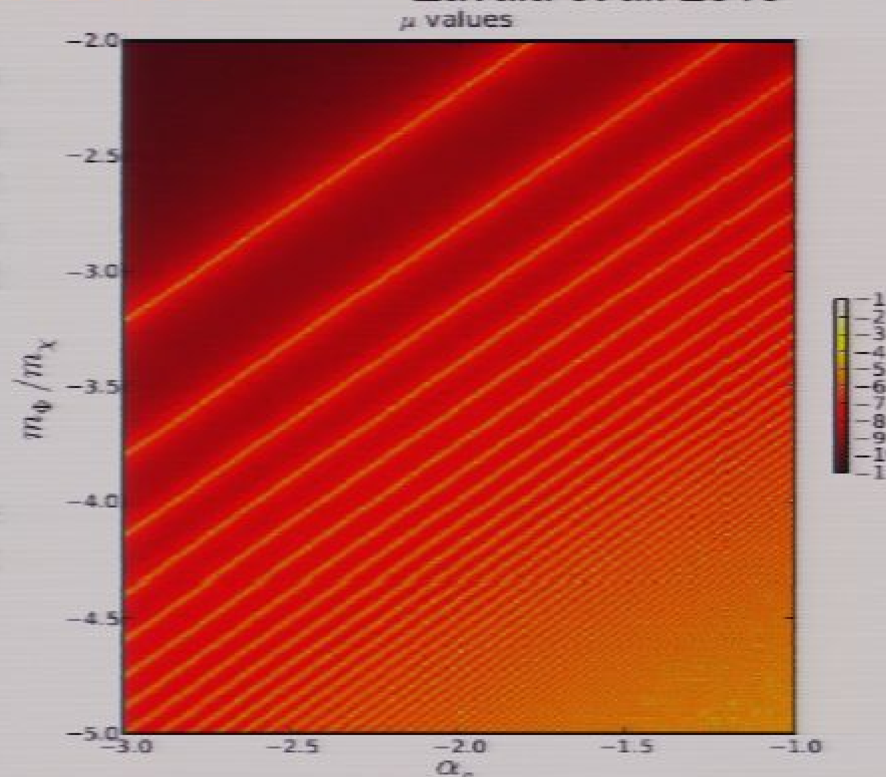

CMB energy spectrum: energy injection at $10^4<z<10^6$ effectively produces a Bose-Einstein energy spectrum with chemical potential μ instead of the pure black body spectrum (Illarionov and Sunyaev 1975). Limit by COBE/FIRAS $|\mu|<9\times10^{-5}$. "f" is the fraction that ionizes and heats the IGM.

$$\mu = 1.4\frac{\delta\rho_\gamma}{\rho_\gamma} = 1.4\int_{t_1}^{t_2}\frac{\dot{\rho}_\gamma}{\rho_\gamma}dt = 1.4\int_{t_1}^{t_2}\frac{f m_\chi \langle\sigma v\rangle n_\chi^2}{\rho_{\gamma,0}a^{-4}}dt,$$

Injection at $10^3<z<10^4$ produces a y-type distortion to the CMB (Hannestad and Tram 2011). Both are weak constraints.

Slatyer et al. 2009

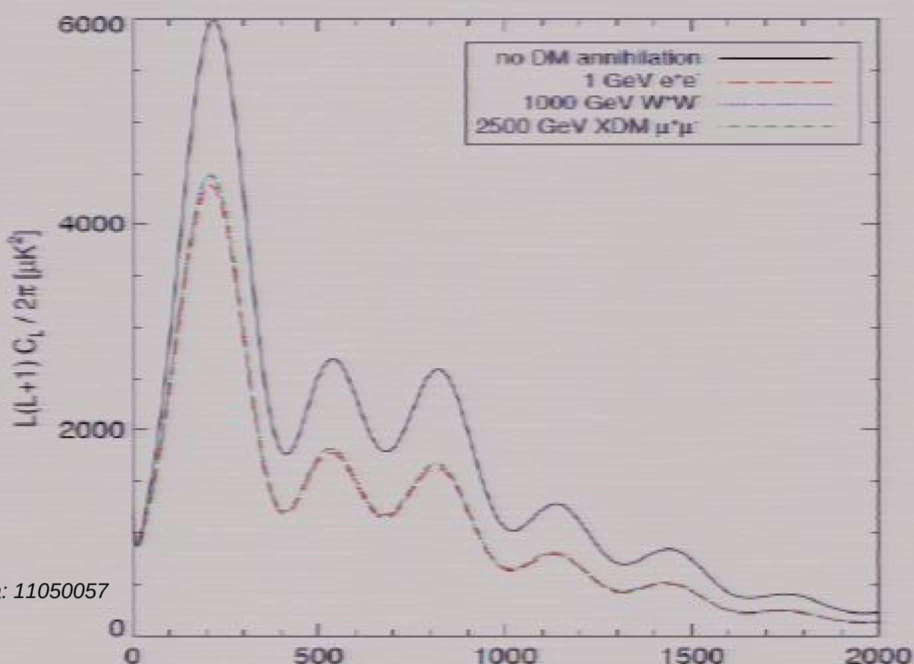

CMB power spectrum: e.g. Slatyer et al. 2009, limits based on WMAP5:

$$\frac{\lim_{v\to 0}\langle\sigma v\rangle}{3\times 10^{-26}\mathrm{cm}^3/\mathrm{s}} \lesssim \frac{120}{f}\left(\frac{m_\chi}{1\mathrm{TeV}}\right)$$

f~0.25 for annihilation into SM particles, except electrons (f~0.7) and neutrinos (f~0)

Finkbeiner et al. 2011, $m_0 \sim m_\varphi$

$$BF_{\mathrm{now}} \lesssim (250/f)(m_0/1\mathrm{GeV})$$

CMB constraints

Zavala et al. 2010

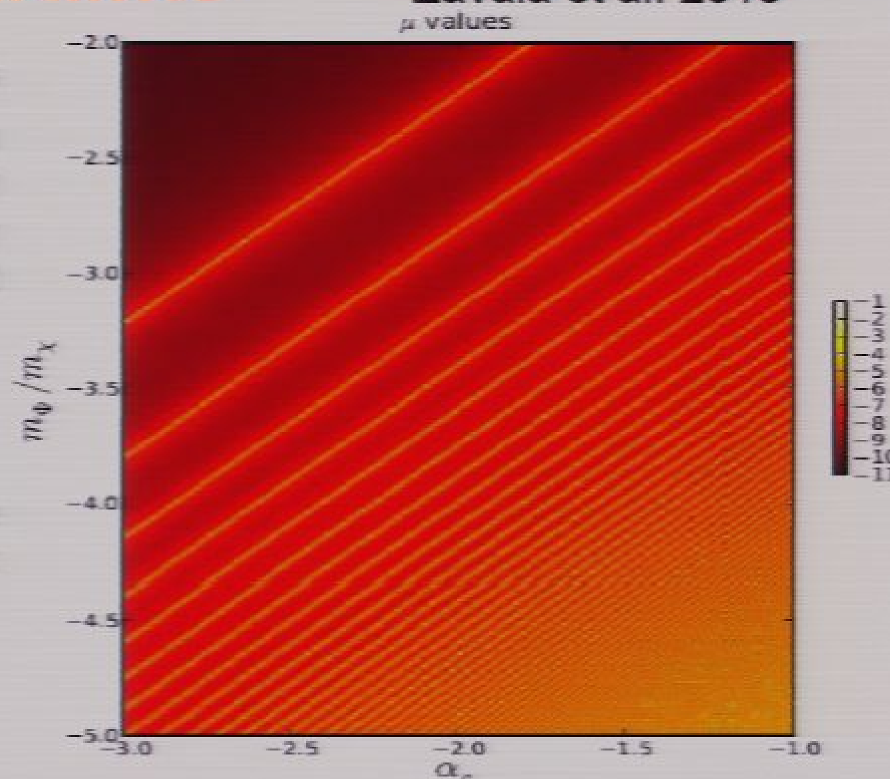

CMB energy spectrum: energy injection at $10^4<z<10^6$ effectively produces a Bose-Einstein energy spectrum with chemical potential μ instead of the pure black body spectrum (Illarionov and Sunyaev 1975). Limit by COBE/FIRAS $|\mu|<9\times10^{-5}$. "f" is the fraction that ionizes and heats the IGM.

$$\mu = 1.4\frac{\delta\rho_\gamma}{\rho_\gamma} = 1.4\int_{t_1}^{t_2}\frac{\dot\rho_\gamma}{\rho_\gamma}dt = 1.4\int_{t_1}^{t_2}\frac{f m_\chi\langle\sigma v\rangle n_\chi^2}{\rho_{\gamma,0}a^{-4}}dt.$$

Injection at $10^3<z<10^4$ produces a y-type distortion to the CMB (Hannestad and Tram 2011). Both are weak constraints.

Slatyer et al. 2009

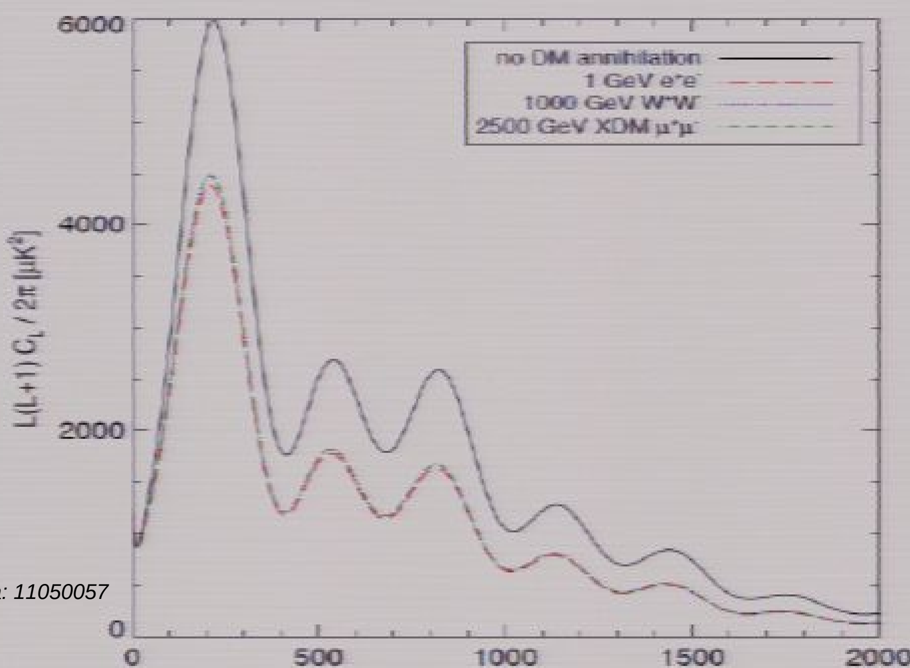

CMB power spectrum: e.g. Slatyer et al. 2009, limits based on WMAP5:

$$\frac{\lim_{v\to0}\langle\sigma v\rangle}{3\times10^{-26}\mathrm{cm}^3/\mathrm{s}} \lesssim \frac{120}{f}\left(\frac{m_\chi}{1\mathrm{TeV}}\right)$$

f~0.25 for annihilation into SM particles, except electrons (f~0.7) and neutrinos (f~0)

Finkbeiner et al. 2011, $m_0 \sim m_\varphi$

$$BF_{\mathrm{now}} \lesssim (250/f)(m_0/1\mathrm{GeV})$$

Cosmic background radiation from dark matter annihilation

- Energy of photons per unit area, time, solid angle and energy range received by an observer located at z=0.

$$I = \frac{1}{4\pi} \int \mathcal{E}(E_0(1+z), z) \frac{\mathrm{d}r}{(1+z)^4} e^{-\tau(E_0, z)}$$

- Contribution from all dark matter structures along the line of sight of the observer.

- In general, the volume emissivity of photons (energy of photons produced per unit volume, time and energy range) can be written as:

$$\mathcal{E} = \frac{f_{\mathrm{WIMP}}}{2} E \rho_\chi(\vec{x})^2$$

- Properties of dark matter as a particle (WIMP factor):

$$f_{\mathrm{WIMP}} = \frac{\mathrm{d}N}{\mathrm{d}E} \frac{\langle \sigma v \rangle_0}{m_\chi^2}$$

- The density squared dependence is connected to the gravitational interactions of dark matter (astrophysical factor).

Photon yield

- In situ photons: Directly created in the annihilation process (annihilation channels).

Fig. from Scott et al. 2009

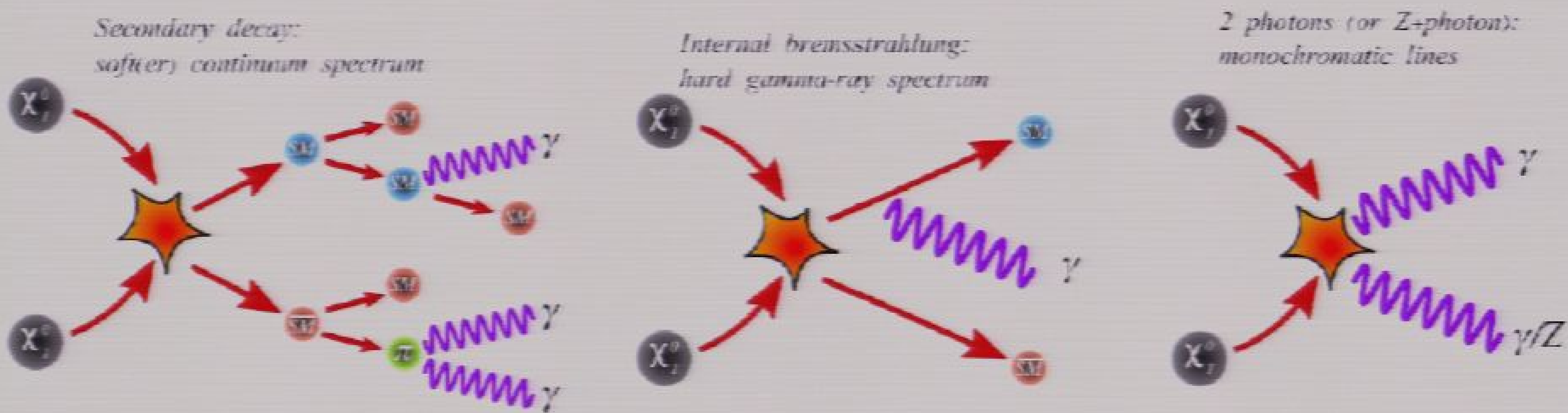

- Up-scattered photons: Background photons gain energy through Inverse Compton scattering with electrons and positrons produced in the annihilation: e+e- injection spectra → e+e- equilibrium solution → photon background → final IC photon spectrum.

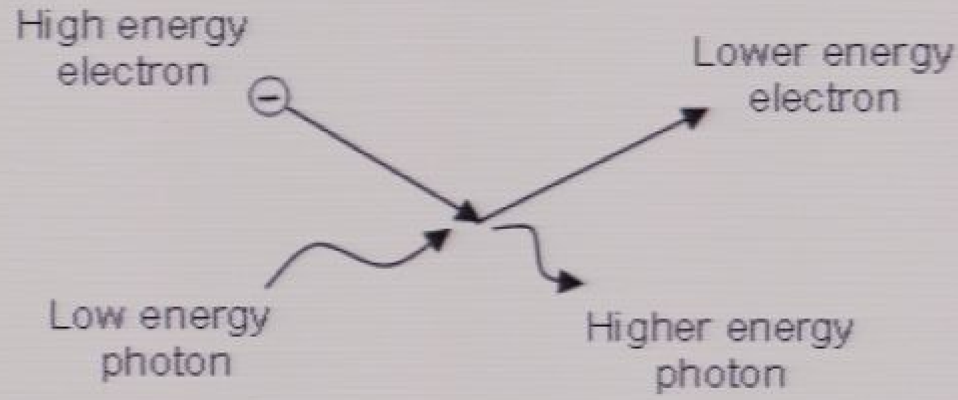

Photon spectrum

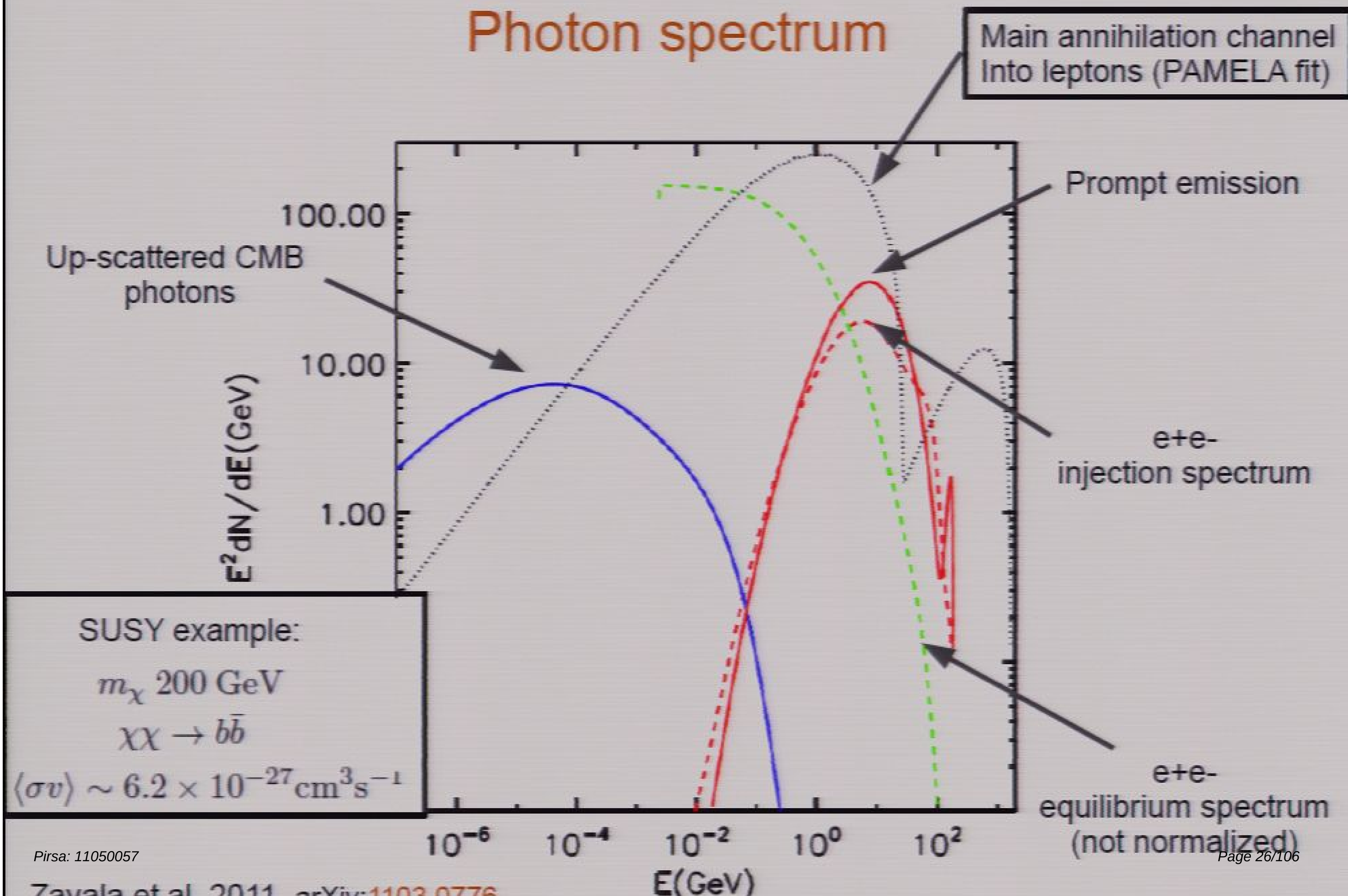

Zavala et al. 2011, arXiv:1103.0776

Simulating the past light cone

Millennium-II
(Boylan-Kolchin et al. 2009)

Same cosmology as Millennium I

100 Mpc/h box and ε=1kpc/h

$N_p=2160^3$, $m_{DM}=6.89\times10^5$Msun/h

Bound substructures found using SUBFIND (Springel et al. 2001):

11×10^6 subs at z=0

M_{sb} (min)~1.4×10^8Msun/h

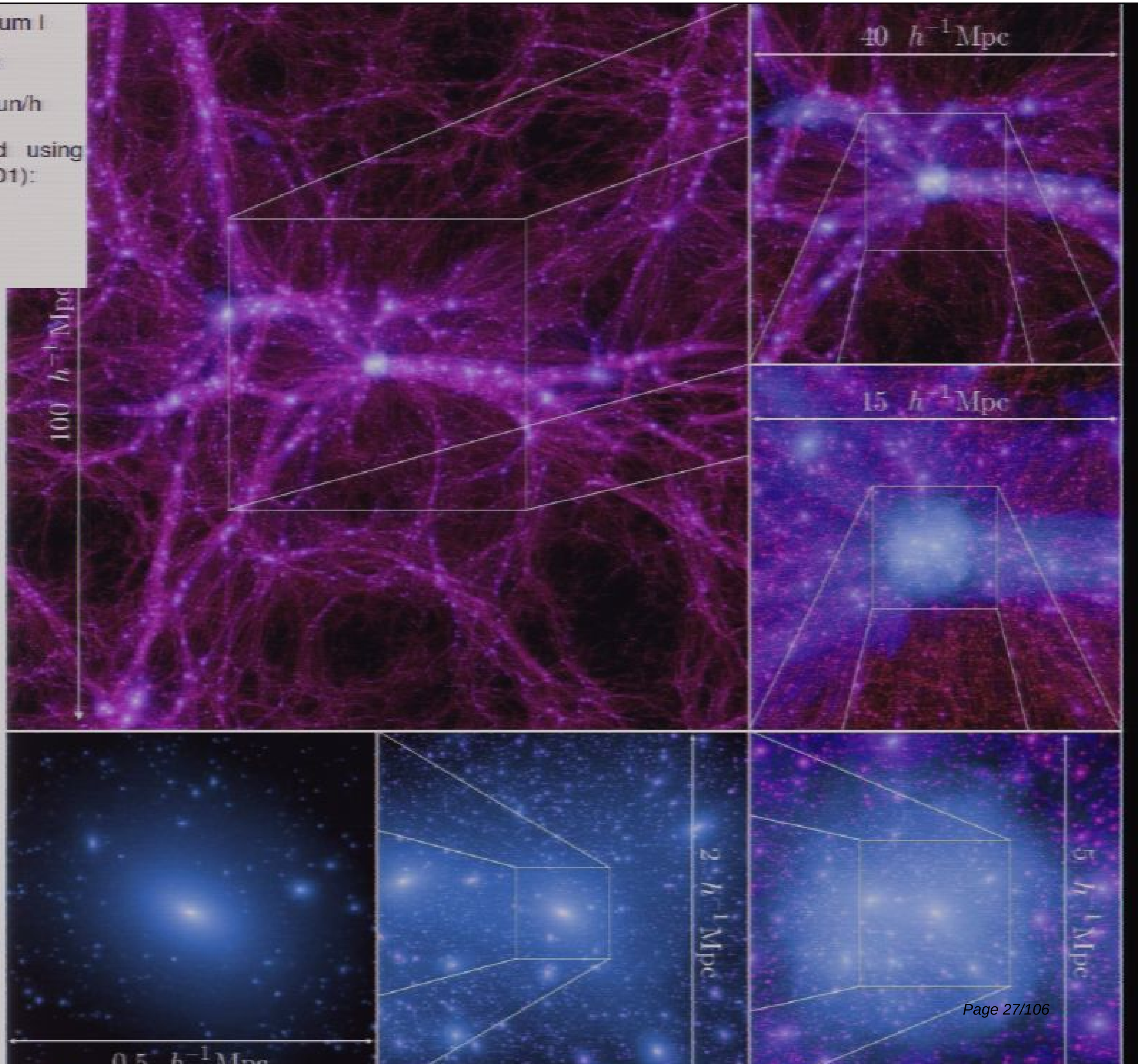

Astrophysical factor (DM halos)

- For a given region of volume V, the annihilation luminosity is proportional to:

$$L_\gamma \propto \int_V \rho_\chi^2(\vec{x})\, d^3x$$

- For a smooth DM halo (Springel et al. 2008): $L'_{\mathrm{h}} = \int \rho^2_{\mathrm{NFW}}(r)\,\mathrm{d}V = \frac{1.23\, V^4_{\mathrm{max}}}{G^2 r_{\mathrm{max}}}$
- Formula agrees with summation over particle densities in high resolution simulations:

Virgo Consortium's Aquarius Project (MW-like haloes), hi-res: m_{DM}~1500 Msun

Substructures within haloes have a significant role for external observers. Their contribution to the total luminosity is ~200 times the contribution of the smooth component for a MW-like halo.

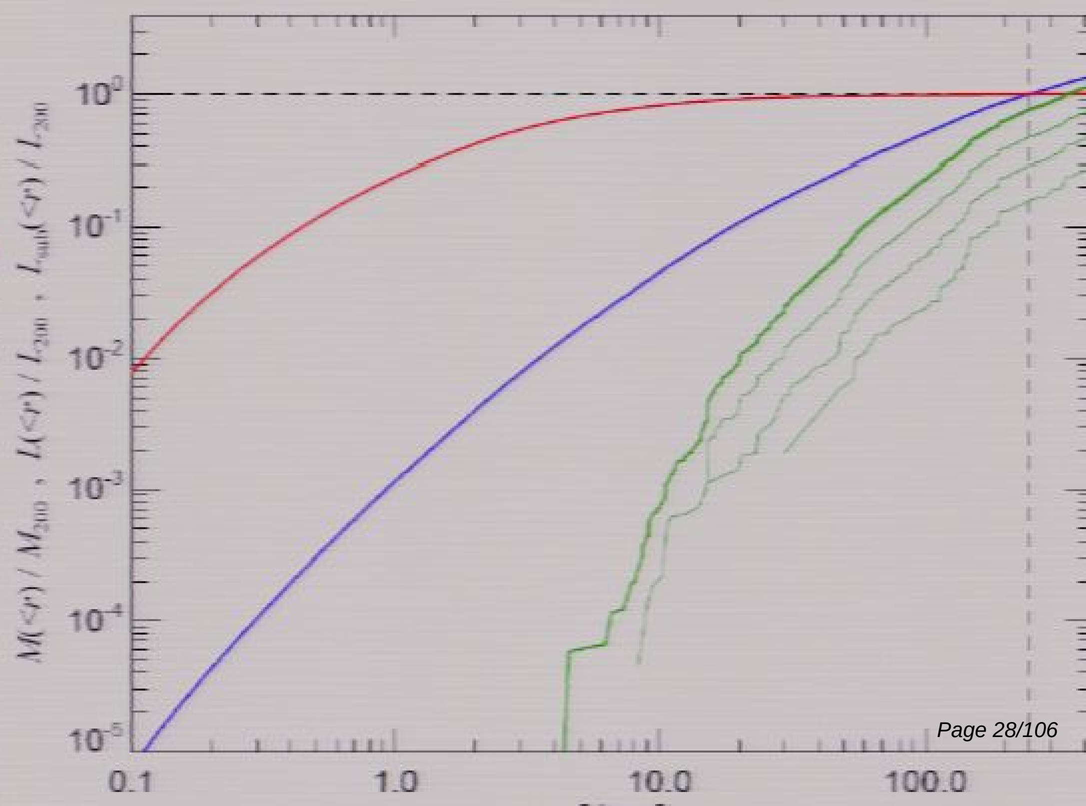

Astrophysical factor (DM halos)

- For a given region of volume V, the annihilation luminosity is proportional to:

$$L_\gamma \propto \int_V \rho_\chi^2(\vec{x})\, d^3x$$

- For a smooth DM halo (Springel et al. 2008): $L'_{\rm h} = \int \rho^2_{\rm NFW}(r)\,{\rm d}V = \frac{1.23\, V^4_{\rm max}}{G^2 r_{\rm max}}$
- Formula agrees with summation over particle densities in high resolution simulations:

Virgo Consortium's Aquarius Project (MW-like haloes), hi-res: m_{DM}~1500 Msun

Substructures within haloes have a significant role for external observers. Their contribution to the total luminosity is ~200 times the contribution of the smooth component for a MW-like halo.

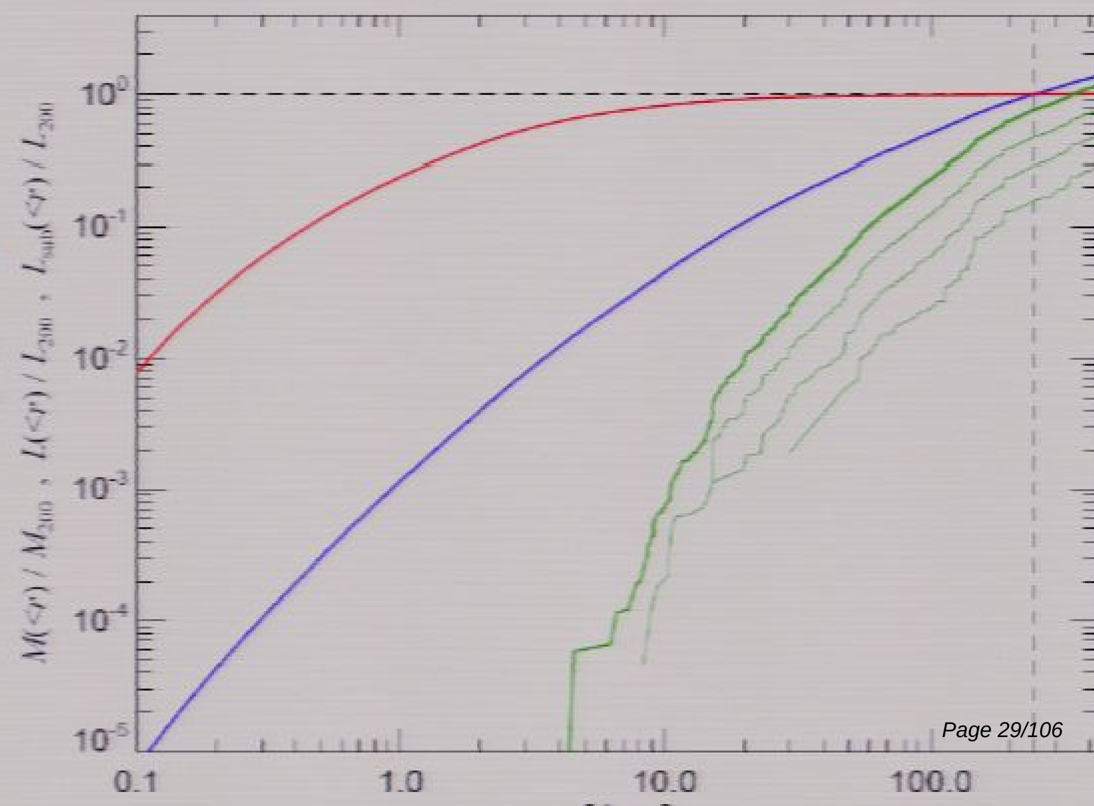

Astrophysical factor (DM halos)

- For a given region of volume V, the annihilation luminosity is proportional to:

$$L_\gamma \propto \int_V \rho_\chi^2(\vec{x}) d^3x$$

- For a smooth DM halo (Springel et al. 2008): $L'_{\rm h} = \int \rho^2_{\rm NFW}(r)\,{\rm d}V = \frac{1.23\,V^4_{\rm max}}{G^2 r_{\rm max}}$
- Formula agrees with summation over particle densities in high resolution simulations:

Virgo Consortium's Aquarius Project (MW-like haloes), hi-res: m_{DM}~1500 Msun

Substructures within haloes have a significant role for external observers. Their contribution to the total luminosity is ~200 times the contribution of the smooth component for a MW-like halo.

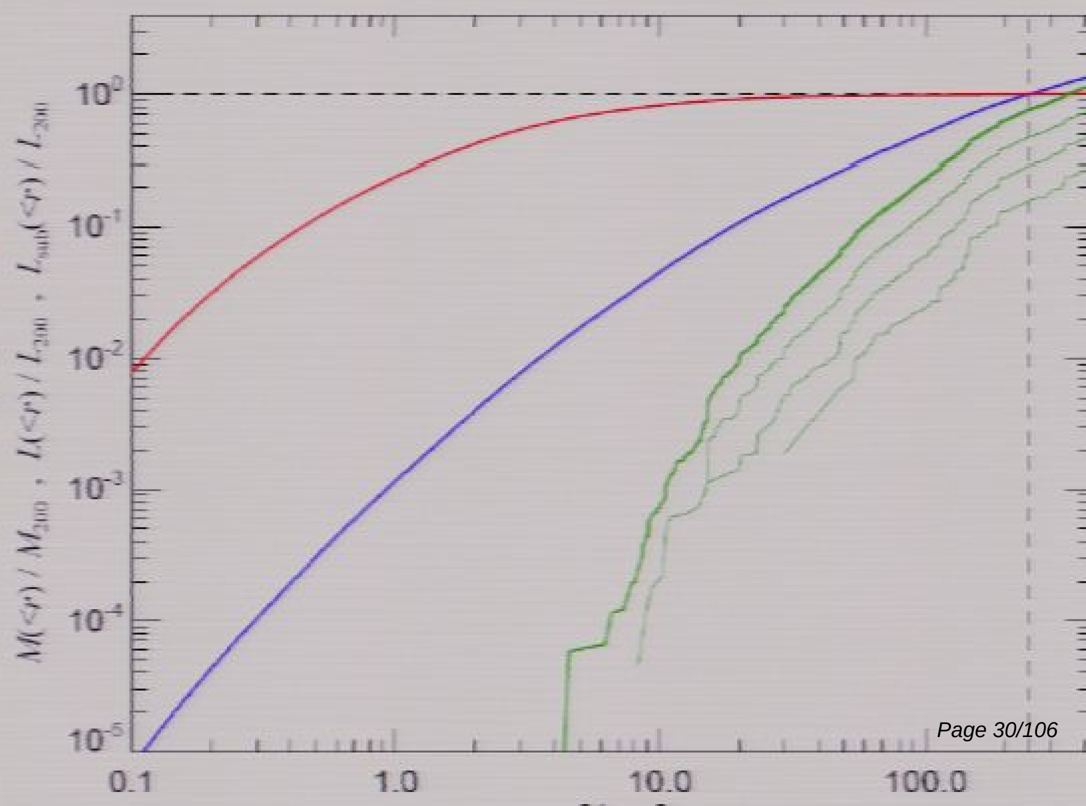

Simulating the past light cone

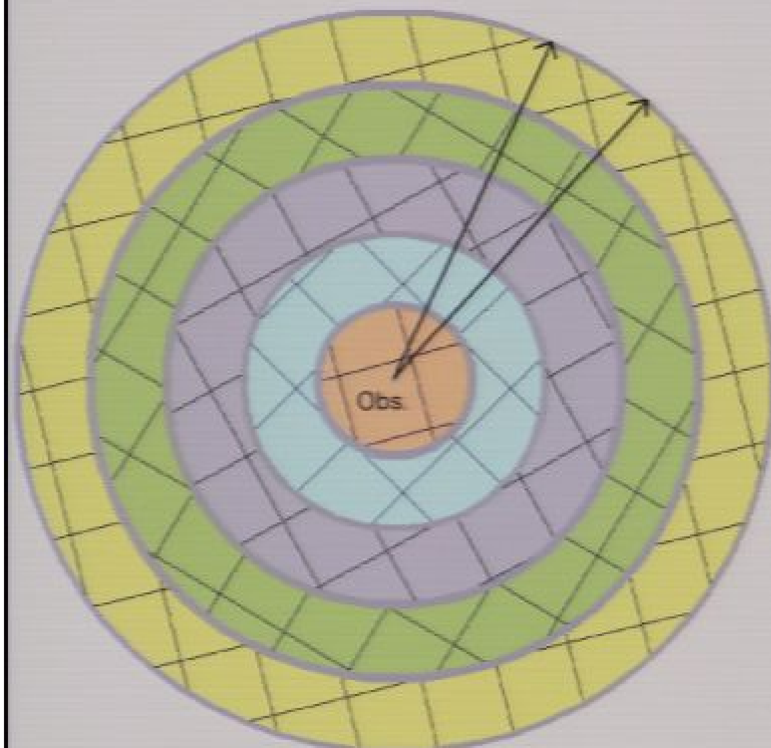

Value per pixel:

$$I_{\gamma,0}(\Delta\Omega_{\mathrm{pix}}) = \frac{1}{8\pi} \sum_{h \epsilon \Delta\Omega_{pix}} L_h w(d_h, r_h) E_{\gamma,0} f_{\mathrm{SUSY}}(z_h)|_{E_{\gamma,0}}$$

Local structures (First shell, 30 Mpc)

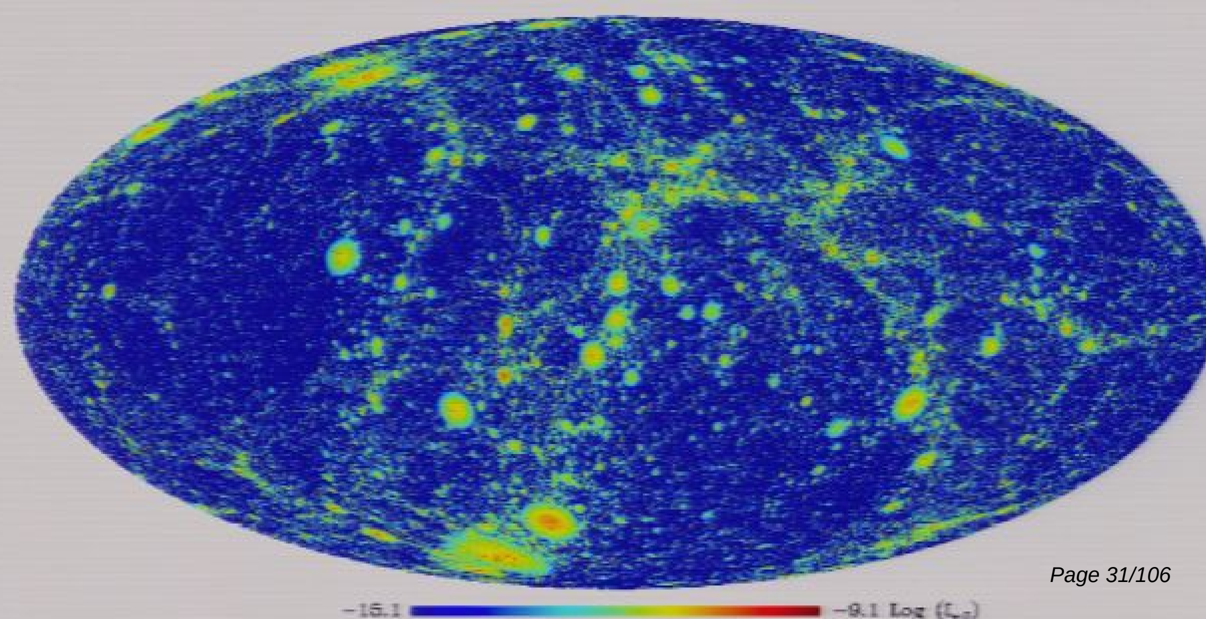

All-sky maps
(resolved structures up to z~10, E=10GeV)

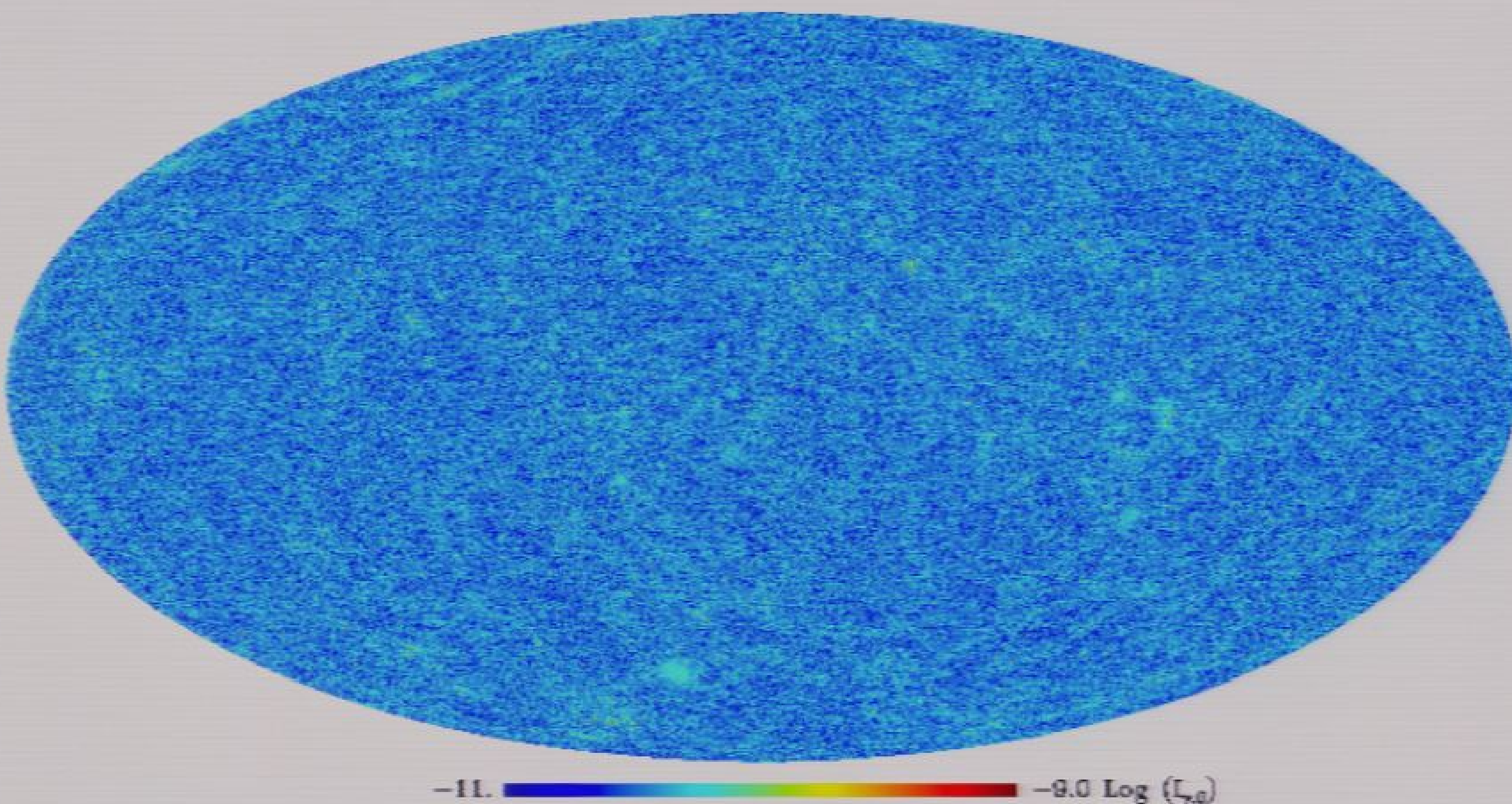

N_{pix}=12(512)^2~3x10^6 ang. res. ~ 0.115°

Extrapolation for unresolved halos down to earth masses (~2 orders of magnitude uncertainty)

Isotropic component

$m_\chi \sim 200\,GeV, \chi\chi \to b\bar{b}$ and $\langle \sigma v \rangle \sim 6.2 \times 10^{-27} \mathrm{cm}^3 \mathrm{s}^{-1}$

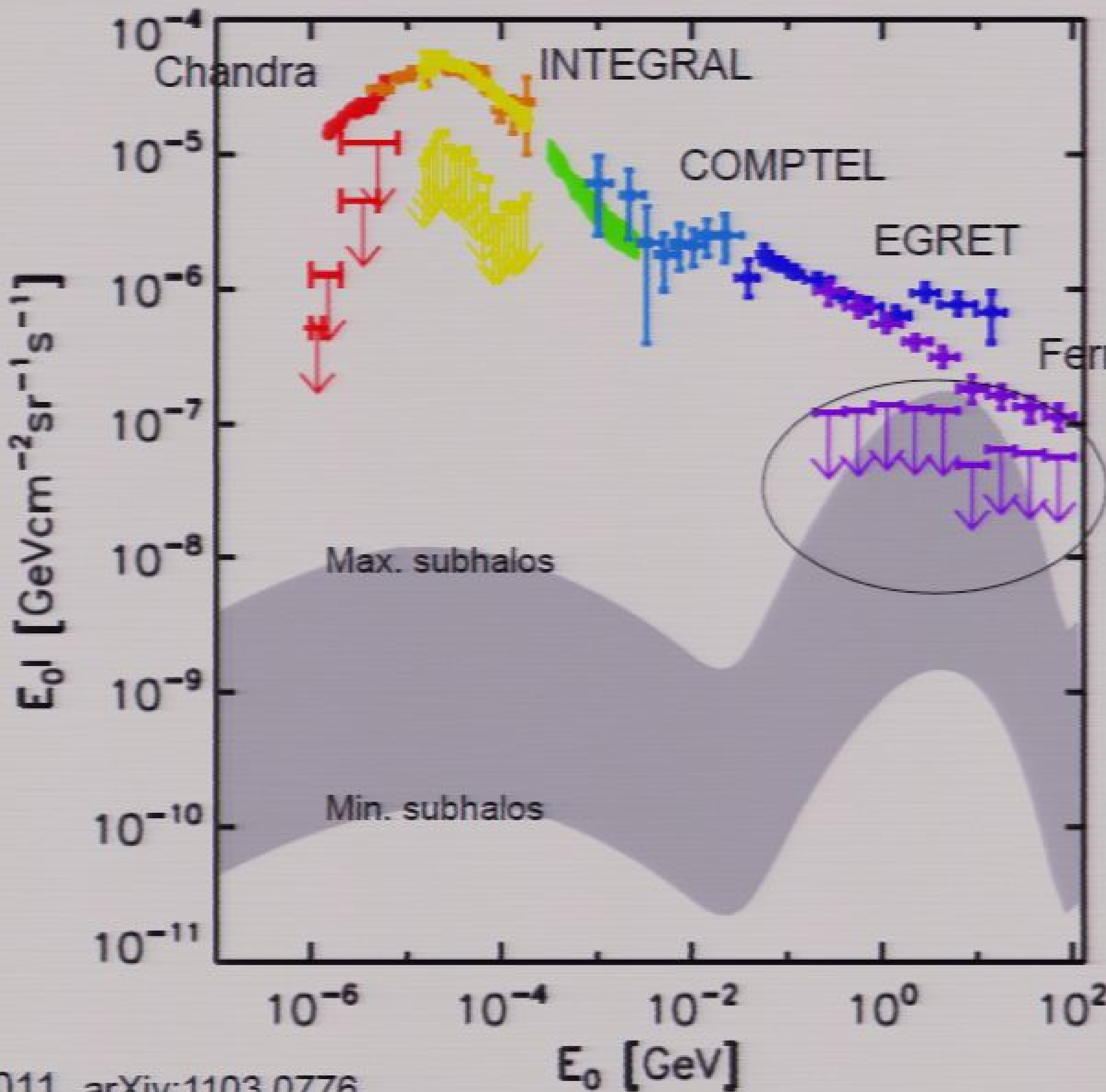

Star forming galaxies (53%) and blazars (16%)

Zavala et al. 2011, arXiv:1103.0776

Isotropic component (annihilation channel)

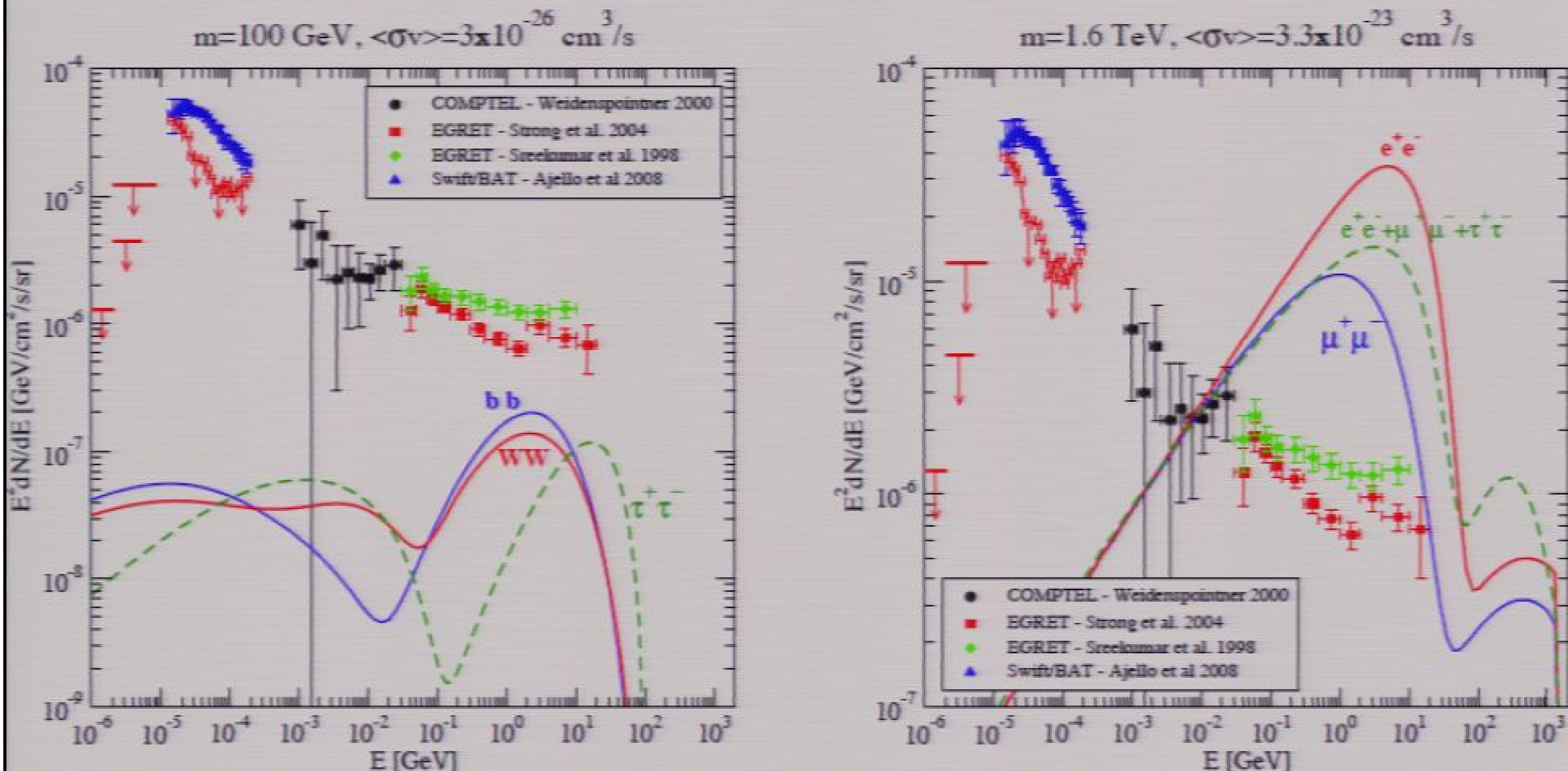

Profumo and Jeltema 2010

Isotropic component

$$m_\chi \sim 200\,GeV, \chi\chi \to b\bar{b} \text{ and } \langle\sigma v\rangle \sim 6.2 \times 10^{-27}\text{cm}^3\text{s}^{-1}$$

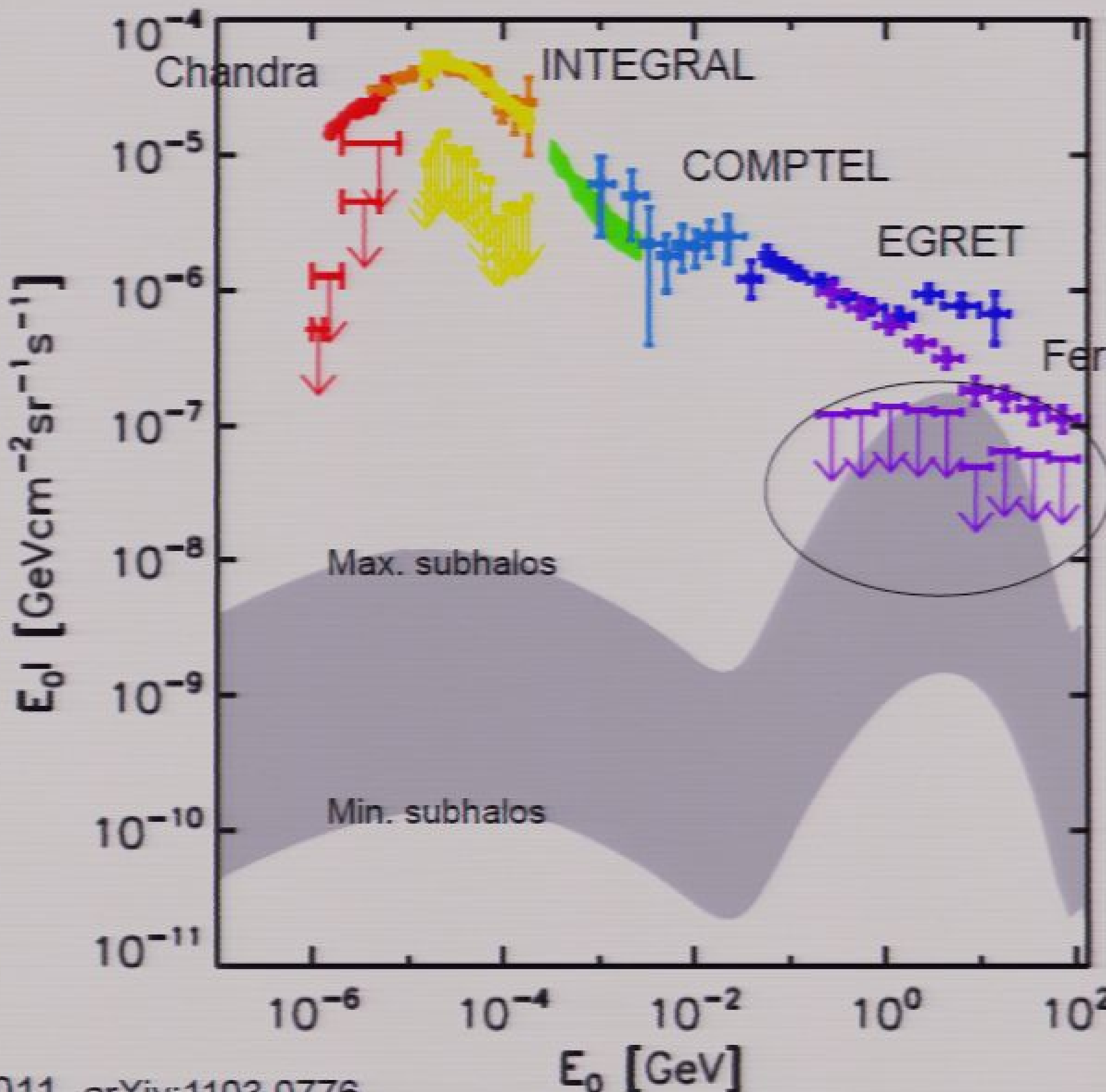

Star forming galaxies (53%) and blazars (16%)

Zavala et al. 2011, arXiv:1103.0776

Isotropic component (annihilation channel)

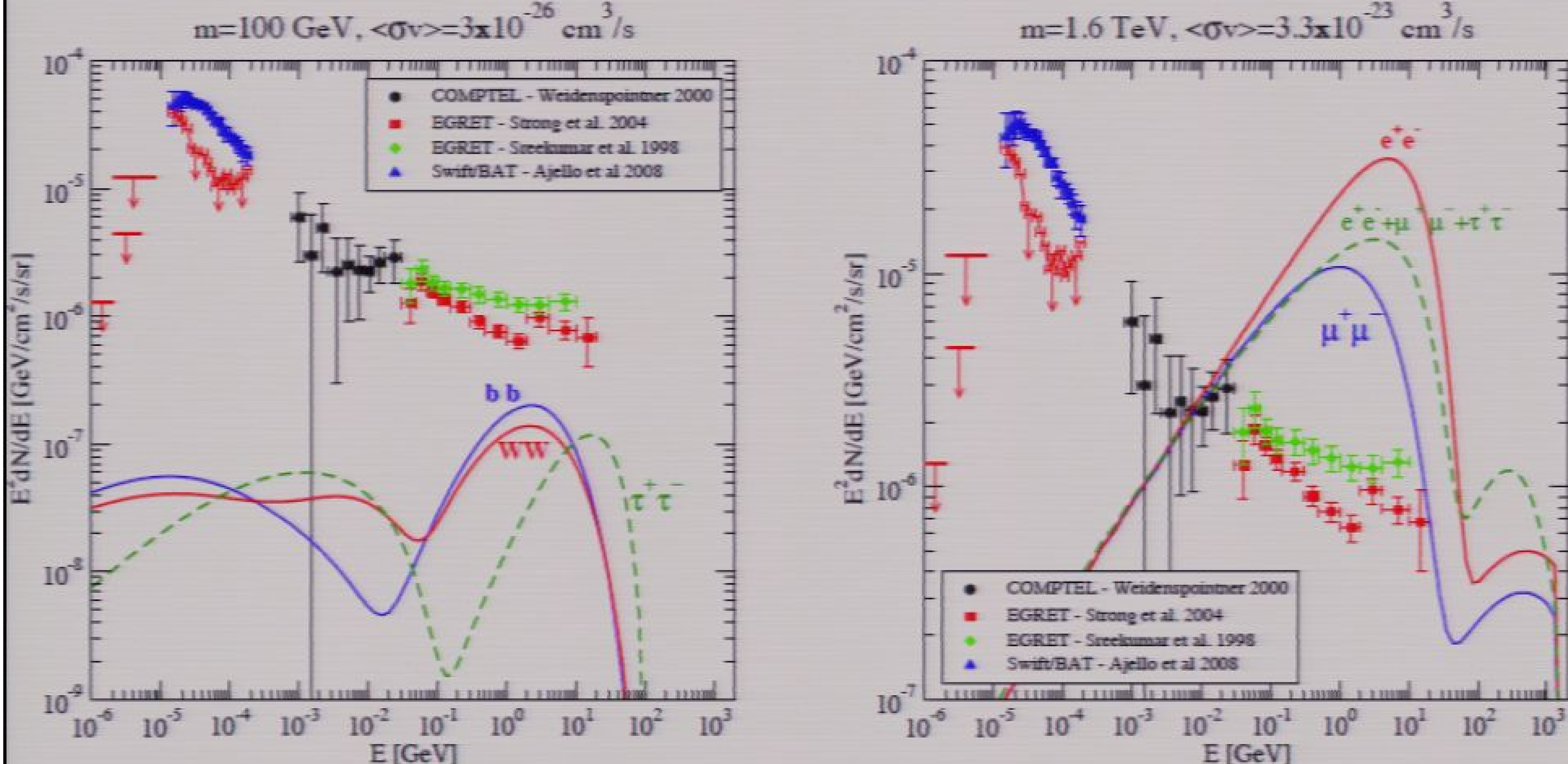

Profumo and Jeltema 2010

Constraints on particle physics models

"factoring out" the astrophysical part of the signal

$$I(E_0) = \frac{c}{8\pi} E_0 f_{\mathrm{WIMP}}(E_0(1+z^*)) \int \frac{\rho_\chi^2(\vec{x}, z)}{(1+z)^3} \frac{e^{-\tau(E_0,z)}}{H(z)} \mathrm{d}z$$

$z^* < 4$ for X-rays
$z^* < 1$ for E>10GeV

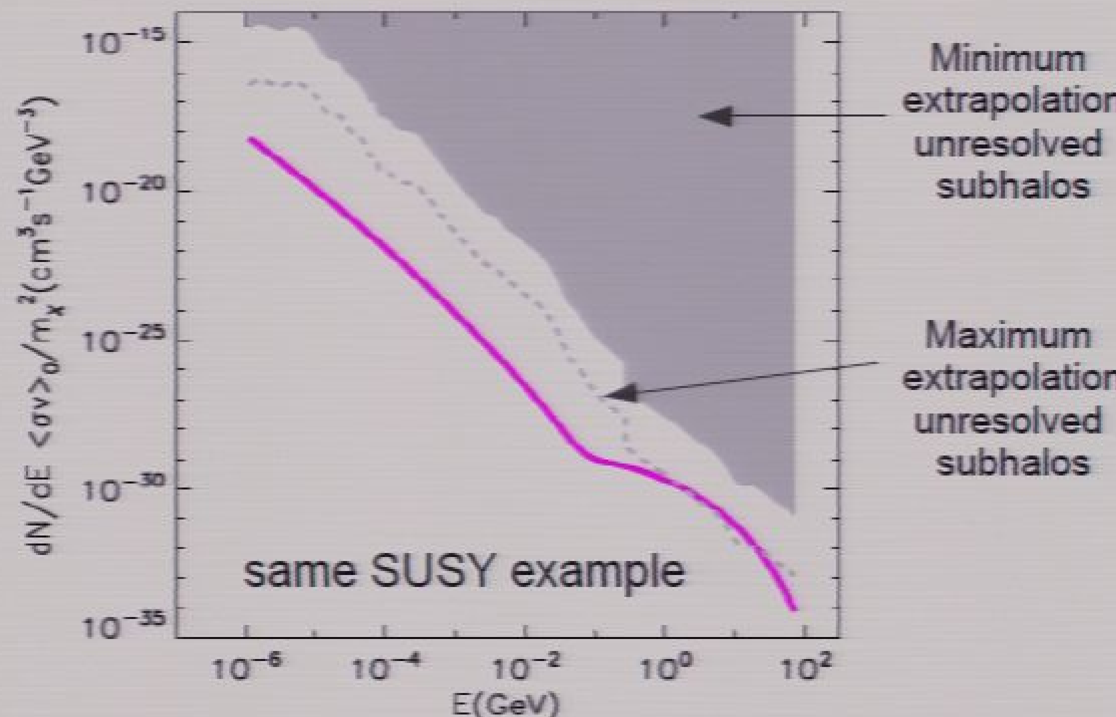

Photon yield spectrum from particle physics model

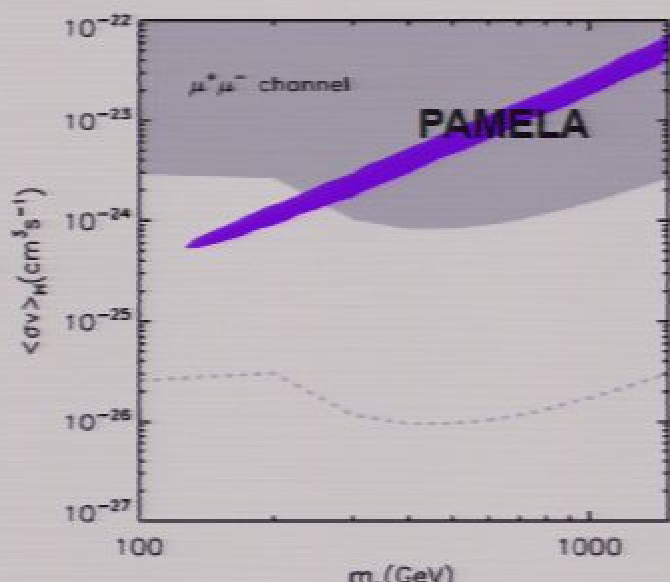

Isotropic component (annihilation channel)

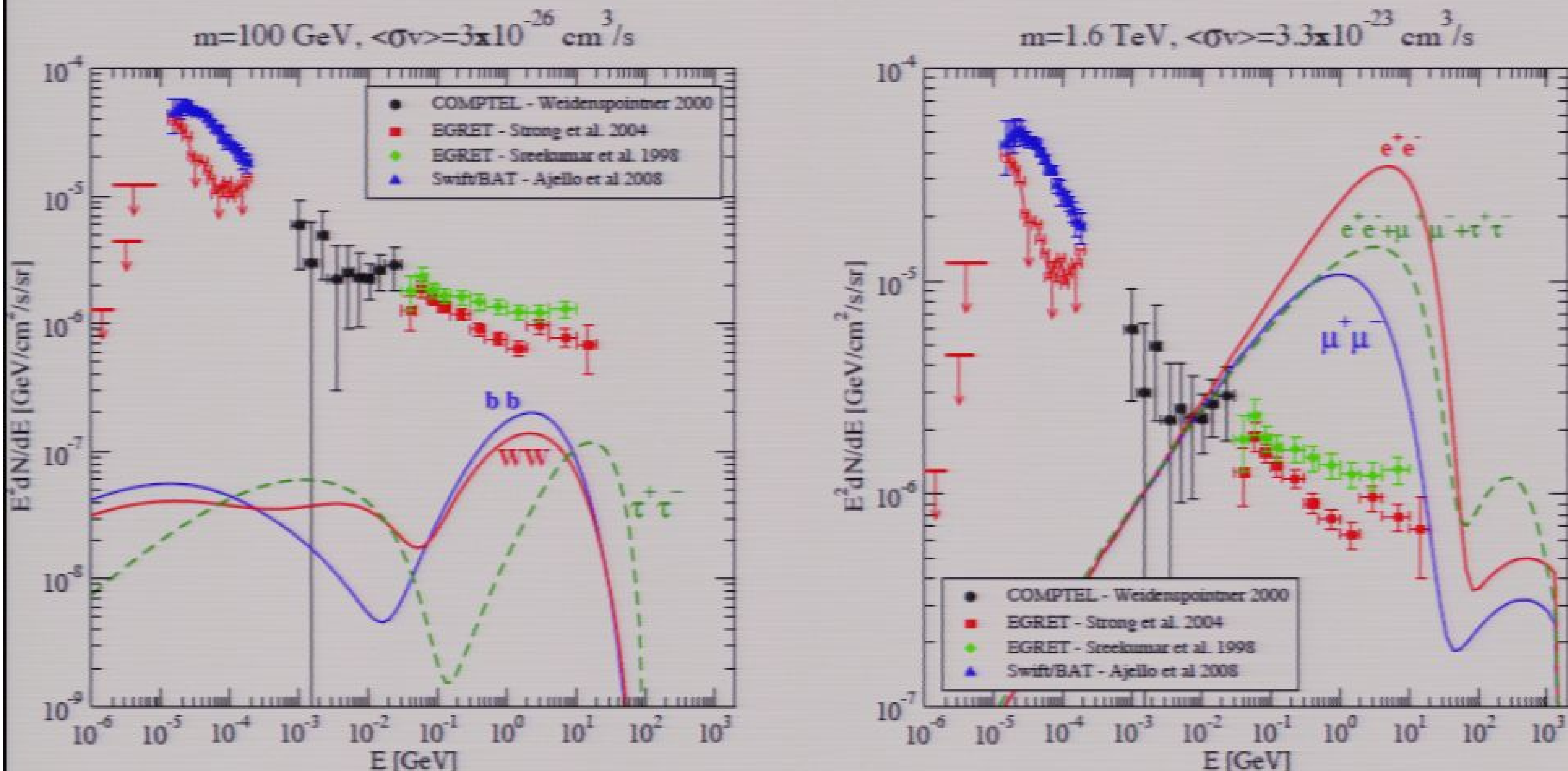

Profumo and Jeltema 2010

Constraints on particle physics models

"factoring out" the astrophysical part of the signal

$$I(E_0) = \frac{c}{8\pi} E_0 f_{\rm WIMP}(E_0(1+z^*)) \int \frac{\rho_\chi^2(\vec{x},z)}{(1+z)^3} \frac{e^{-\tau(E_0,z)}}{H(z)} \mathrm{d}z$$

$z^* < 4$ for X-rays
$z^* < 1$ for E>10GeV

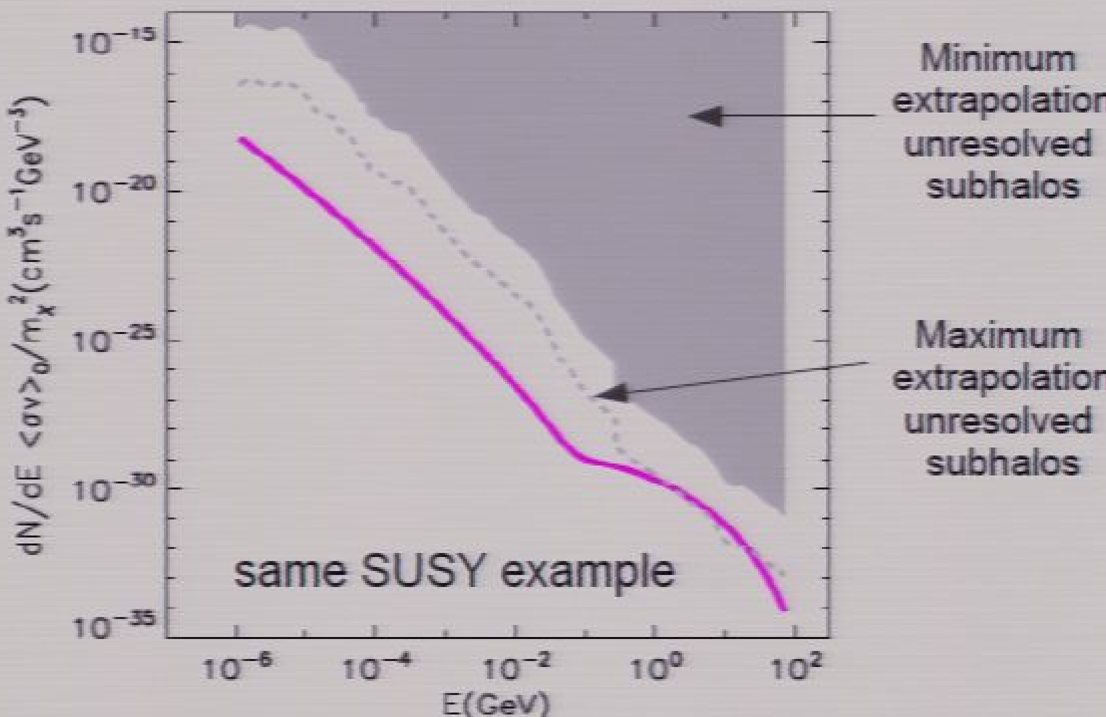

Photon yield spectrum from particle physics model

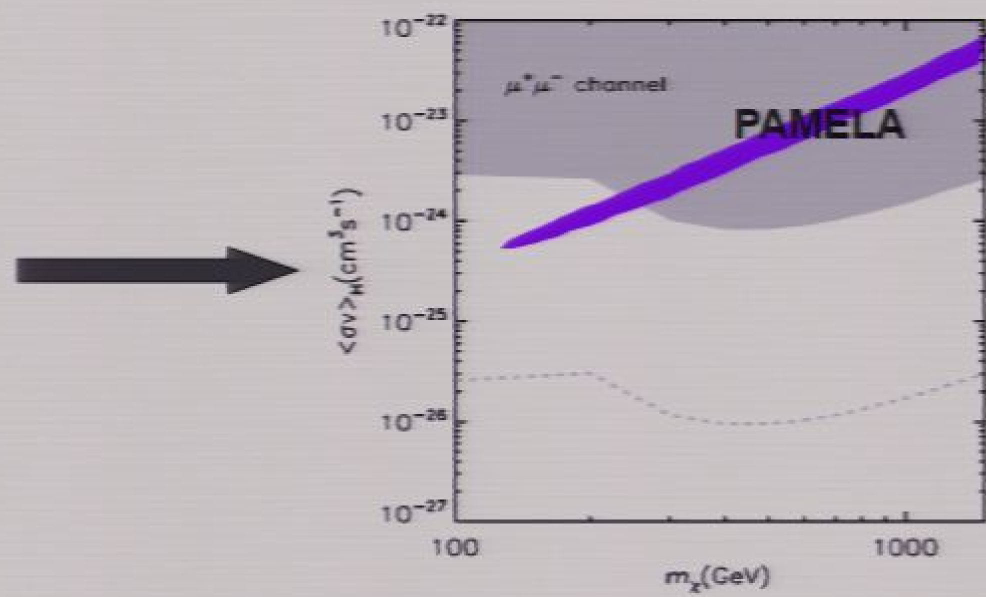

Sommerfeld-enhanced models fitting the cosmic ray excesses (Finkbeiner et al. 2011)

Benchmark no.	Annihilation Channel	m_ϕ (MeV)	m_χ (TeV)	α_c	δ (MeV)	$\frac{S_{max}\langle\sigma v\rangle_0}{3\times10^{-26}\mathrm{cm}^3\,\mathrm{s}^{-1}}$
1	1:1:2 $e^\pm : \mu^\pm : \pi^\pm$	900	1.68	0.04067	0.15	530
2	1:1:2 $e^\pm : \mu^\pm : \pi^\pm$	900	1.52	0.03725	1.34	360
3	1:1:1 $e^\pm : \mu^\pm : \pi^\pm$	580	1.55	0.03523	1.49	437
4	1:1:1 $e^\pm : \mu^\pm : \pi^\pm$	580	1.20	0.03054	1.00	374
5	1:1 $e^\pm : \mu^\pm$	350	1.33	0.02643	1.10	339
6	$e^\pm$ only	200	1.00	0.01622	0.70	171

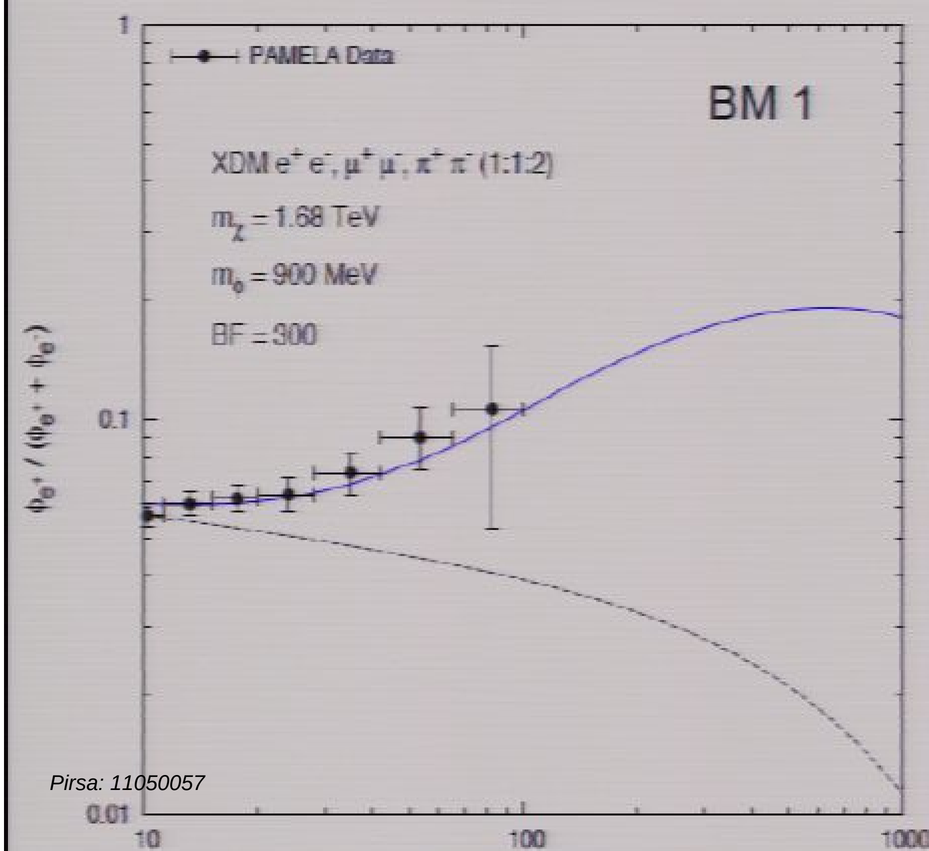

- New force carrier in the "dark sector"
- Annihilation cross section enhanced by a Sommerfeld mechanism:

$$\langle\sigma v\rangle = \langle\sigma v\rangle_0 S(\sigma_{\mathrm{vel}})$$

- Correct relic density
- Fit to the cosmic ray excesses measured by PAMELA and Fermi
- Allowed by bounds on Smax from the CMB
- IC contribution dominates the photon yield

Sommerfeld-enhanced models fitting the cosmic ray excesses (Finkbeiner et al. 2011)

Benchmark no.	Annihilation Channel	m_ϕ (MeV)	m_χ (TeV)	α_c	δ (MeV)	$\frac{S_{\max}\langle\sigma v\rangle_0}{3\times10^{-26}\,\mathrm{cm}^3\,\mathrm{s}^{-1}}$
1	1:1:2 $e^\pm : \mu^\pm : \pi^\pm$	900	1.68	0.04067	0.15	530
2	1:1:2 $e^\pm : \mu^\pm : \pi^\pm$	900	1.52	0.03725	1.34	360
3	1:1:1 $e^\pm : \mu^\pm : \pi^\pm$	580	1.55	0.03523	1.49	437
4	1:1:1 $e^\pm : \mu^\pm : \pi^\pm$	580	1.20	0.03054	1.00	374
5	1:1 $e^\pm : \mu^\pm$	350	1.33	0.02643	1.10	339
6	$e^\pm$ only	200	1.00	0.01622	0.70	171

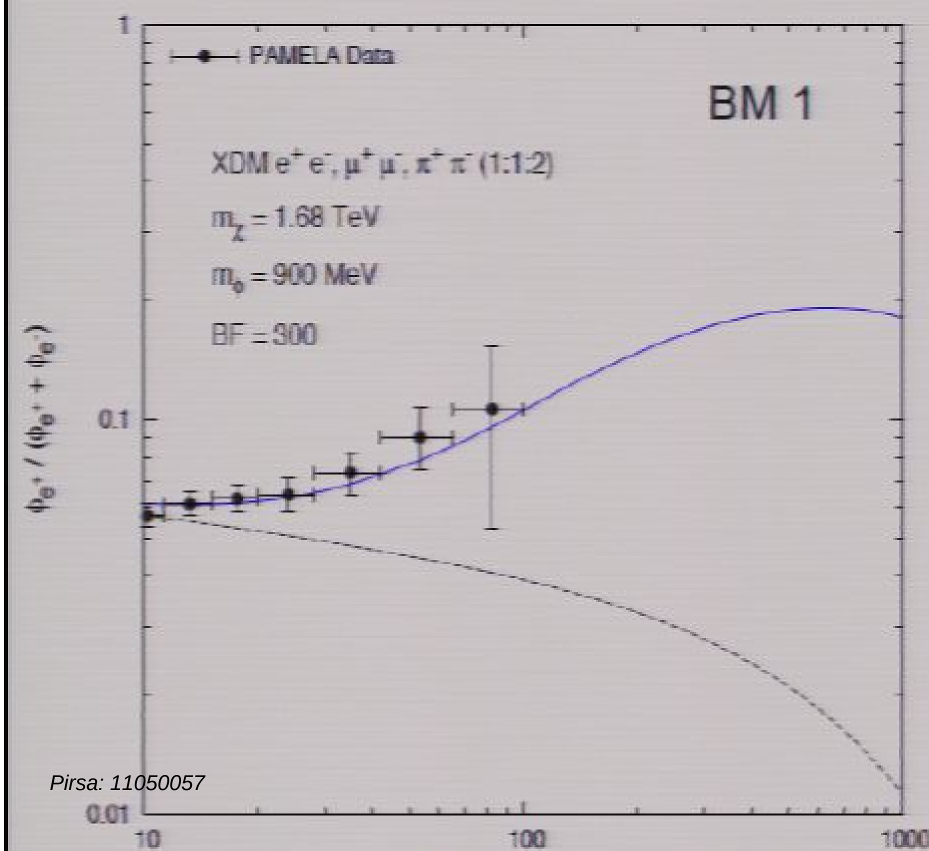

- New force carrier in the "dark sector"
- Annihilation cross section enhanced by a Sommerfeld mechanism:

$$\langle\sigma v\rangle = \langle\sigma v\rangle_0 S(\sigma_{\mathrm{vel}})$$

- Correct relic density
- Fit to the cosmic ray excesses measured by PAMELA and Fermi
- Allowed by bounds on Smax from the CMB
- IC contribution dominates the photon yield

Sommerfeld-enhanced models fitting the cosmic ray excesses (Finkbeiner et al. 2011)

Benchmark no.	Annihilation Channel	m_ϕ (MeV)	m_χ (TeV)	α_c	δ (MeV)	$\frac{S_{max}\langle\sigma v\rangle_0}{3\times10^{-26}\mathrm{cm}^3\,\mathrm{s}^{-1}}$
1	1:1:2 $e^\pm : \mu^\pm : \pi^\pm$	900	1.68	0.04067	0.15	530
2	1:1:2 $e^\pm : \mu^\pm : \pi^\pm$	900	1.52	0.03725	1.34	360
3	1:1:1 $e^\pm : \mu^\pm : \pi^\pm$	580	1.55	0.03523	1.49	437
4	1:1:1 $e^\pm : \mu^\pm : \pi^\pm$	580	1.20	0.03054	1.00	374
5	1:1 $e^\pm : \mu^\pm$	350	1.33	0.02643	1.10	339
6	$e^\pm$ only	200	1.00	0.01622	0.70	171

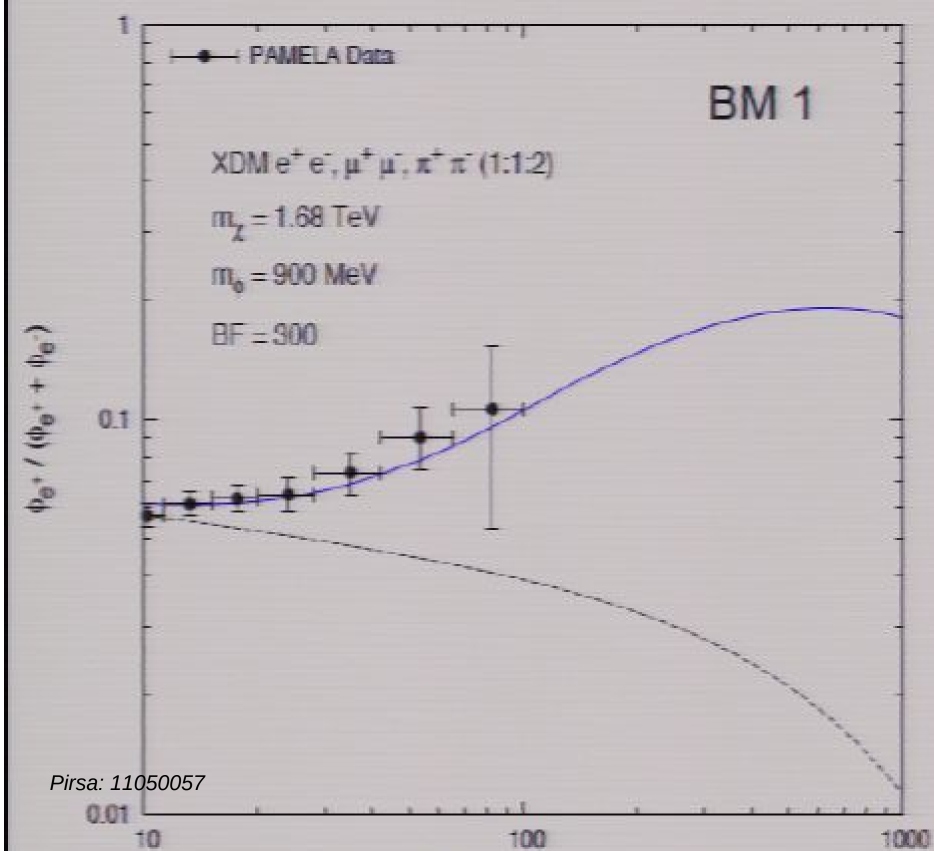

- New force carrier in the "dark sector"
- Annihilation cross section enhanced by a Sommerfeld mechanism:

$$\langle\sigma v\rangle = \langle\sigma v\rangle_0 S(\sigma_{\rm vel})$$

- Correct relic density
- Fit to the cosmic ray excesses measured by PAMELA and Fermi
- Allowed by bounds on Smax from the CMB
- IC contribution dominates the photon yield

Sommerfeld-enhanced models fitting the cosmic ray excesses (Finkbeiner et al. 2011)

Benchmark no.	Annihilation Channel	m_ϕ (MeV)	m_χ (TeV)	α_c	δ (MeV)	$\frac{S_{max}\langle\sigma v\rangle_0}{3\times10^{-26}\mathrm{cm}^3\,\mathrm{s}^{-1}}$
1	1:1:2 $e^\pm : \mu^\pm : \pi^\pm$	900	1.68	0.04067	0.15	530
2	1:1:2 $e^\pm : \mu^\pm : \pi^\pm$	900	1.52	0.03725	1.34	360
3	1:1:1 $e^\pm : \mu^\pm : \pi^\pm$	580	1.55	0.03523	1.49	437
4	1:1:1 $e^\pm : \mu^\pm : \pi^\pm$	580	1.20	0.03054	1.00	374
5	1:1 $e^\pm : \mu^\pm$	350	1.33	0.02643	1.10	339
6	$e^\pm$ only	200	1.00	0.01622	0.70	171

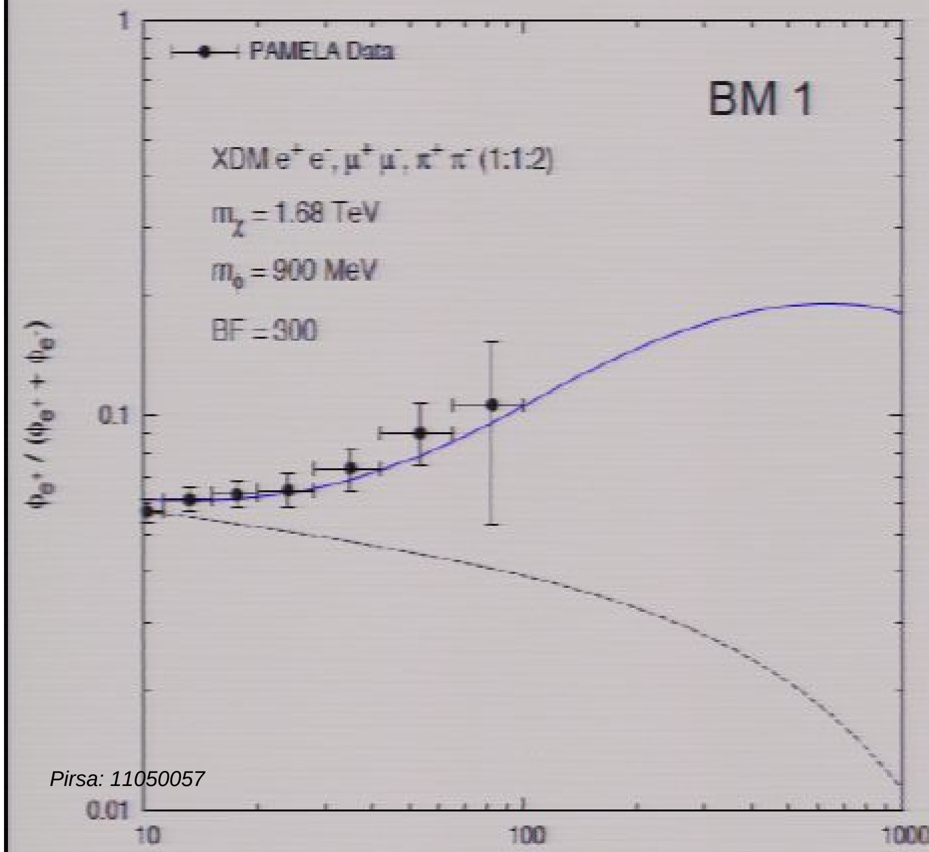

- New force carrier in the "dark sector"
- Annihilation cross section enhanced by a Sommerfeld mechanism:

$$\langle \sigma v\rangle = \langle \sigma v\rangle_0 S(\sigma_{\rm vel})$$

- Correct relic density
- Fit to the cosmic ray excesses measured by PAMELA and Fermi
- Allowed by bounds on Smax from the CMB
- IC contribution dominates the photon yield

Sommerfeld-enhanced models fitting the cosmic ray excesses (Finkbeiner et al. 2011)

Benchmark no.	Annihilation Channel	m_ϕ (MeV)	m_χ (TeV)	α_c	δ (MeV)	$\frac{S_{max}\langle\sigma v\rangle_0}{3\times10^{-26}\text{cm}^3\text{ s}^{-1}}$
1	1:1:2 $e^\pm : \mu^\pm : \pi^\pm$	900	1.68	0.04067	0.15	530
2	1:1:2 $e^\pm : \mu^\pm : \pi^\pm$	900	1.52	0.03725	1.34	360
3	1:1:1 $e^\pm : \mu^\pm : \pi^\pm$	580	1.55	0.03523	1.49	437
4	1:1:1 $e^\pm : \mu^\pm : \pi^\pm$	580	1.20	0.03054	1.00	374
5	1:1 $e^\pm : \mu^\pm$	350	1.33	0.02643	1.10	339
6	$e^\pm$ only	200	1.00	0.01622	0.70	171

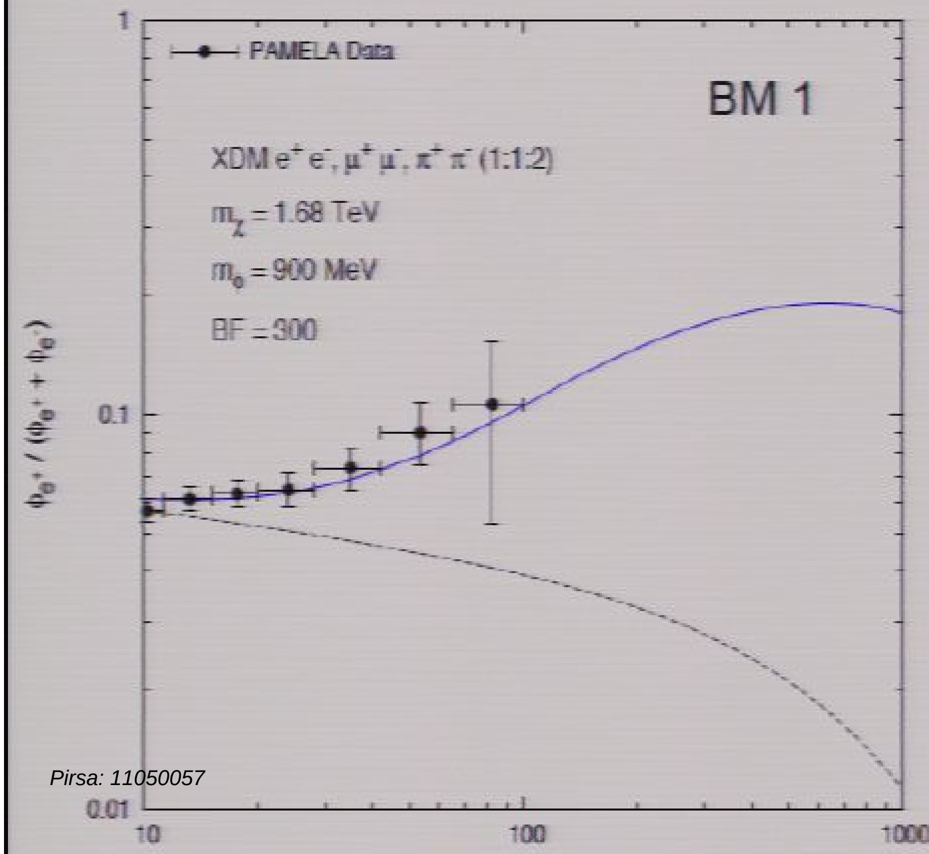

- New force carrier in the "dark sector"
- Annihilation cross section enhanced by a Sommerfeld mechanism:

$$\langle\sigma v\rangle = \langle\sigma v\rangle_0 S(\sigma_{\rm vel})$$

- Correct relic density
- Fit to the cosmic ray excesses measured by PAMELA and Fermi
- Allowed by bounds on Smax from the CMB
- IC contribution dominates the photon yield

Sommerfeld-enhanced models fitting the cosmic ray excesses (Finkbeiner et al. 2011)

Benchmark no.	Annihilation Channel	m_ϕ (MeV)	m_χ (TeV)	α_c	δ (MeV)	$\frac{S_{max}\langle\sigma v\rangle_0}{3\times10^{-26}\mathrm{cm}^3\,\mathrm{s}^{-1}}$
1	1:1:2 $e^\pm : \mu^\pm : \pi^\pm$	900	1.68	0.04067	0.15	530
2	1:1:2 $e^\pm : \mu^\pm : \pi^\pm$	900	1.52	0.03725	1.34	360
3	1:1:1 $e^\pm : \mu^\pm : \pi^\pm$	580	1.55	0.03523	1.49	437
4	1:1:1 $e^\pm : \mu^\pm : \pi^\pm$	580	1.20	0.03054	1.00	374
5	1:1 $e^\pm : \mu^\pm$	350	1.33	0.02643	1.10	339
6	$e^\pm$ only	200	1.00	0.01622	0.70	171

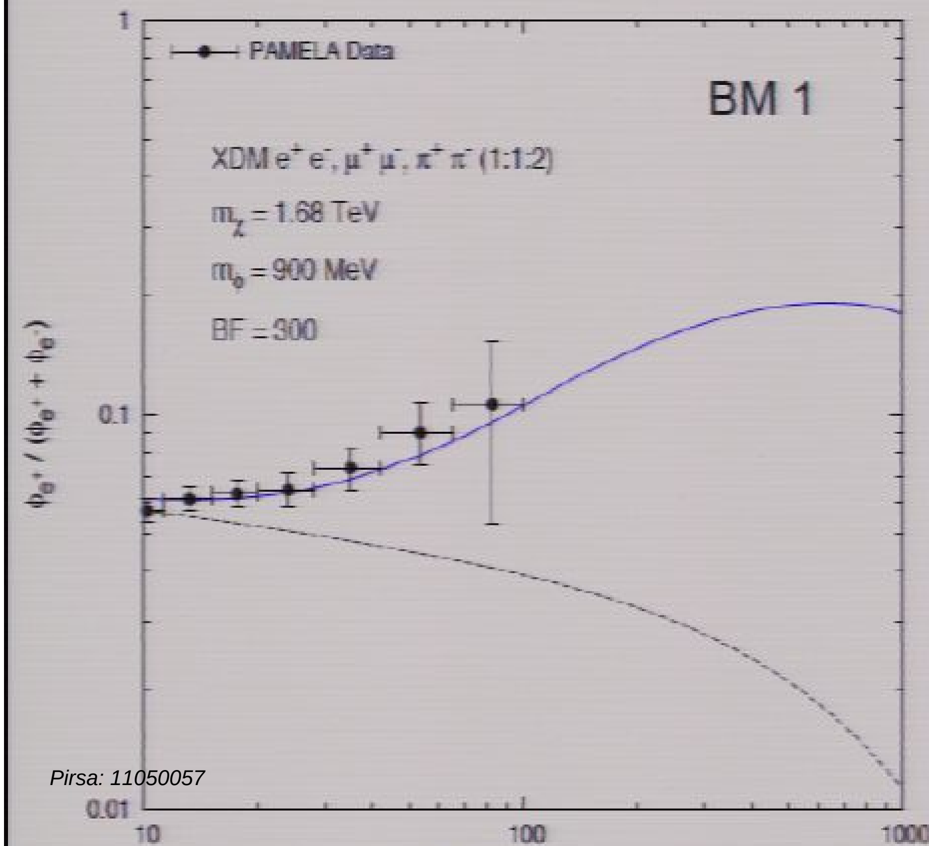

- New force carrier in the "dark sector"
- Annihilation cross section enhanced by a Sommerfeld mechanism:

$$\langle\sigma v\rangle = \langle\sigma v\rangle_0 S(\sigma_{\rm vel})$$

- Correct relic density
- Fit to the cosmic ray excesses measured by PAMELA and Fermi
- Allowed by bounds on Smax from the CMB
- IC contribution dominates the photon yield

Sommerfeld-enhanced models fitting the cosmic ray excesses (Finkbeiner et al. 2011)

Benchmark no.	Annihilation Channel	m_ϕ (MeV)	m_χ (TeV)	α_c	δ (MeV)	$\frac{S_{\max}\langle\sigma v\rangle_0}{3\times10^{-26}\mathrm{cm}^3\,\mathrm{s}^{-1}}$
1	1:1:2 $e^\pm : \mu^\pm : \pi^\pm$	900	1.68	0.04067	0.15	530
2	1:1:2 $e^\pm : \mu^\pm : \pi^\pm$	900	1.52	0.03725	1.34	360
3	1:1:1 $e^\pm : \mu^\pm : \pi^\pm$	580	1.55	0.03523	1.49	437
4	1:1:1 $e^\pm : \mu^\pm : \pi^\pm$	580	1.20	0.03054	1.00	374
5	1:1 $e^\pm : \mu^\pm$	350	1.33	0.02643	1.10	339
6	$e^\pm$ only	200	1.00	0.01622	0.70	171

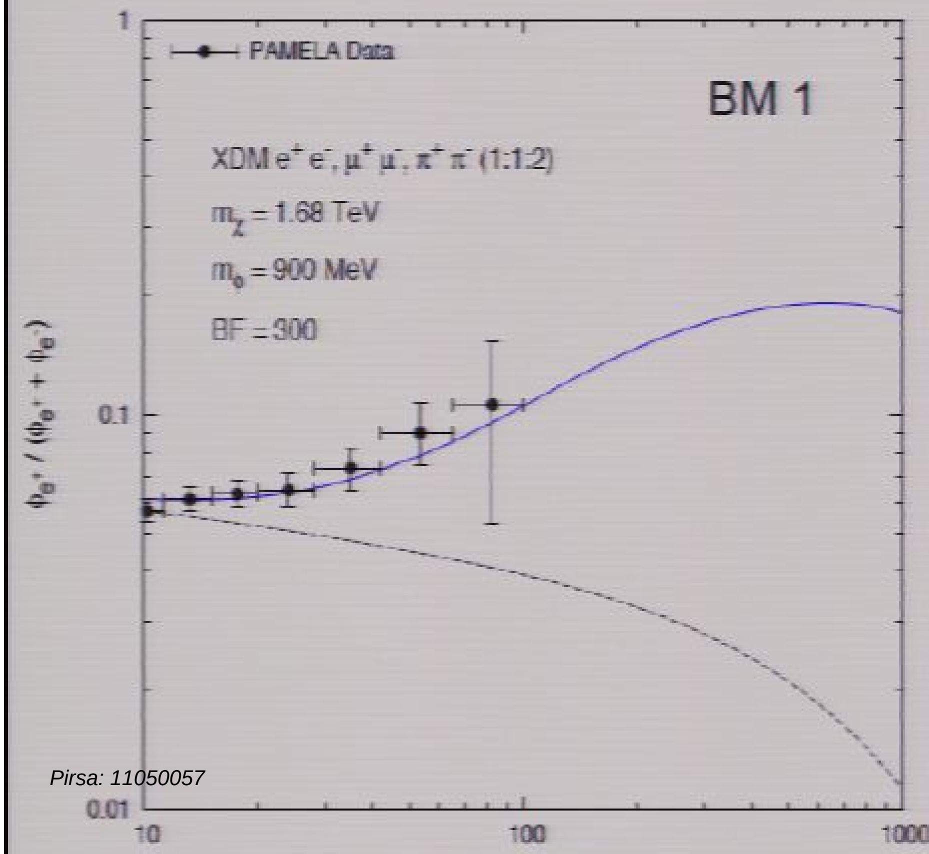

- New force carrier in the "dark sector"
- Annihilation cross section enhanced by a Sommerfeld mechanism:

$$\langle\sigma v\rangle = \langle\sigma v\rangle_0 S(\sigma_{\mathrm{vel}})$$

- Correct relic density
- Fit to the cosmic ray excesses measured by PAMELA and Fermi
- Allowed by bounds on Smax from the CMB
- IC contribution dominates the photon yield

Sommerfeld-enhanced models fitting the cosmic ray excesses (Finkbeiner et al. 2011)

Benchmark no.	Annihilation Channel	m_ϕ (MeV)	m_χ (TeV)	α_c	δ (MeV)	$\frac{S_{\max}\langle\sigma v\rangle_0}{3\times10^{-26}\text{cm}^3\text{ s}^{-1}}$
1	1:1:2 $e^\pm : \mu^\pm : \pi^\pm$	900	1.68	0.04067	0.15	530
2	1:1:2 $e^\pm : \mu^\pm : \pi^\pm$	900	1.52	0.03725	1.34	360
3	1:1:1 $e^\pm : \mu^\pm : \pi^\pm$	580	1.55	0.03523	1.49	437
4	1:1:1 $e^\pm : \mu^\pm : \pi^\pm$	580	1.20	0.03054	1.00	374
5	1:1 $e^\pm : \mu^\pm$	350	1.33	0.02643	1.10	339
6	$e^\pm$ only	200	1.00	0.01622	0.70	171

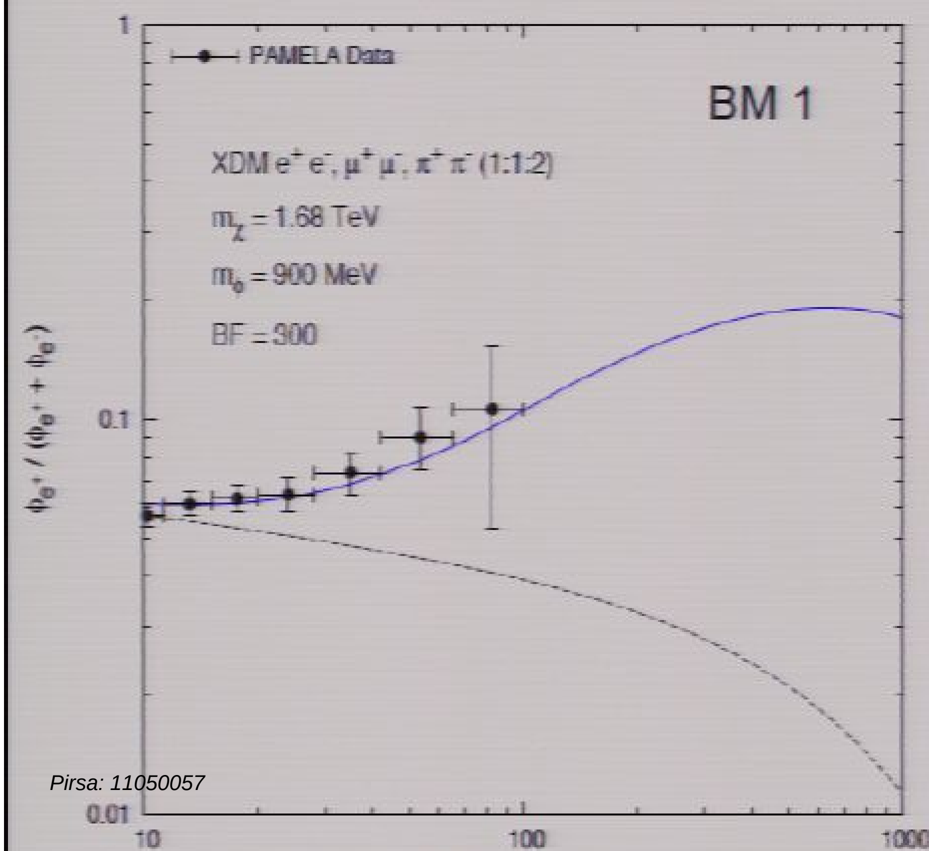

- New force carrier in the "dark sector"
- Annihilation cross section enhanced by a Sommerfeld mechanism:

$$\langle\sigma v\rangle = \langle\sigma v\rangle_0 S(\sigma_{\rm vel})$$

- Correct relic density
- Fit to the cosmic ray excesses measured by PAMELA and Fermi
- Allowed by bounds on Smax from the CMB
- IC contribution dominates the photon yield

Sommerfeld-enhanced models fitting the cosmic ray excesses (Finkbeiner et al. 2011)

Benchmark no.	Annihilation Channel	m_ϕ (MeV)	m_χ (TeV)	α_c	δ (MeV)	$\frac{S_{max}\langle\sigma v\rangle_0}{3\times10^{-26}\mathrm{cm}^3\,\mathrm{s}^{-1}}$
1	1:1:2 $e^\pm : \mu^\pm : \pi^\pm$	900	1.68	0.04067	0.15	530
2	1:1:2 $e^\pm : \mu^\pm : \pi^\pm$	900	1.52	0.03725	1.34	360
3	1:1:1 $e^\pm : \mu^\pm : \pi^\pm$	580	1.55	0.03523	1.49	437
4	1:1:1 $e^\pm : \mu^\pm : \pi^\pm$	580	1.20	0.03054	1.00	374
5	1:1 $e^\pm : \mu^\pm$	350	1.33	0.02643	1.10	339
6	$e^\pm$ only	200	1.00	0.01622	0.70	171

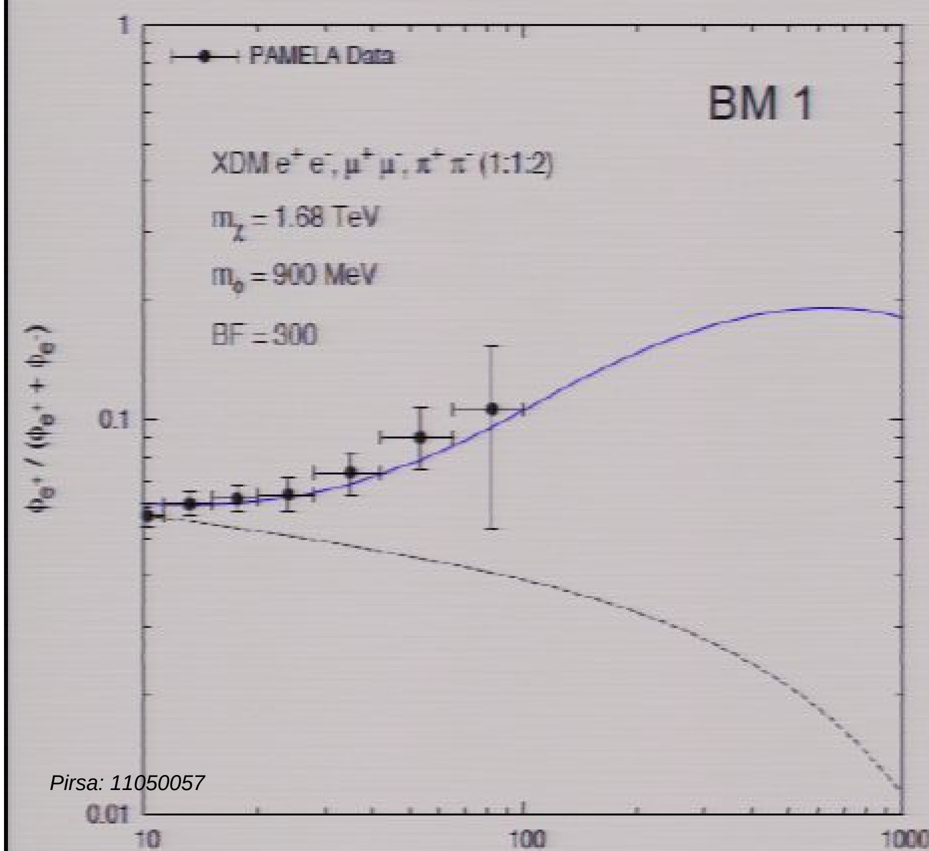

- New force carrier in the "dark sector"
- Annihilation cross section enhanced by a Sommerfeld mechanism:

$$\langle\sigma v\rangle = \langle\sigma v\rangle_0 S(\sigma_{\rm vel})$$

- Correct relic density
- Fit to the cosmic ray excesses measured by PAMELA and Fermi
- Allowed by bounds on Smax from the CMB
- IC contribution dominates the photon yield

Sommerfeld-enhanced models fitting the cosmic ray excesses (Finkbeiner et al. 2011)

Benchmark no.	Annihilation Channel	m_ϕ (MeV)	m_χ (TeV)	α_c	δ (MeV)	$\frac{S_{max}\langle\sigma v\rangle_0}{3\times10^{-26}\text{cm}^3\text{ s}^{-1}}$
1	1:1:2 $e^\pm : \mu^\pm : \pi^\pm$	900	1.68	0.04067	0.15	530
2	1:1:2 $e^\pm : \mu^\pm : \pi^\pm$	900	1.52	0.03725	1.34	360
3	1:1:1 $e^\pm : \mu^\pm : \pi^\pm$	580	1.55	0.03523	1.49	437
4	1:1:1 $e^\pm : \mu^\pm : \pi^\pm$	580	1.20	0.03054	1.00	374
5	1:1 $e^\pm : \mu^\pm$	350	1.33	0.02643	1.10	339
6	$e^\pm$ only	200	1.00	0.01622	0.70	171

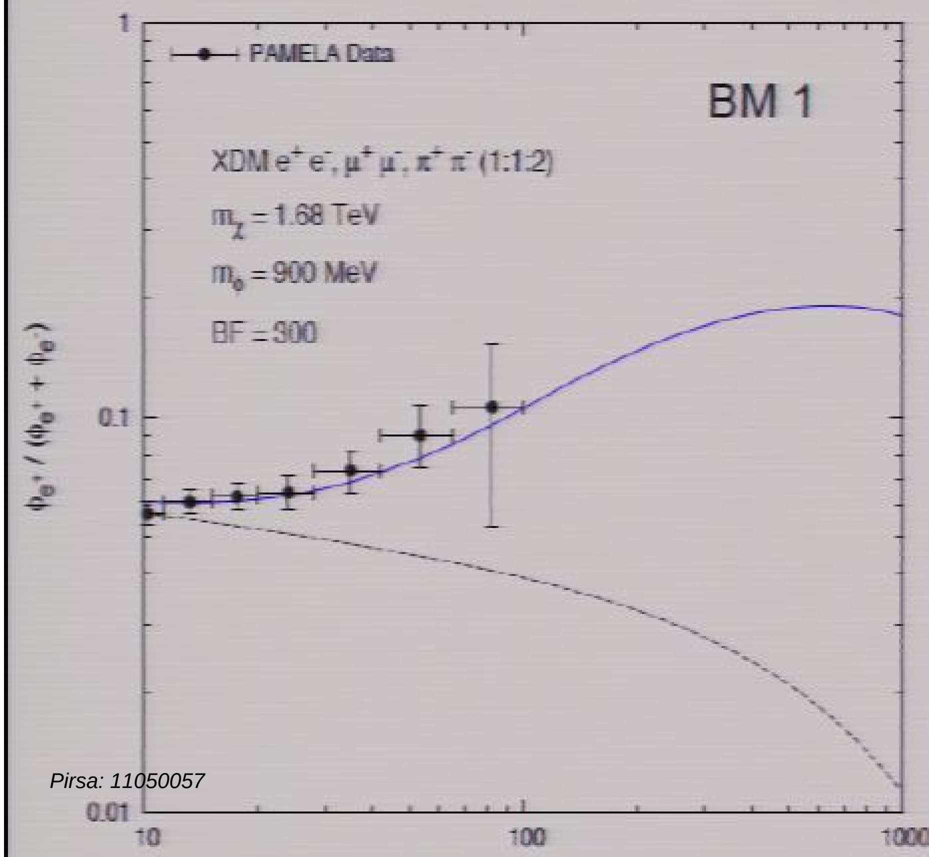

- New force carrier in the "dark sector"
- Annihilation cross section enhanced by a Sommerfeld mechanism:

$$\langle\sigma v\rangle = \langle\sigma v\rangle_0 S(\sigma_{\text{vel}})$$

- Correct relic density
- Fit to the cosmic ray excesses measured by PAMELA and Fermi
- Allowed by bounds on Smax from the CMB
- IC contribution dominates the photon yield

Sommerfeld-enhanced models fitting the cosmic ray excesses (Finkbeiner et al. 2011)

Benchmark no.	Annihilation Channel	m_ϕ (MeV)	m_χ (TeV)	α_c	δ (MeV)	$\frac{S_{max}\langle\sigma v\rangle_0}{3\times10^{-26}\mathrm{cm}^3\mathrm{s}^{-1}}$
1	1:1:2 $e^\pm : \mu^\pm : \pi^\pm$	900	1.68	0.04067	0.15	530
2	1:1:2 $e^\pm : \mu^\pm : \pi^\pm$	900	1.52	0.03725	1.34	360
3	1:1:1 $e^\pm : \mu^\pm : \pi^\pm$	580	1.55	0.03523	1.49	437
4	1:1:1 $e^\pm : \mu^\pm : \pi^\pm$	580	1.20	0.03054	1.00	374
5	1:1 $e^\pm : \mu^\pm$	350	1.33	0.02643	1.10	339
6	$e^\pm$ only	200	1.00	0.01622	0.70	171

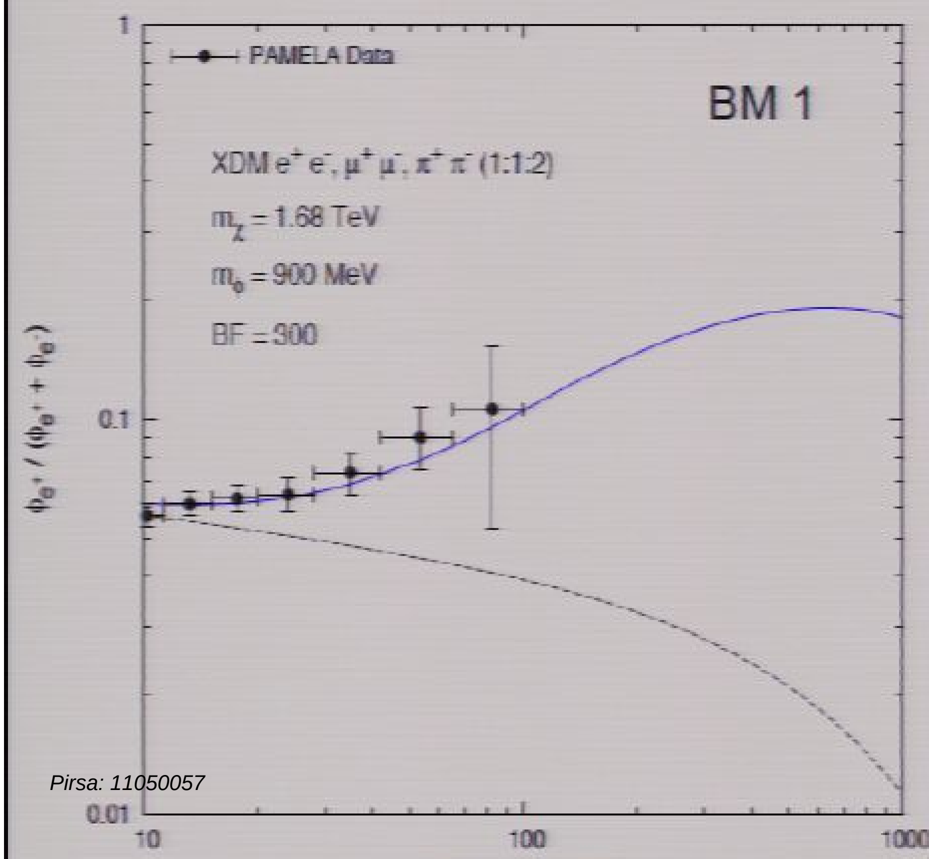

- New force carrier in the "dark sector"
- Annihilation cross section enhanced by a Sommerfeld mechanism:

$$\langle\sigma v\rangle = \langle\sigma v\rangle_0 S(\sigma_{vel})$$

- Correct relic density
- Fit to the cosmic ray excesses measured by PAMELA and Fermi
- Allowed by bounds on Smax from the CMB
- IC contribution dominates the photon yield

Sommerfeld-enhanced models fitting the cosmic ray excesses (Finkbeiner et al. 2011)

Benchmark no.	Annihilation Channel	m_ϕ (MeV)	m_χ (TeV)	α_c	δ (MeV)	$\frac{S_{max}\langle\sigma v\rangle_0}{3\times10^{-26}\mathrm{cm}^3\,\mathrm{s}^{-1}}$
1	1:1:2 $e^\pm : \mu^\pm : \pi^\pm$	900	1.68	0.04067	0.15	530
2	1:1:2 $e^\pm : \mu^\pm : \pi^\pm$	900	1.52	0.03725	1.34	360
3	1:1:1 $e^\pm : \mu^\pm : \pi^\pm$	580	1.55	0.03523	1.49	437
4	1:1:1 $e^\pm : \mu^\pm : \pi^\pm$	580	1.20	0.03054	1.00	374
5	1:1 $e^\pm : \mu^\pm$	350	1.33	0.02643	1.10	339
6	$e^\pm$ only	200	1.00	0.01622	0.70	171

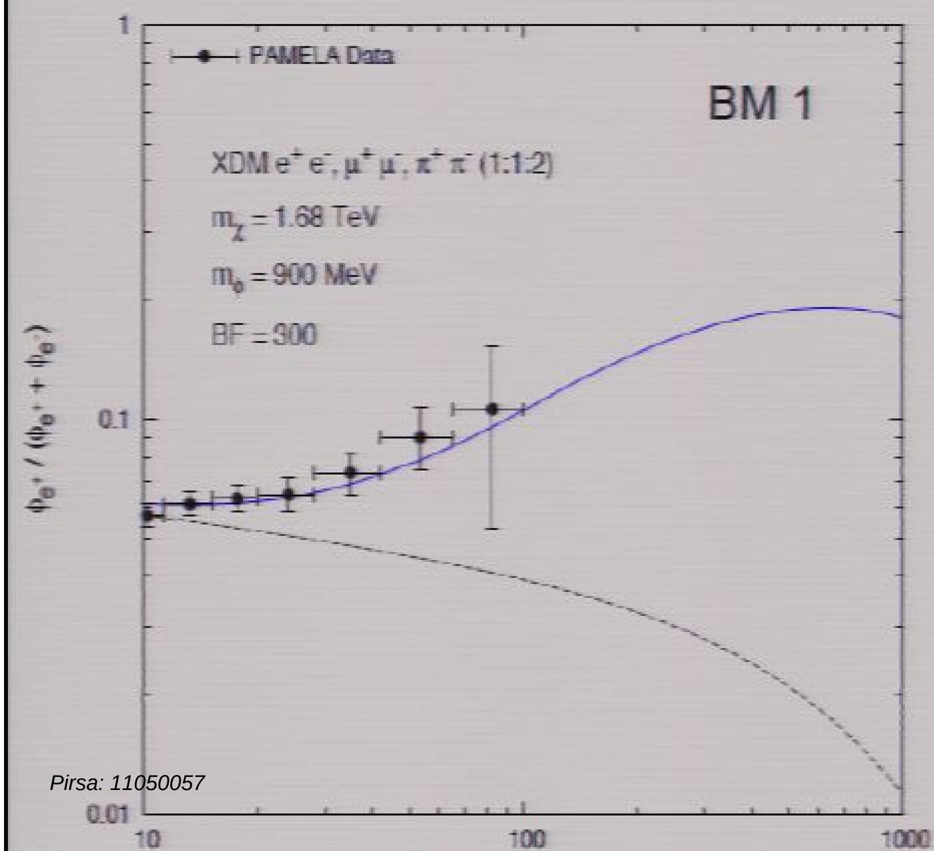

- New force carrier in the "dark sector"
- Annihilation cross section enhanced by a Sommerfeld mechanism:

$$\langle\sigma v\rangle = \langle\sigma v\rangle_0 S(\sigma_{\rm vel})$$

- Correct relic density
- Fit to the cosmic ray excesses measured by PAMELA and Fermi
- Allowed by bounds on Smax from the CMB
- IC contribution dominates the photon yield

Sommerfeld-enhanced models fitting the cosmic ray excesses (Finkbeiner et al. 2011)

Benchmark no.	Annihilation Channel	m_ϕ (MeV)	m_χ (TeV)	α_c	δ (MeV)	$\frac{S_{\max}\langle\sigma v\rangle_0}{3\times10^{-26}\mathrm{cm}^3\,\mathrm{s}^{-1}}$
1	1:1:2 $e^\pm : \mu^\pm : \pi^\pm$	900	1.68	0.04067	0.15	530
2	1:1:2 $e^\pm : \mu^\pm : \pi^\pm$	900	1.52	0.03725	1.34	360
3	1:1:1 $e^\pm : \mu^\pm : \pi^\pm$	580	1.55	0.03523	1.49	437
4	1:1:1 $e^\pm : \mu^\pm : \pi^\pm$	580	1.20	0.03054	1.00	374
5	1:1 $e^\pm : \mu^\pm$	350	1.33	0.02643	1.10	339
6	$e^\pm$ only	200	1.00	0.01622	0.70	171

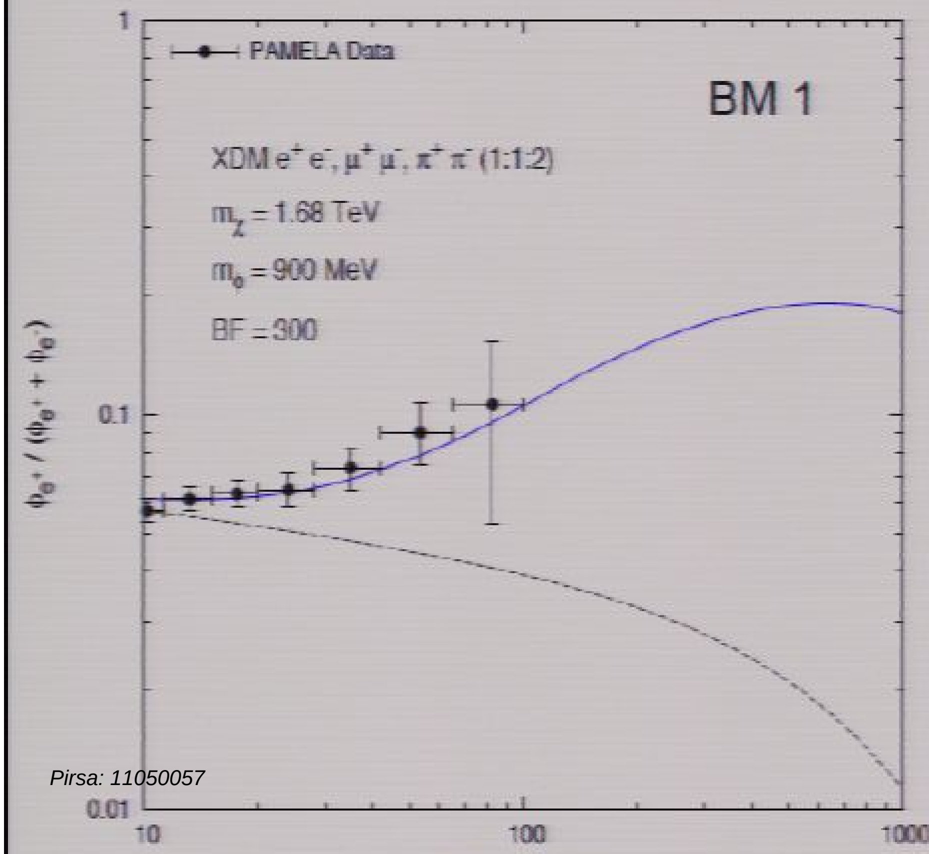

- New force carrier in the "dark sector"
- Annihilation cross section enhanced by a Sommerfeld mechanism:

$$\langle\sigma v\rangle = \langle\sigma v\rangle_0 S(\sigma_{\rm vel})$$

- Correct relic density
- Fit to the cosmic ray excesses measured by PAMELA and Fermi
- Allowed by bounds on Smax from the CMB
- IC contribution dominates the photon yield

Sommerfeld-enhanced models fitting the cosmic ray excesses (Finkbeiner et al. 2011)

Benchmark no.	Annihilation Channel	m_ϕ (MeV)	m_χ (TeV)	α_c	δ (MeV)	$\frac{S_{max}\langle\sigma v\rangle_0}{3\times10^{-26}\mathrm{cm}^3\,\mathrm{s}^{-1}}$
1	1:1:2 $e^\pm : \mu^\pm : \pi^\pm$	900	1.68	0.04067	0.15	530
2	1:1:2 $e^\pm : \mu^\pm : \pi^\pm$	900	1.52	0.03725	1.34	360
3	1:1:1 $e^\pm : \mu^\pm : \pi^\pm$	580	1.55	0.03523	1.49	437
4	1:1:1 $e^\pm : \mu^\pm : \pi^\pm$	580	1.20	0.03054	1.00	374
5	1:1 $e^\pm : \mu^\pm$	350	1.33	0.02643	1.10	339
6	$e^\pm$ only	200	1.00	0.01622	0.70	171

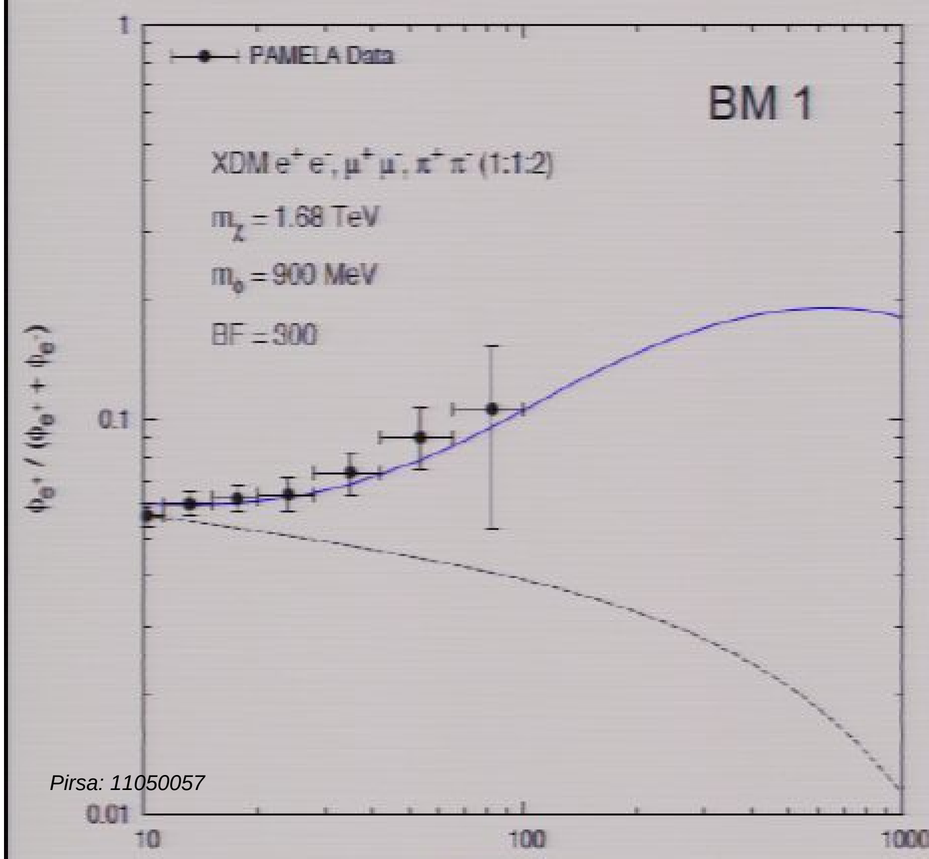

- New force carrier in the "dark sector"
- Annihilation cross section enhanced by a Sommerfeld mechanism:

$$\langle\sigma v\rangle = \langle\sigma v\rangle_0 S(\sigma_{\rm vel})$$

- Correct relic density
- Fit to the cosmic ray excesses measured by PAMELA and Fermi
- Allowed by bounds on Smax from the CMB
- IC contribution dominates the photon yield

Sommerfeld-enhanced models fitting the cosmic ray excesses (Finkbeiner et al. 2011)

Benchmark no.	Annihilation Channel	m_ϕ (MeV)	m_χ (TeV)	α_c	δ (MeV)	$\frac{S_{max}\langle\sigma v\rangle_0}{3\times10^{-26}\mathrm{cm}^3\,\mathrm{s}^{-1}}$
1	1:1:2 $e^\pm : \mu^\pm : \pi^\pm$	900	1.68	0.04067	0.15	530
2	1:1:2 $e^\pm : \mu^\pm : \pi^\pm$	900	1.52	0.03725	1.34	360
3	1:1:1 $e^\pm : \mu^\pm : \pi^\pm$	580	1.55	0.03523	1.49	437
4	1:1:1 $e^\pm : \mu^\pm : \pi^\pm$	580	1.20	0.03054	1.00	374
5	1:1 $e^\pm : \mu^\pm$	350	1.33	0.02643	1.10	339
6	$e^\pm$ only	200	1.00	0.01622	0.70	171

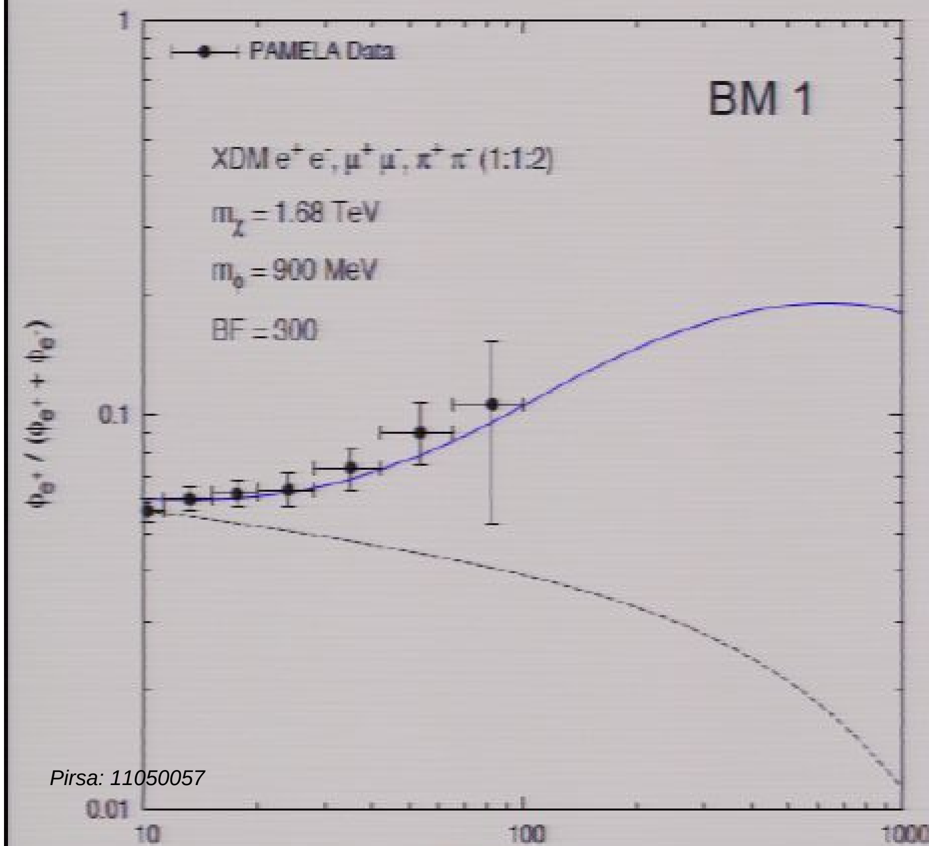

- New force carrier in the "dark sector"
- Annihilation cross section enhanced by a Sommerfeld mechanism:

$$\langle\sigma v\rangle = \langle\sigma v\rangle_0 S(\sigma_{\mathrm{vel}})$$

- Correct relic density
- Fit to the cosmic ray excesses measured by PAMELA and Fermi
- Allowed by bounds on Smax from the CMB
- IC contribution dominates the photon yield

Sommerfeld-enhanced models fitting the cosmic ray excesses

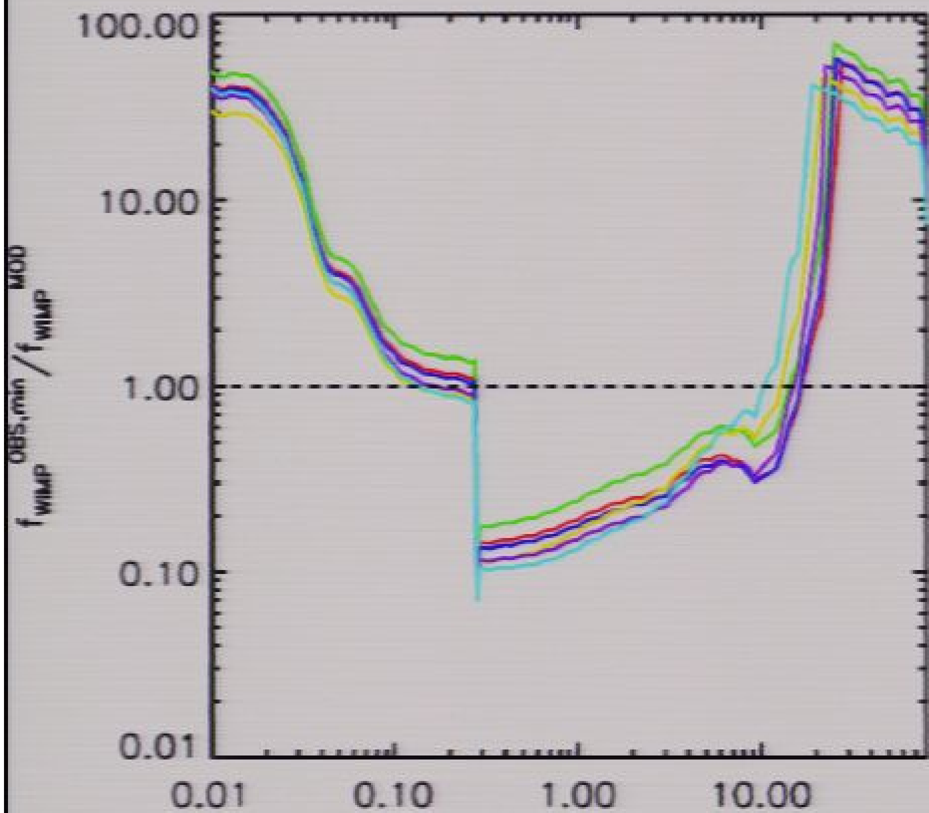

- Minimum contribution from subhalos
- SFG = 53%of EGB(E>1GeV)
- Blazars = 16% of EGB (E>1GeV)

Benchmark no.	Annihilation Channel	m_ϕ (MeV)	m_χ (TeV)	α_c	δ (MeV)	$\frac{S_{max}\langle\sigma v\rangle_0}{3\times10^{-26}\mathrm{cm^3\,s^{-1}}}$
1	$1{:}1{:}2\ e^\pm : \mu^\pm : \pi^\pm$	900	1.68	0.04067	0.15	530
2	$1{:}1{:}2\ e^\pm : \mu^\pm : \pi^\pm$	900	1.52	0.03725	1.34	360
3	$1{:}1{:}1\ e^\pm : \mu^\pm : \pi^\pm$	580	1.55	0.03523	1.49	437
4	$1{:}1{:}1\ e^\pm : \mu^\pm : \pi^\pm$	580	1.20	0.03054	1.00	374
5	$1{:}1\ e^\pm : \mu^\pm$	350	1.33	0.02643	1.10	339
6	$e^\pm$ only	200	1.00	0.01622	0.70	171

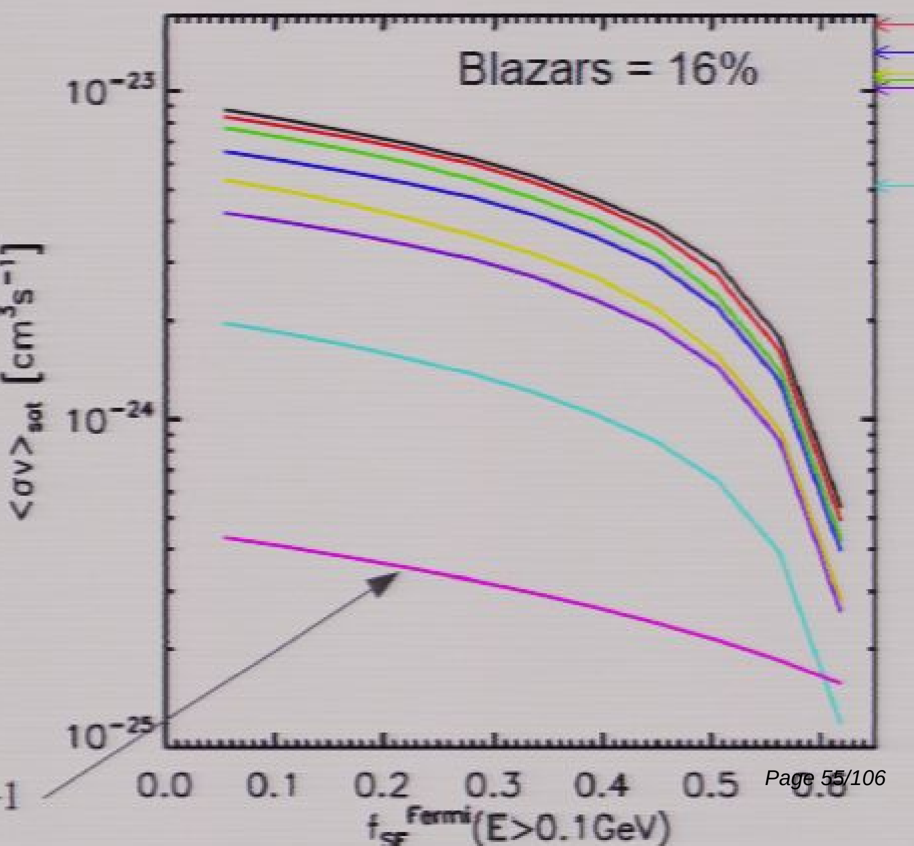

$$m_\chi \sim 200\,GeV,\ \chi\chi \rightarrow b\bar{b} \text{ and } \langle\sigma v\rangle \sim 6.2\times10^{-27}\mathrm{cm^3 s^{-1}}$$

Isotropic component

$m_\chi \sim 200\, GeV, \chi\chi \to b\bar{b}$ and $\langle \sigma v \rangle \sim 6.2 \times 10^{-27} \mathrm{cm}^3 \mathrm{s}^{-1}$

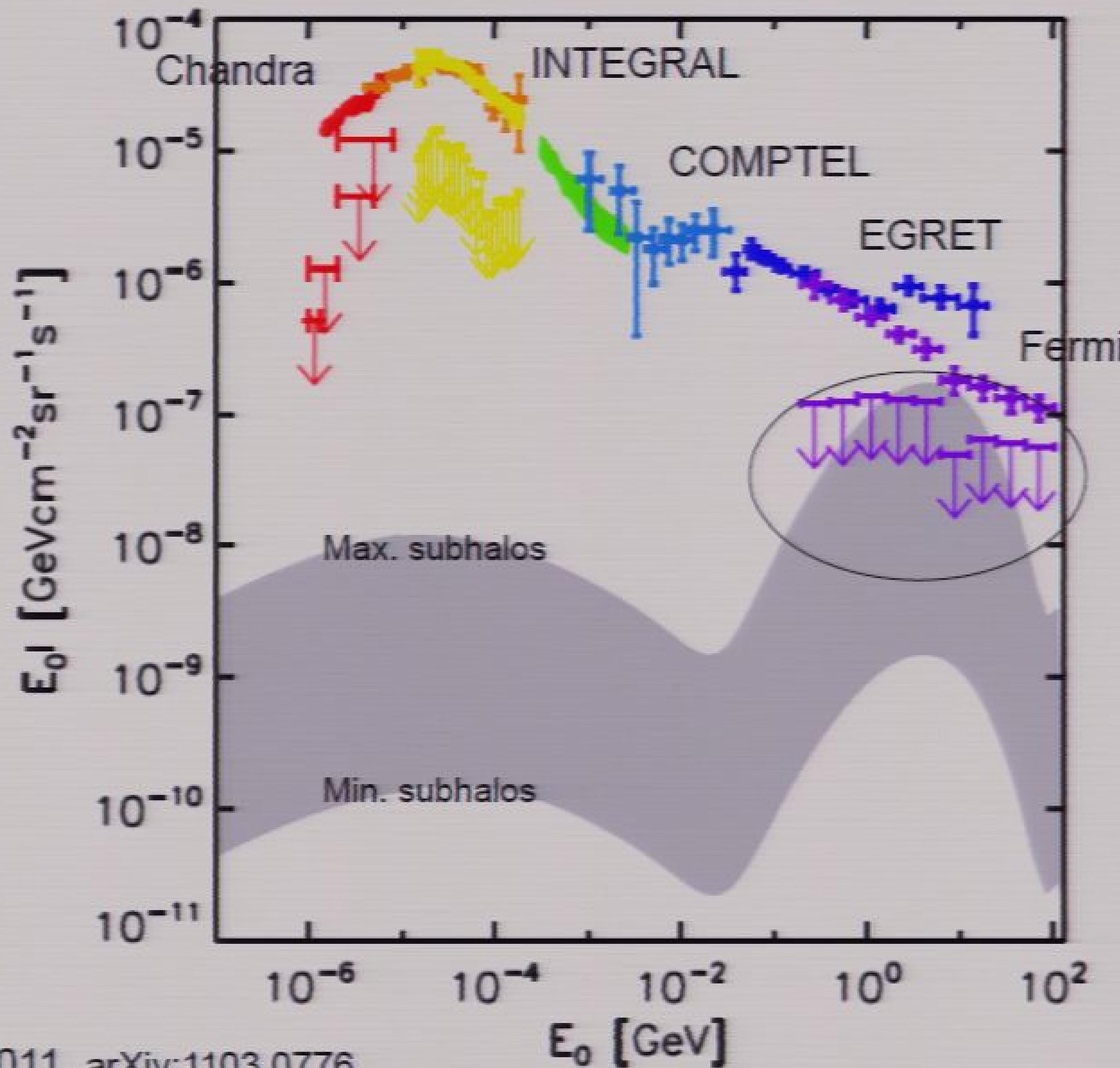

Star forming galaxies (53%) and blazars (16%)

Zavala et al. 2011, arXiv:1103.0776

Sommerfeld-enhanced models fitting the cosmic ray excesses (Finkbeiner et al. 2011)

Benchmark no.	Annihilation Channel	m_ϕ (MeV)	m_χ (TeV)	α_c	δ (MeV)	$\frac{S_{max}\langle\sigma v\rangle_0}{3\times10^{-26}\mathrm{cm}^3\,\mathrm{s}^{-1}}$
1	1:1:2 $e^\pm : \mu^\pm : \pi^\pm$	900	1.68	0.04067	0.15	530
2	1:1:2 $e^\pm : \mu^\pm : \pi^\pm$	900	1.52	0.03725	1.34	360
3	1:1:1 $e^\pm : \mu^\pm : \pi^\pm$	580	1.55	0.03523	1.49	437
4	1:1:1 $e^\pm : \mu^\pm : \pi^\pm$	580	1.20	0.03054	1.00	374
5	1:1 $e^\pm : \mu^\pm$	350	1.33	0.02643	1.10	339
6	$e^\pm$ only	200	1.00	0.01622	0.70	171

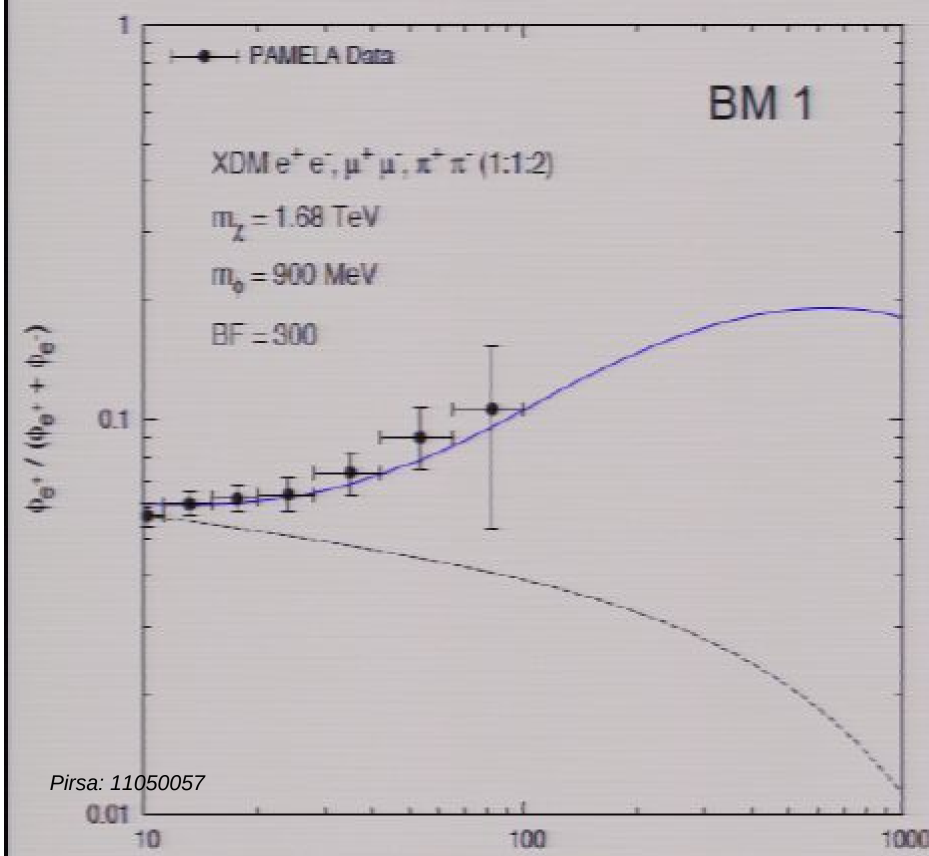

- New force carrier in the "dark sector"
- Annihilation cross section enhanced by a Sommerfeld mechanism:

$$\langle\sigma v\rangle = \langle\sigma v\rangle_0 S(\sigma_{\rm vel})$$

- Correct relic density
- Fit to the cosmic ray excesses measured by PAMELA and Fermi
- Allowed by bounds on Smax from the CMB
- IC contribution dominates the photon yield

Sommerfeld-enhanced models fitting the cosmic ray excesses

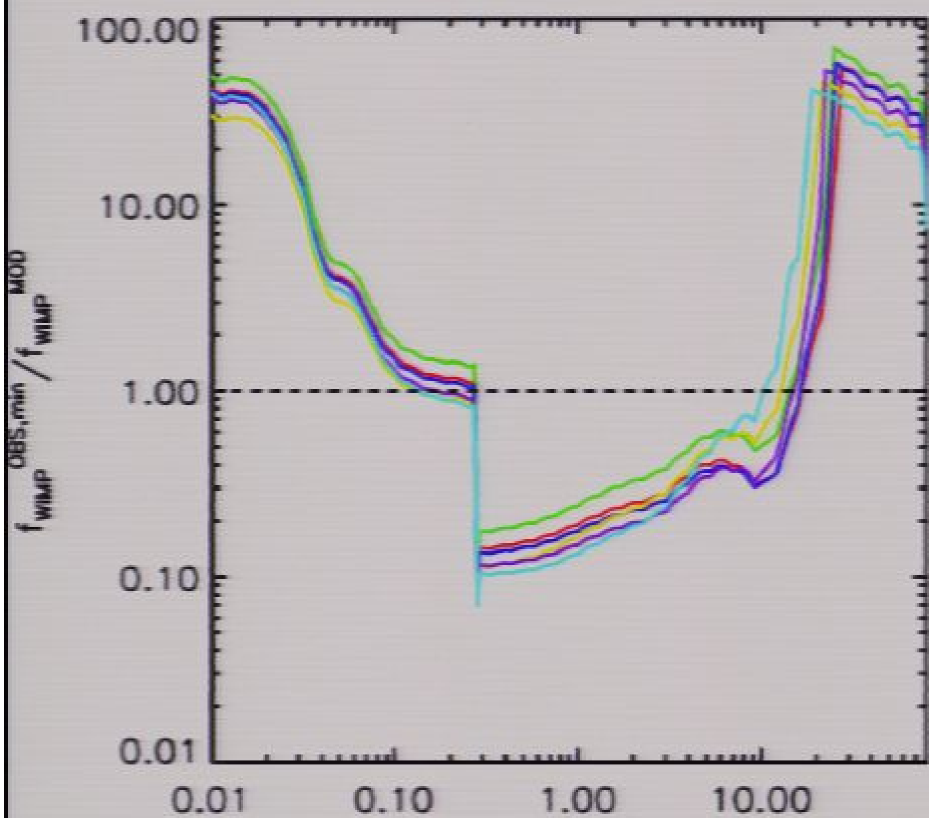

- Minimum contribution from subhalos
- SFG = 53%of EGB(E>1GeV)
- Blazars = 16% of EGB (E>1GeV)

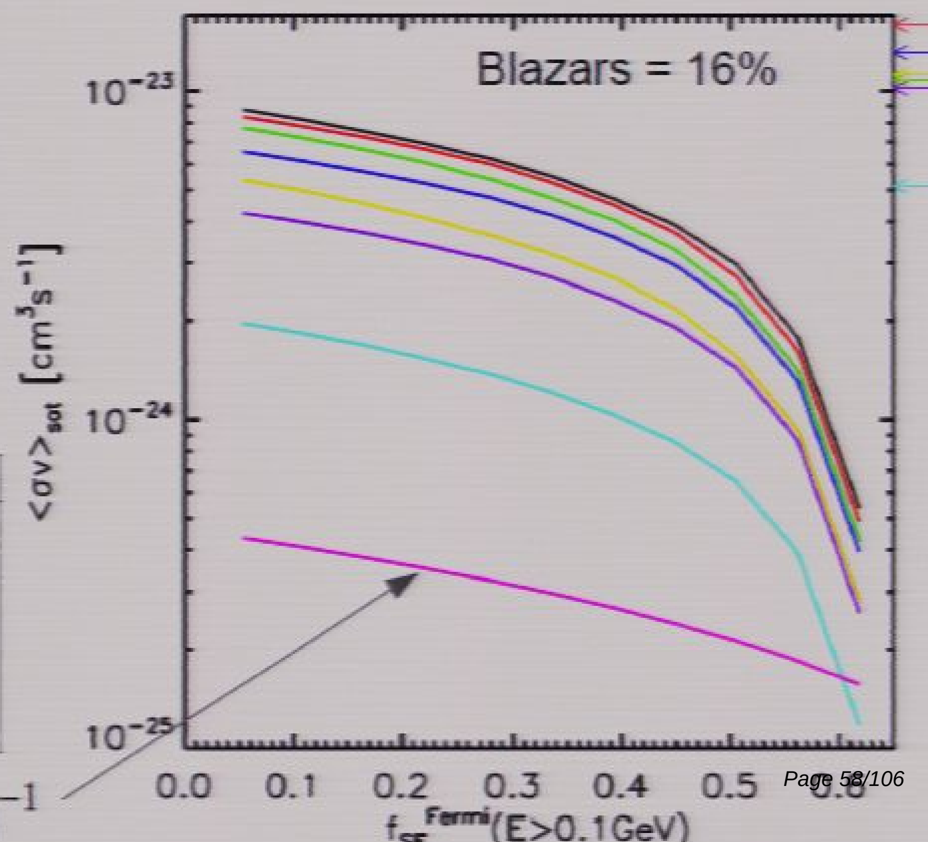

Benchmark no.	Annihilation Channel	m_ϕ (MeV)	m_χ (TeV)	α_c	δ (MeV)	$\frac{S_{max}\langle\sigma v\rangle_0}{3\times10^{-26} cm^3 s^{-1}}$
1	$1{:}1{:}2\ e^\pm : \mu^\pm : \pi^\pm$	900	1.68	0.04067	0.15	530
2	$1{:}1{:}2\ e^\pm : \mu^\pm : \pi^\pm$	900	1.52	0.03725	1.34	360
3	$1{:}1{:}1\ e^\pm : \mu^\pm : \pi^\pm$	580	1.55	0.03523	1.49	437
4	$1{:}1{:}1\ e^\pm : \mu^\pm : \pi^\pm$	580	1.20	0.03054	1.00	374
5	$1{:}1\ e^\pm : \mu^\pm$	350	1.33	0.02643	1.10	339
6	$e^\pm$ only	200	1.00	0.01622	0.70	171

$m_\chi \sim 200\,GeV, \chi\chi \to b\bar{b}$ and $\langle\sigma v\rangle \sim 6.2\times 10^{-27} cm^3 s^{-1}$

Isotropic component (annihilation channel)

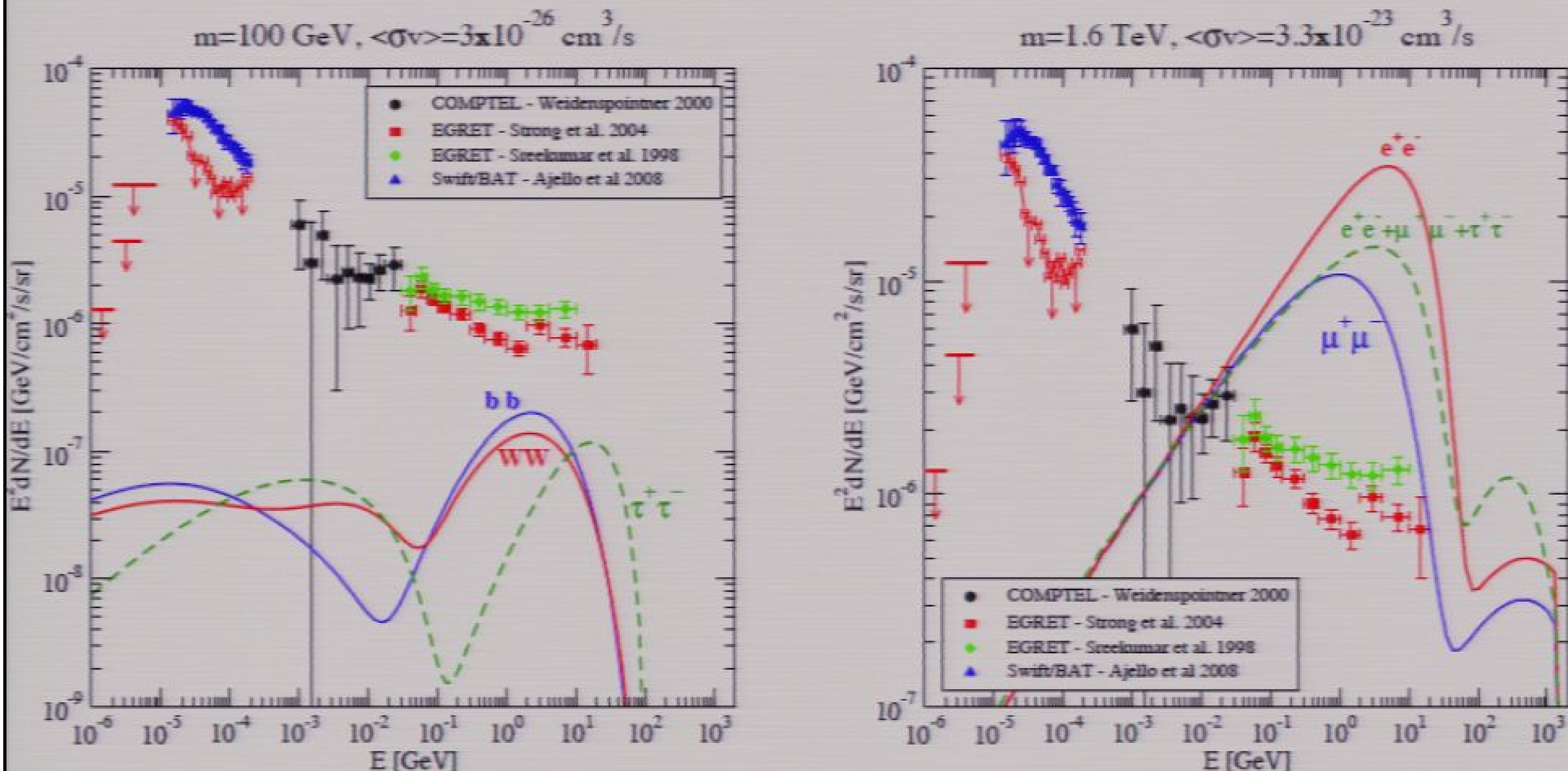

Profumo and Jeltema 2010

Isotropic component

$m_\chi \sim 200\,GeV, \chi\chi \to b\bar{b}$ and $\langle\sigma v\rangle \sim 6.2 \times 10^{-27}\mathrm{cm}^3\mathrm{s}^{-1}$

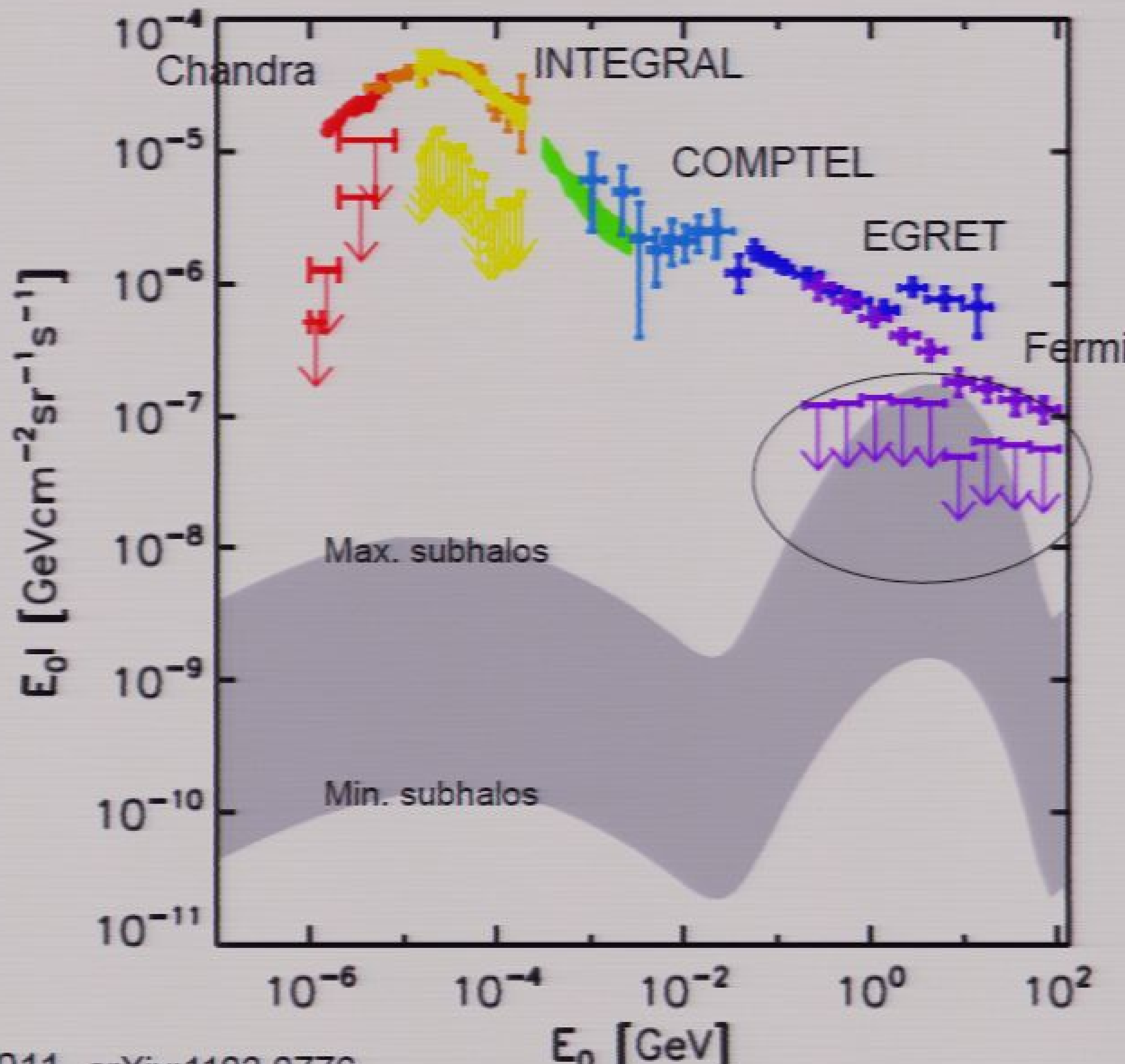

Star forming galaxies (53%) and blazars (16%)

Zavala et al. 2011, arXiv:1103.0776

Sommerfeld-enhanced models fitting the cosmic ray excesses (Finkbeiner et al. 2011)

Benchmark no.	Annihilation Channel	m_ϕ (MeV)	m_χ (TeV)	α_c	δ (MeV)	$\frac{S_{\max}\langle\sigma v\rangle_0}{3\times10^{-26}\mathrm{cm}^3\ \mathrm{s}^{-1}}$
1	1:1:2 $e^\pm : \mu^\pm : \pi^\pm$	900	1.68	0.04067	0.15	530
2	1:1:2 $e^\pm : \mu^\pm : \pi^\pm$	900	1.52	0.03725	1.34	360
3	1:1:1 $e^\pm : \mu^\pm : \pi^\pm$	580	1.55	0.03523	1.49	437
4	1:1:1 $e^\pm : \mu^\pm : \pi^\pm$	580	1.20	0.03054	1.00	374
5	1:1 $e^\pm : \mu^\pm$	350	1.33	0.02643	1.10	339
6	$e^\pm$ only	200	1.00	0.01622	0.70	171

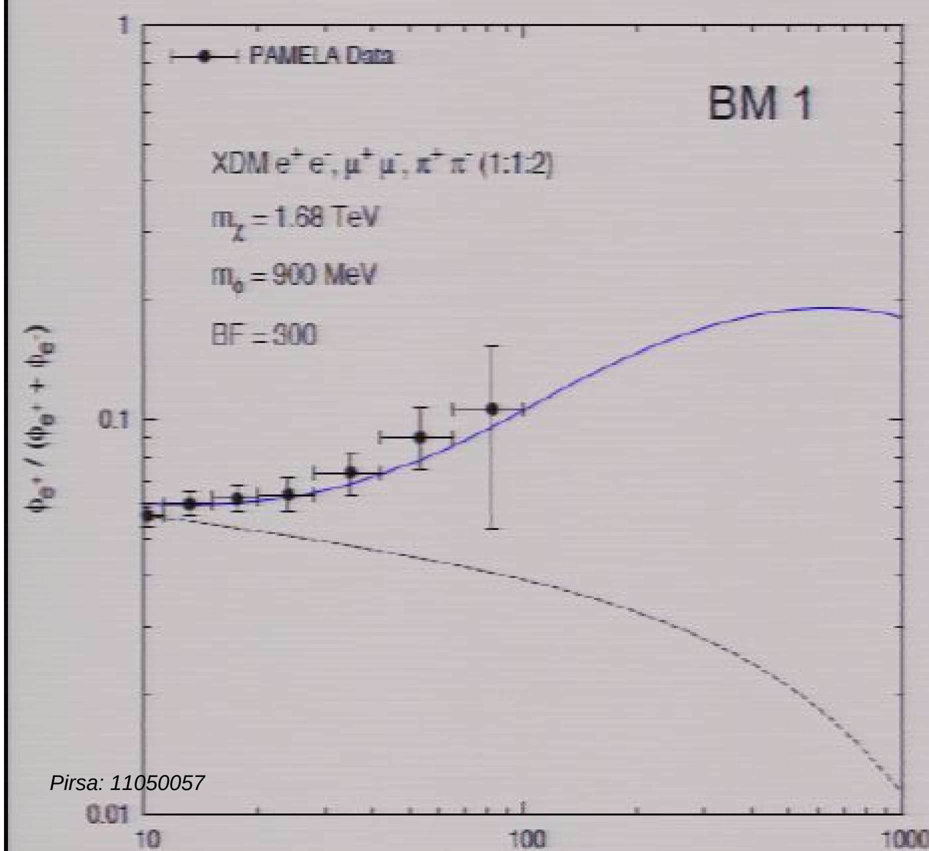

- New force carrier in the "dark sector"
- Annihilation cross section enhanced by a Sommerfeld mechanism:

$$\langle\sigma v\rangle = \langle\sigma v\rangle_0 S(\sigma_{\mathrm{vel}})$$

- Correct relic density
- Fit to the cosmic ray excesses measured by PAMELA and Fermi
- Allowed by bounds on Smax from the CMB
- IC contribution dominates the photon yield

Sommerfeld-enhanced models fitting the cosmic ray excesses

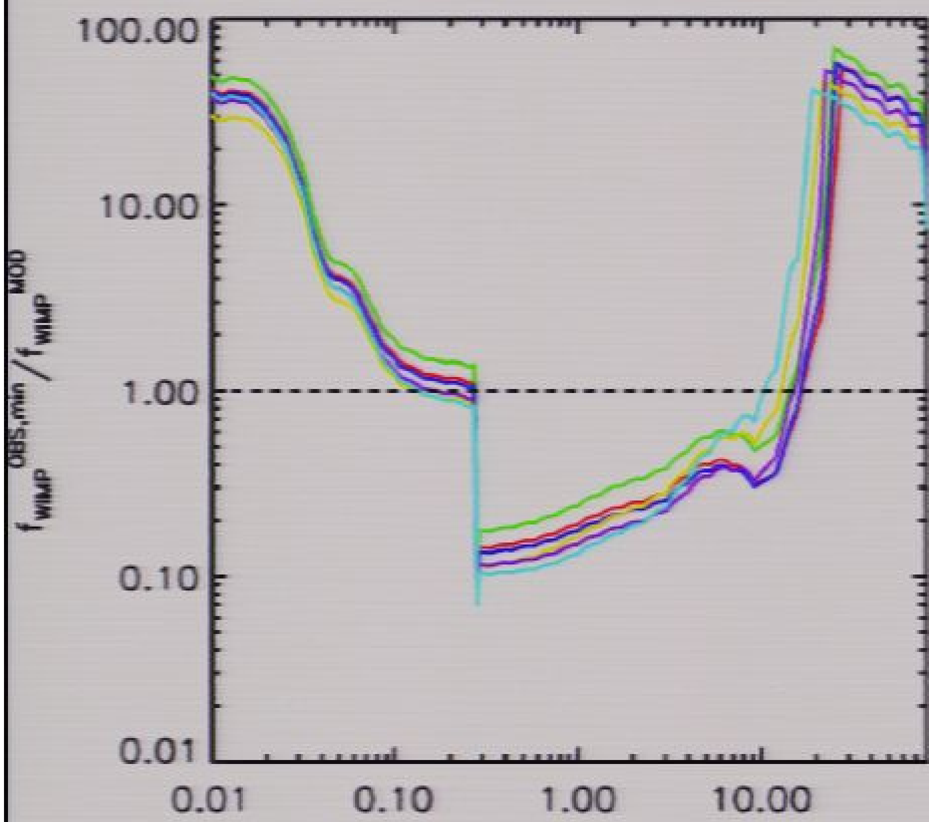

- Minimum contribution from subhalos
- SFG = 53%of EGB(E>1GeV)
- Blazars = 16% of EGB (E>1GeV)

Benchmark no.	Annihilation Channel	m_ϕ (MeV)	m_χ (TeV)	α_c	δ (MeV)	$\frac{S_{max}\langle\sigma v\rangle_0}{3\times10^{-26}\mathrm{cm^3\,s^{-1}}}$
1	1:1:2 $e^\pm : \mu^\pm : \pi^\pm$	900	1.68	0.04067	0.15	530
2	1:1:2 $e^\pm : \mu^\pm : \pi^\pm$	900	1.52	0.03725	1.34	360
3	1:1:1 $e^\pm : \mu^\pm : \pi^\pm$	580	1.55	0.03523	1.49	437
4	1:1:1 $e^\pm : \mu^\pm : \pi^\pm$	580	1.20	0.03054	1.00	374
5	1:1 $e^\pm : \mu^\pm$	350	1.33	0.02643	1.10	339
6	$e^\pm$ only	200	1.00	0.01622	0.70	171

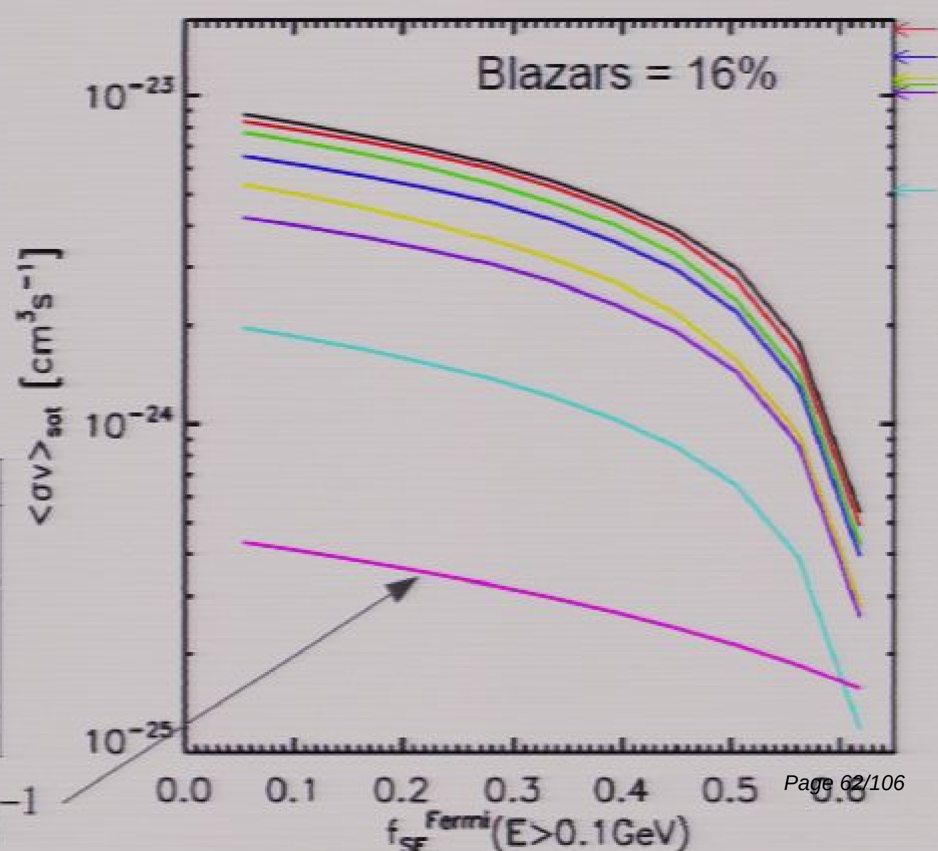

$m_\chi \sim 200\, GeV,\, \chi\chi \to b\bar{b}$ and $\langle\sigma v\rangle \sim 6.2\times10^{-27}\mathrm{cm^3 s^{-1}}$

Summary and Conclusions

- Sommerfeld-enhanced models can explain the cosmic-ray anomalies, but they need to be consistent with independent astrophysical constraints.
- The local boost factors are less than ~100 for a scalar boson as the force carrier and a Yukawa interaction (relic density constraint).
- We have obtained predictions from the simulated all-sky maps of the cosmic X- and gamma-ray background from DM annihilation including:
  - Photon yield given by a WIMP model (in situ photons and up-scattered photons of the CMB). Model-independent, can be used for Sommerfeld-enhanced models.
  - Dark matter spatial distribution using Millennium-II simulation, uncertainty of ~2 orders of magnitude in extrapolation to unresolved structures.
- Isotropic component constrained by observations of the cosmic background, and contributions from blazars and star forming galaxies: although is not as clean as the CMB, it is more powerful to constrain the intrinsic properties of dark matter.

Summary and Conclusions

- Sommerfeld-enhanced models can explain the cosmic-ray anomalies, but they need to be consistent with independent astrophysical constraints.
- The local boost factors are less than ~100 for a scalar boson as the force carrier and a Yukawa interaction (relic density constraint).
- We have obtained predictions from the simulated all-sky maps of the cosmic X- and gamma-ray background from DM annihilation including:
  - Photon yield given by a WIMP model (in situ photons and up-scattered photons of the CMB). Model-independent, can be used for Sommerfeld-enhanced models.
  - Dark matter spatial distribution using Millennium-II simulation, uncertainty of ~2 orders of magnitude in extrapolation to unresolved structures.
- Isotropic component constrained by observations of the cosmic background, and contributions from blazars and star forming galaxies: although is not as clean as the CMB, it is more powerful to constrain the intrinsic properties of dark matter.

Summary and Conclusions

- Sommerfeld-enhanced models can explain the cosmic-ray anomalies, but they need to be consistent with independent astrophysical constraints.
- The local boost factors are less than ~100 for a scalar boson as the force carrier and a Yukawa interaction (relic density constraint).
- We have obtained predictions from the simulated all-sky maps of the cosmic X- and gamma-ray background from DM annihilation including:
  - Photon yield given by a WIMP model (in situ photons and up-scattered photons of the CMB). Model-independent, can be used for Sommerfeld-enhanced models.
  - Dark matter spatial distribution using Millennium-II simulation, uncertainty of ~2 orders of magnitude in extrapolation to unresolved structures.
- Isotropic component constrained by observations of the cosmic background, and contributions from blazars and star forming galaxies: although is not as clean as the CMB, it is more powerful to constrain the intrinsic properties of dark matter.

Summary and Conclusions

- Sommerfeld-enhanced models can explain the cosmic-ray anomalies, but they need to be consistent with independent astrophysical constraints.
- The local boost factors are less than ~100 for a scalar boson as the force carrier and a Yukawa interaction (relic density constraint).
- We have obtained predictions from the simulated all-sky maps of the cosmic X- and gamma-ray background from DM annihilation including:
  - Photon yield given by a WIMP model (in situ photons and up-scattered photons of the CMB). Model-independent, can be used for Sommerfeld-enhanced models.
  - Dark matter spatial distribution using Millennium-II simulation, uncertainty of ~2 orders of magnitude in extrapolation to unresolved structures.
- Isotropic component constrained by observations of the cosmic background, and contributions from blazars and star forming galaxies: although is not as clean as the CMB, it is more powerful to constrain the intrinsic properties of dark matter.

Summary and Conclusions

- Sommerfeld-enhanced models can explain the cosmic-ray anomalies, but they need to be consistent with independent astrophysical constraints.
- The local boost factors are less than ~100 for a scalar boson as the force carrier and a Yukawa interaction (relic density constraint).
- We have obtained predictions from the simulated all-sky maps of the cosmic X- and gamma-ray background from DM annihilation including:
  - Photon yield given by a WIMP model (in situ photons and up-scattered photons of the CMB). Model-independent, can be used for Sommerfeld-enhanced models.
  - Dark matter spatial distribution using Millennium-II simulation, uncertainty of ~2 orders of magnitude in extrapolation to unresolved structures.
- Isotropic component constrained by observations of the cosmic background, and contributions from blazars and star forming galaxies: although is not as clean as the CMB, it is more powerful to constrain the intrinsic properties of dark matter.

Summary and Conclusions

- Sommerfeld-enhanced models can explain the cosmic-ray anomalies, but they need to be consistent with independent astrophysical constraints.
- The local boost factors are less than ~100 for a scalar boson as the force carrier and a Yukawa interaction (relic density constraint).
- We have obtained predictions from the simulated all-sky maps of the cosmic X- and gamma-ray background from DM annihilation including:
  - Photon yield given by a WIMP model (in situ photons and up-scattered photons of the CMB). Model-independent, can be used for Sommerfeld-enhanced models.
  - Dark matter spatial distribution using Millennium-II simulation, uncertainty of ~2 orders of magnitude in extrapolation to unresolved structures.
- Isotropic component constrained by observations of the cosmic background, and contributions from blazars and star forming galaxies: although is not as clean as the CMB, it is more powerful to constrain the intrinsic properties of dark matter.

Summary and Conclusions

- Sommerfeld-enhanced models can explain the cosmic-ray anomalies, but they need to be consistent with independent astrophysical constraints.
- The local boost factors are less than ~100 for a scalar boson as the force carrier and a Yukawa interaction (relic density constraint).
- We have obtained predictions from the simulated all-sky maps of the cosmic X- and gamma-ray background from DM annihilation including:
  - Photon yield given by a WIMP model (in situ photons and up-scattered photons of the CMB). Model-independent, can be used for Sommerfeld-enhanced models.
  - Dark matter spatial distribution using Millennium-II simulation, uncertainty of ~2 orders of magnitude in extrapolation to unresolved structures.
- Isotropic component constrained by observations of the cosmic background, and contributions from blazars and star forming galaxies: although is not as clean as the CMB, it is more powerful to constrain the intrinsic properties of dark matter.

Summary and Conclusions

- Sommerfeld-enhanced models can explain the cosmic-ray anomalies, but they need to be consistent with independent astrophysical constraints.
- The local boost factors are less than ~100 for a scalar boson as the force carrier and a Yukawa interaction (relic density constraint).
- We have obtained predictions from the simulated all-sky maps of the cosmic X- and gamma-ray background from DM annihilation including:
  - Photon yield given by a WIMP model (in situ photons and up-scattered photons of the CMB). Model-independent, can be used for Sommerfeld-enhanced models.
  - Dark matter spatial distribution using Millennium-II simulation, uncertainty of ~2 orders of magnitude in extrapolation to unresolved structures.
- Isotropic component constrained by observations of the cosmic background, and contributions from blazars and star forming galaxies: although is not as clean as the CMB, it is more powerful to constrain the intrinsic properties of dark matter.

Summary and Conclusions

- Sommerfeld-enhanced models can explain the cosmic-ray anomalies, but they need to be consistent with independent astrophysical constraints.
- The local boost factors are less than ~100 for a scalar boson as the force carrier and a Yukawa interaction (relic density constraint).
- We have obtained predictions from the simulated all-sky maps of the cosmic X- and gamma-ray background from DM annihilation including:
  - Photon yield given by a WIMP model (in situ photons and up-scattered photons of the CMB). Model-independent, can be used for Sommerfeld-enhanced models.
  - Dark matter spatial distribution using Millennium-II simulation, uncertainty of ~2 orders of magnitude in extrapolation to unresolved structures.
- Isotropic component constrained by observations of the cosmic background, and contributions from blazars and star forming galaxies: although is not as clean as the CMB, it is more powerful to constrain the intrinsic properties of dark matter.

Summary and Conclusions

- Sommerfeld-enhanced models can explain the cosmic-ray anomalies, but they need to be consistent with independent astrophysical constraints.
- The local boost factors are less than ~100 for a scalar boson as the force carrier and a Yukawa interaction (relic density constraint).
- We have obtained predictions from the simulated all-sky maps of the cosmic X- and gamma-ray background from DM annihilation including:
  - Photon yield given by a WIMP model (in situ photons and up-scattered photons of the CMB). Model-independent, can be used for Sommerfeld-enhanced models.
  - Dark matter spatial distribution using Millennium-II simulation, uncertainty of ~2 orders of magnitude in extrapolation to unresolved structures.
- Isotropic component constrained by observations of the cosmic background, and contributions from blazars and star forming galaxies: although is not as clean as the CMB, it is more powerful to constrain the intrinsic properties of dark matter.

Summary and Conclusions

- Sommerfeld-enhanced models can explain the cosmic-ray anomalies, but they need to be consistent with independent astrophysical constraints.
- The local boost factors are less than ~100 for a scalar boson as the force carrier and a Yukawa interaction (relic density constraint).
- We have obtained predictions from the simulated all-sky maps of the cosmic X- and gamma-ray background from DM annihilation including:
  - Photon yield given by a WIMP model (in situ photons and up-scattered photons of the CMB). Model-independent, can be used for Sommerfeld-enhanced models.
  - Dark matter spatial distribution using Millennium-II simulation, uncertainty of ~2 orders of magnitude in extrapolation to unresolved structures.
- Isotropic component constrained by observations of the cosmic background, and contributions from blazars and star forming galaxies: although is not as clean as the CMB, it is more powerful to constrain the intrinsic properties of dark matter.

Summary and Conclusions

- Sommerfeld-enhanced models can explain the cosmic-ray anomalies, but they need to be consistent with independent astrophysical constraints.
- The local boost factors are less than ~100 for a scalar boson as the force carrier and a Yukawa interaction (relic density constraint).
- We have obtained predictions from the simulated all-sky maps of the cosmic X- and gamma-ray background from DM annihilation including:
  - Photon yield given by a WIMP model (in situ photons and up-scattered photons of the CMB). Model-independent, can be used for Sommerfeld-enhanced models.
  - Dark matter spatial distribution using Millennium-II simulation, uncertainty of ~2 orders of magnitude in extrapolation to unresolved structures.
- Isotropic component constrained by observations of the cosmic background, and contributions from blazars and star forming galaxies: although is not as clean as the CMB, it is more powerful to constrain the intrinsic properties of dark matter.

Summary and Conclusions

- Sommerfeld-enhanced models can explain the cosmic-ray anomalies, but they need to be consistent with independent astrophysical constraints.
- The local boost factors are less than ~100 for a scalar boson as the force carrier and a Yukawa interaction (relic density constraint).
- We have obtained predictions from the simulated all-sky maps of the cosmic X- and gamma-ray background from DM annihilation including:
  - Photon yield given by a WIMP model (in situ photons and up-scattered photons of the CMB). Model-independent, can be used for Sommerfeld-enhanced models.
  - Dark matter spatial distribution using Millennium-II simulation, uncertainty of ~2 orders of magnitude in extrapolation to unresolved structures.
- Isotropic component constrained by observations of the cosmic background, and contributions from blazars and star forming galaxies: although is not as clean as the CMB, it is more powerful to constrain the intrinsic properties of dark matter.

Summary and Conclusions

- Sommerfeld-enhanced models can explain the cosmic-ray anomalies, but they need to be consistent with independent astrophysical constraints.
- The local boost factors are less than ~100 for a scalar boson as the force carrier and a Yukawa interaction (relic density constraint).
- We have obtained predictions from the simulated all-sky maps of the cosmic X- and gamma-ray background from DM annihilation including:
  - Photon yield given by a WIMP model (in situ photons and up-scattered photons of the CMB). Model-independent, can be used for Sommerfeld-enhanced models.
  - Dark matter spatial distribution using Millennium-II simulation, uncertainty of ~2 orders of magnitude in extrapolation to unresolved structures.
- Isotropic component constrained by observations of the cosmic background, and contributions from blazars and star forming galaxies: although is not as clean as the CMB, it is more powerful to constrain the intrinsic properties of dark matter.

Summary and Conclusions

- Sommerfeld-enhanced models can explain the cosmic-ray anomalies, but they need to be consistent with independent astrophysical constraints.
- The local boost factors are less than ~100 for a scalar boson as the force carrier and a Yukawa interaction (relic density constraint).
- We have obtained predictions from the simulated all-sky maps of the cosmic X- and gamma-ray background from DM annihilation including:
  - Photon yield given by a WIMP model (in situ photons and up-scattered photons of the CMB). Model-independent, can be used for Sommerfeld-enhanced models.
  - Dark matter spatial distribution using Millennium-II simulation, uncertainty of ~2 orders of magnitude in extrapolation to unresolved structures.
- Isotropic component constrained by observations of the cosmic background, and contributions from blazars and star forming galaxies: although is not as clean as the CMB, it is more powerful to constrain the intrinsic properties of dark matter.

Summary and Conclusions

- Sommerfeld-enhanced models can explain the cosmic-ray anomalies, but they need to be consistent with independent astrophysical constraints.
- The local boost factors are less than ~100 for a scalar boson as the force carrier and a Yukawa interaction (relic density constraint).
- We have obtained predictions from the simulated all-sky maps of the cosmic X- and gamma-ray background from DM annihilation including:
  - Photon yield given by a WIMP model (in situ photons and up-scattered photons of the CMB). Model-independent, can be used for Sommerfeld-enhanced models.
  - Dark matter spatial distribution using Millennium-II simulation, uncertainty of ~2 orders of magnitude in extrapolation to unresolved structures.
- Isotropic component constrained by observations of the cosmic background, and contributions from blazars and star forming galaxies: although is not as clean as the CMB, it is more powerful to constrain the intrinsic properties of dark matter.

Summary and Conclusions

- Sommerfeld-enhanced models can explain the cosmic-ray anomalies, but they need to be consistent with independent astrophysical constraints.
- The local boost factors are less than ~100 for a scalar boson as the force carrier and a Yukawa interaction (relic density constraint).
- We have obtained predictions from the simulated all-sky maps of the cosmic X- and gamma-ray background from DM annihilation including:
  - Photon yield given by a WIMP model (in situ photons and up-scattered photons of the CMB). Model-independent, can be used for Sommerfeld-enhanced models.
  - Dark matter spatial distribution using Millennium-II simulation, uncertainty of ~2 orders of magnitude in extrapolation to unresolved structures.
- Isotropic component constrained by observations of the cosmic background, and contributions from blazars and star forming galaxies: although is not as clean as the CMB, it is more powerful to constrain the intrinsic properties of dark matter.

Summary and Conclusions

- Sommerfeld-enhanced models can explain the cosmic-ray anomalies, but they need to be consistent with independent astrophysical constraints.
- The local boost factors are less than ~100 for a scalar boson as the force carrier and a Yukawa interaction (relic density constraint).
- We have obtained predictions from the simulated all-sky maps of the cosmic X- and gamma-ray background from DM annihilation including:
  - Photon yield given by a WIMP model (in situ photons and up-scattered photons of the CMB). Model-independent, can be used for Sommerfeld-enhanced models.
  - Dark matter spatial distribution using Millennium-II simulation, uncertainty of ~2 orders of magnitude in extrapolation to unresolved structures.
- Isotropic component constrained by observations of the cosmic background, and contributions from blazars and star forming galaxies: although is not as clean as the CMB, it is more powerful to constrain the intrinsic properties of dark matter.

Summary and Conclusions

- Sommerfeld-enhanced models can explain the cosmic-ray anomalies, but they need to be consistent with independent astrophysical constraints.
- The local boost factors are less than ~100 for a scalar boson as the force carrier and a Yukawa interaction (relic density constraint).
- We have obtained predictions from the simulated all-sky maps of the cosmic X- and gamma-ray background from DM annihilation including:
  - Photon yield given by a WIMP model (in situ photons and up-scattered photons of the CMB). Model-independent, can be used for Sommerfeld-enhanced models.
  - Dark matter spatial distribution using Millennium-II simulation, uncertainty of ~2 orders of magnitude in extrapolation to unresolved structures.
- Isotropic component constrained by observations of the cosmic background, and contributions from blazars and star forming galaxies: although is not as clean as the CMB, it is more powerful to constrain the intrinsic properties of dark matter.

Summary and Conclusions

- Sommerfeld-enhanced models can explain the cosmic-ray anomalies, but they need to be consistent with independent astrophysical constraints.
- The local boost factors are less than ~100 for a scalar boson as the force carrier and a Yukawa interaction (relic density constraint).
- We have obtained predictions from the simulated all-sky maps of the cosmic X- and gamma-ray background from DM annihilation including:
  - Photon yield given by a WIMP model (in situ photons and up-scattered photons of the CMB). Model-independent, can be used for Sommerfeld-enhanced models.
  - Dark matter spatial distribution using Millennium-II simulation, uncertainty of ~2 orders of magnitude in extrapolation to unresolved structures.
- Isotropic component constrained by observations of the cosmic background, and contributions from blazars and star forming galaxies: although is not as clean as the CMB, it is more powerful to constrain the intrinsic properties of dark matter.

Summary and Conclusions

- Sommerfeld-enhanced models can explain the cosmic-ray anomalies, but they need to be consistent with independent astrophysical constraints.
- The local boost factors are less than ~100 for a scalar boson as the force carrier and a Yukawa interaction (relic density constraint).
- We have obtained predictions from the simulated all-sky maps of the cosmic X- and gamma-ray background from DM annihilation including:
  - Photon yield given by a WIMP model (in situ photons and up-scattered photons of the CMB). Model-independent, can be used for Sommerfeld-enhanced models.
  - Dark matter spatial distribution using Millennium-II simulation, uncertainty of ~2 orders of magnitude in extrapolation to unresolved structures.
- Isotropic component constrained by observations of the cosmic background, and contributions from blazars and star forming galaxies: although is not as clean as the CMB, it is more powerful to constrain the intrinsic properties of dark matter.

Summary and Conclusions

- Sommerfeld-enhanced models can explain the cosmic-ray anomalies, but they need to be consistent with independent astrophysical constraints.
- The local boost factors are less than ~100 for a scalar boson as the force carrier and a Yukawa interaction (relic density constraint).
- We have obtained predictions from the simulated all-sky maps of the cosmic X- and gamma-ray background from DM annihilation including:
  - Photon yield given by a WIMP model (in situ photons and up-scattered photons of the CMB). Model-independent, can be used for Sommerfeld-enhanced models.
  - Dark matter spatial distribution using Millennium-II simulation, uncertainty of ~2 orders of magnitude in extrapolation to unresolved structures.
- Isotropic component constrained by observations of the cosmic background, and contributions from blazars and star forming galaxies: although is not as clean as the CMB, it is more powerful to constrain the intrinsic properties of dark matter.

Summary and Conclusions

- Sommerfeld-enhanced models can explain the cosmic-ray anomalies, but they need to be consistent with independent astrophysical constraints.
- The local boost factors are less than ~100 for a scalar boson as the force carrier and a Yukawa interaction (relic density constraint).
- We have obtained predictions from the simulated all-sky maps of the cosmic X- and gamma-ray background from DM annihilation including:
  - Photon yield given by a WIMP model (in situ photons and up-scattered photons of the CMB). Model-independent, can be used for Sommerfeld-enhanced models.
  - Dark matter spatial distribution using Millennium-II simulation, uncertainty of ~2 orders of magnitude in extrapolation to unresolved structures.
- Isotropic component constrained by observations of the cosmic background, and contributions from blazars and star forming galaxies: although is not as clean as the CMB, it is more powerful to constrain the intrinsic properties of dark matter.

Summary and Conclusions

- Sommerfeld-enhanced models can explain the cosmic-ray anomalies, but they need to be consistent with independent astrophysical constraints.
- The local boost factors are less than ~100 for a scalar boson as the force carrier and a Yukawa interaction (relic density constraint).
- We have obtained predictions from the simulated all-sky maps of the cosmic X- and gamma-ray background from DM annihilation including:
  - Photon yield given by a WIMP model (in situ photons and up-scattered photons of the CMB). Model-independent, can be used for Sommerfeld-enhanced models.
  - Dark matter spatial distribution using Millennium-II simulation, uncertainty of ~2 orders of magnitude in extrapolation to unresolved structures.
- Isotropic component constrained by observations of the cosmic background, and contributions from blazars and star forming galaxies: although is not as clean as the CMB, it is more powerful to constrain the intrinsic properties of dark matter.

Summary and Conclusions

- Sommerfeld-enhanced models can explain the cosmic-ray anomalies, but they need to be consistent with independent astrophysical constraints.
- The local boost factors are less than ~100 for a scalar boson as the force carrier and a Yukawa interaction (relic density constraint).
- We have obtained predictions from the simulated all-sky maps of the cosmic X- and gamma-ray background from DM annihilation including:
  - Photon yield given by a WIMP model (in situ photons and up-scattered photons of the CMB). Model-independent, can be used for Sommerfeld-enhanced models.
  - Dark matter spatial distribution using Millennium-II simulation, uncertainty of ~2 orders of magnitude in extrapolation to unresolved structures.
- Isotropic component constrained by observations of the cosmic background, and contributions from blazars and star forming galaxies: although is not as clean as the CMB, it is more powerful to constrain the intrinsic properties of dark matter.

Summary and Conclusions

- Sommerfeld-enhanced models can explain the cosmic-ray anomalies, but they need to be consistent with independent astrophysical constraints.
- The local boost factors are less than ~100 for a scalar boson as the force carrier and a Yukawa interaction (relic density constraint).
- We have obtained predictions from the simulated all-sky maps of the cosmic X- and gamma-ray background from DM annihilation including:
  - Photon yield given by a WIMP model (in situ photons and up-scattered photons of the CMB). Model-independent, can be used for Sommerfeld-enhanced models.
  - Dark matter spatial distribution using Millennium-II simulation, uncertainty of ~2 orders of magnitude in extrapolation to unresolved structures.
- Isotropic component constrained by observations of the cosmic background, and contributions from blazars and star forming galaxies: although is not as clean as the CMB, it is more powerful to constrain the intrinsic properties of dark matter.

Summary and Conclusions

- Sommerfeld-enhanced models can explain the cosmic-ray anomalies, but they need to be consistent with independent astrophysical constraints.
- The local boost factors are less than ~100 for a scalar boson as the force carrier and a Yukawa interaction (relic density constraint).
- We have obtained predictions from the simulated all-sky maps of the cosmic X- and gamma-ray background from DM annihilation including:
  - Photon yield given by a WIMP model (in situ photons and up-scattered photons of the CMB). Model-independent, can be used for Sommerfeld-enhanced models.
  - Dark matter spatial distribution using Millennium-II simulation, uncertainty of ~2 orders of magnitude in extrapolation to unresolved structures.
- Isotropic component constrained by observations of the cosmic background, and contributions from blazars and star forming galaxies: although is not as clean as the CMB, it is more powerful to constrain the intrinsic properties of dark matter.

Summary and Conclusions

- Sommerfeld-enhanced models can explain the cosmic-ray anomalies, but they need to be consistent with independent astrophysical constraints.
- The local boost factors are less than ~100 for a scalar boson as the force carrier and a Yukawa interaction (relic density constraint).
- We have obtained predictions from the simulated all-sky maps of the cosmic X- and gamma-ray background from DM annihilation including:
  - Photon yield given by a WIMP model (in situ photons and up-scattered photons of the CMB). Model-independent, can be used for Sommerfeld-enhanced models.
  - Dark matter spatial distribution using Millennium-II simulation, uncertainty of ~2 orders of magnitude in extrapolation to unresolved structures.
- Isotropic component constrained by observations of the cosmic background, and contributions from blazars and star forming galaxies: although is not as clean as the CMB, it is more powerful to constrain the intrinsic properties of dark matter.

Summary and Conclusions

- Sommerfeld-enhanced models can explain the cosmic-ray anomalies, but they need to be consistent with independent astrophysical constraints.
- The local boost factors are less than ~100 for a scalar boson as the force carrier and a Yukawa interaction (relic density constraint).
- We have obtained predictions from the simulated all-sky maps of the cosmic X- and gamma-ray background from DM annihilation including:
  - Photon yield given by a WIMP model (in situ photons and up-scattered photons of the CMB). Model-independent, can be used for Sommerfeld-enhanced models.
  - Dark matter spatial distribution using Millennium-II simulation, uncertainty of ~2 orders of magnitude in extrapolation to unresolved structures.
- Isotropic component constrained by observations of the cosmic background, and contributions from blazars and star forming galaxies: although is not as clean as the CMB, it is more powerful to constrain the intrinsic properties of dark matter.

Summary and Conclusions

- Sommerfeld-enhanced models can explain the cosmic-ray anomalies, but they need to be consistent with independent astrophysical constraints.
- The local boost factors are less than ~100 for a scalar boson as the force carrier and a Yukawa interaction (relic density constraint).
- We have obtained predictions from the simulated all-sky maps of the cosmic X- and gamma-ray background from DM annihilation including:
  - Photon yield given by a WIMP model (in situ photons and up-scattered photons of the CMB). Model-independent, can be used for Sommerfeld-enhanced models.
  - Dark matter spatial distribution using Millennium-II simulation, uncertainty of ~2 orders of magnitude in extrapolation to unresolved structures.
- Isotropic component constrained by observations of the cosmic background, and contributions from blazars and star forming galaxies: although is not as clean as the CMB, it is more powerful to constrain the intrinsic properties of dark matter.

Summary and Conclusions

- Sommerfeld-enhanced models can explain the cosmic-ray anomalies, but they need to be consistent with independent astrophysical constraints.
- The local boost factors are less than ~100 for a scalar boson as the force carrier and a Yukawa interaction (relic density constraint).
- We have obtained predictions from the simulated all-sky maps of the cosmic X- and gamma-ray background from DM annihilation including:
  - Photon yield given by a WIMP model (in situ photons and up-scattered photons of the CMB). Model-independent, can be used for Sommerfeld-enhanced models.
  - Dark matter spatial distribution using Millennium-II simulation, uncertainty of ~2 orders of magnitude in extrapolation to unresolved structures.
- Isotropic component constrained by observations of the cosmic background, and contributions from blazars and star forming galaxies: although is not as clean as the CMB, it is more powerful to constrain the intrinsic properties of dark matter.

Summary and Conclusions

- Sommerfeld-enhanced models can explain the cosmic-ray anomalies, but they need to be consistent with independent astrophysical constraints.
- The local boost factors are less than ~100 for a scalar boson as the force carrier and a Yukawa interaction (relic density constraint).
- We have obtained predictions from the simulated all-sky maps of the cosmic X- and gamma-ray background from DM annihilation including:
  - Photon yield given by a WIMP model (in situ photons and up-scattered photons of the CMB). Model-independent, can be used for Sommerfeld-enhanced models.
  - Dark matter spatial distribution using Millennium-II simulation, uncertainty of ~2 orders of magnitude in extrapolation to unresolved structures.
- Isotropic component constrained by observations of the cosmic background, and contributions from blazars and star forming galaxies: although is not as clean as the CMB, it is more powerful to constrain the intrinsic properties of dark matter.

Summary and Conclusions

- Sommerfeld-enhanced models can explain the cosmic-ray anomalies, but they need to be consistent with independent astrophysical constraints.
- The local boost factors are less than ~100 for a scalar boson as the force carrier and a Yukawa interaction (relic density constraint).
- We have obtained predictions from the simulated all-sky maps of the cosmic X- and gamma-ray background from DM annihilation including:
  - Photon yield given by a WIMP model (in situ photons and up-scattered photons of the CMB). Model-independent, can be used for Sommerfeld-enhanced models.
  - Dark matter spatial distribution using Millennium-II simulation, uncertainty of ~2 orders of magnitude in extrapolation to unresolved structures.
- Isotropic component constrained by observations of the cosmic background, and contributions from blazars and star forming galaxies: although is not as clean as the CMB, it is more powerful to constrain the intrinsic properties of dark matter.

Summary and Conclusions

- Sommerfeld-enhanced models can explain the cosmic-ray anomalies, but they need to be consistent with independent astrophysical constraints.
- The local boost factors are less than ~100 for a scalar boson as the force carrier and a Yukawa interaction (relic density constraint).
- We have obtained predictions from the simulated all-sky maps of the cosmic X- and gamma-ray background from DM annihilation including:
  - Photon yield given by a WIMP model (in situ photons and up-scattered photons of the CMB). Model-independent, can be used for Sommerfeld-enhanced models.
  - Dark matter spatial distribution using Millennium-II simulation, uncertainty of ~2 orders of magnitude in extrapolation to unresolved structures.
- Isotropic component constrained by observations of the cosmic background, and contributions from blazars and star forming galaxies: although is not as clean as the CMB, it is more powerful to constrain the intrinsic properties of dark matter.

Summary and Conclusions

- Sommerfeld-enhanced models can explain the cosmic-ray anomalies, but they need to be consistent with independent astrophysical constraints.
- The local boost factors are less than ~100 for a scalar boson as the force carrier and a Yukawa interaction (relic density constraint).
- We have obtained predictions from the simulated all-sky maps of the cosmic X- and gamma-ray background from DM annihilation including:
  - Photon yield given by a WIMP model (in situ photons and up-scattered photons of the CMB). Model-independent, can be used for Sommerfeld-enhanced models.
  - Dark matter spatial distribution using Millennium-II simulation, uncertainty of ~2 orders of magnitude in extrapolation to unresolved structures.
- Isotropic component constrained by observations of the cosmic background, and contributions from blazars and star forming galaxies: although is not as clean as the CMB, it is more powerful to constrain the intrinsic properties of dark matter.

Summary and Conclusions

- Sommerfeld-enhanced models can explain the cosmic-ray anomalies, but they need to be consistent with independent astrophysical constraints.
- The local boost factors are less than ~100 for a scalar boson as the force carrier and a Yukawa interaction (relic density constraint).
- We have obtained predictions from the simulated all-sky maps of the cosmic X- and gamma-ray background from DM annihilation including:
  - Photon yield given by a WIMP model (in situ photons and up-scattered photons of the CMB). Model-independent, can be used for Sommerfeld-enhanced models.
  - Dark matter spatial distribution using Millennium-II simulation, uncertainty of ~2 orders of magnitude in extrapolation to unresolved structures.
- Isotropic component constrained by observations of the cosmic background, and contributions from blazars and star forming galaxies: although is not as clean as the CMB, it is more powerful to constrain the intrinsic properties of dark matter.

Summary and Conclusions

- Sommerfeld-enhanced models can explain the cosmic-ray anomalies, but they need to be consistent with independent astrophysical constraints.
- The local boost factors are less than ~100 for a scalar boson as the force carrier and a Yukawa interaction (relic density constraint).
- We have obtained predictions from the simulated all-sky maps of the cosmic X- and gamma-ray background from DM annihilation including:
  - Photon yield given by a WIMP model (in situ photons and up-scattered photons of the CMB). Model-independent, can be used for Sommerfeld-enhanced models.
  - Dark matter spatial distribution using Millennium-II simulation, uncertainty of ~2 orders of magnitude in extrapolation to unresolved structures.
- Isotropic component constrained by observations of the cosmic background, and contributions from blazars and star forming galaxies: although is not as clean as the CMB, it is more powerful to constrain the intrinsic properties of dark matter.

Summary and Conclusions

- Sommerfeld-enhanced models can explain the cosmic-ray anomalies, but they need to be consistent with independent astrophysical constraints.
- The local boost factors are less than ~100 for a scalar boson as the force carrier and a Yukawa interaction (relic density constraint).
- We have obtained predictions from the simulated all-sky maps of the cosmic X- and gamma-ray background from DM annihilation including:
    - Photon yield given by a WIMP model (in situ photons and up-scattered photons of the CMB). Model-independent, can be used for Sommerfeld-enhanced models.
    - Dark matter spatial distribution using Millennium-II simulation, uncertainty of ~2 orders of magnitude in extrapolation to unresolved structures.
- Isotropic component constrained by observations of the cosmic background, and contributions from blazars and star forming galaxies: although is not as clean as the CMB, it is more powerful to constrain the intrinsic properties of dark matter.

Summary and Conclusions

- Sommerfeld-enhanced models can explain the cosmic-ray anomalies, but they need to be consistent with independent astrophysical constraints.
- The local boost factors are less than ~100 for a scalar boson as the force carrier and a Yukawa interaction (relic density constraint).
- We have obtained predictions from the simulated all-sky maps of the cosmic X- and gamma-ray background from DM annihilation including:
  - Photon yield given by a WIMP model (in situ photons and up-scattered photons of the CMB). Model-independent, can be used for Sommerfeld-enhanced models.
  - Dark matter spatial distribution using Millennium-II simulation, uncertainty of ~2 orders of magnitude in extrapolation to unresolved structures.
- Isotropic component constrained by observations of the cosmic background, and contributions from blazars and star forming galaxies: although is not as clean as the CMB, it is more powerful to constrain the intrinsic properties of dark matter.

Summary and Conclusions

- Sommerfeld-enhanced models can explain the cosmic-ray anomalies, but they need to be consistent with independent astrophysical constraints.
- The local boost factors are less than ~100 for a scalar boson as the force carrier and a Yukawa interaction (relic density constraint).
- We have obtained predictions from the simulated all-sky maps of the cosmic X- and gamma-ray background from DM annihilation including:
  - Photon yield given by a WIMP model (in situ photons and up-scattered photons of the CMB). Model-independent, can be used for Sommerfeld-enhanced models.
  - Dark matter spatial distribution using Millennium-II simulation, uncertainty of ~2 orders of magnitude in extrapolation to unresolved structures.
- Isotropic component constrained by observations of the cosmic background, and contributions from blazars and star forming galaxies: although is not as clean as the CMB, it is more powerful to constrain the intrinsic properties of dark matter.

Summary and Conclusions

- Sommerfeld-enhanced models can explain the cosmic-ray anomalies, but they need to be consistent with independent astrophysical constraints.
- The local boost factors are less than ~100 for a scalar boson as the force carrier and a Yukawa interaction (relic density constraint).
- We have obtained predictions from the simulated all-sky maps of the cosmic X- and gamma-ray background from DM annihilation including:
  - Photon yield given by a WIMP model (in situ photons and up-scattered photons of the CMB). Model-independent, can be used for Sommerfeld-enhanced models.
  - Dark matter spatial distribution using Millennium-II simulation, uncertainty of ~2 orders of magnitude in extrapolation to unresolved structures.
- Isotropic component constrained by observations of the cosmic background, and contributions from blazars and star forming galaxies: although is not as clean as the CMB, it is more powerful to constrain the intrinsic properties of dark matter.

Summary and Conclusions

- Sommerfeld-enhanced models can explain the cosmic-ray anomalies, but they need to be consistent with independent astrophysical constraints.
- The local boost factors are less than ~100 for a scalar boson as the force carrier and a Yukawa interaction (relic density constraint).
- We have obtained predictions from the simulated all-sky maps of the cosmic X- and gamma-ray background from DM annihilation including:
  - Photon yield given by a WIMP model (in situ photons and up-scattered photons of the CMB). Model-independent, can be used for Sommerfeld-enhanced models.
  - Dark matter spatial distribution using Millennium-II simulation, uncertainty of ~2 orders of magnitude in extrapolation to unresolved structures.
- Isotropic component constrained by observations of the cosmic background, and contributions from blazars and star forming galaxies: although is not as clean as the CMB, it is more powerful to constrain the intrinsic properties of dark matter.

Summary and Conclusions

- Sommerfeld-enhanced models can explain the cosmic-ray anomalies, but they need to be consistent with independent astrophysical constraints.
- The local boost factors are less than ~100 for a scalar boson as the force carrier and a Yukawa interaction (relic density constraint).
- We have obtained predictions from the simulated all-sky maps of the cosmic X- and gamma-ray background from DM annihilation including:
  - Photon yield given by a WIMP model (in situ photons and up-scattered photons of the CMB). Model-independent, can be used for Sommerfeld-enhanced models.
  - Dark matter spatial distribution using Millennium-II simulation, uncertainty of ~2 orders of magnitude in extrapolation to unresolved structures.
- Isotropic component constrained by observations of the cosmic background, and contributions from blazars and star forming galaxies: although is not as clean as the CMB, it is more powerful to constrain the intrinsic properties of dark matter.

Sommerfeld-enhanced models fitting the cosmic ray excesses

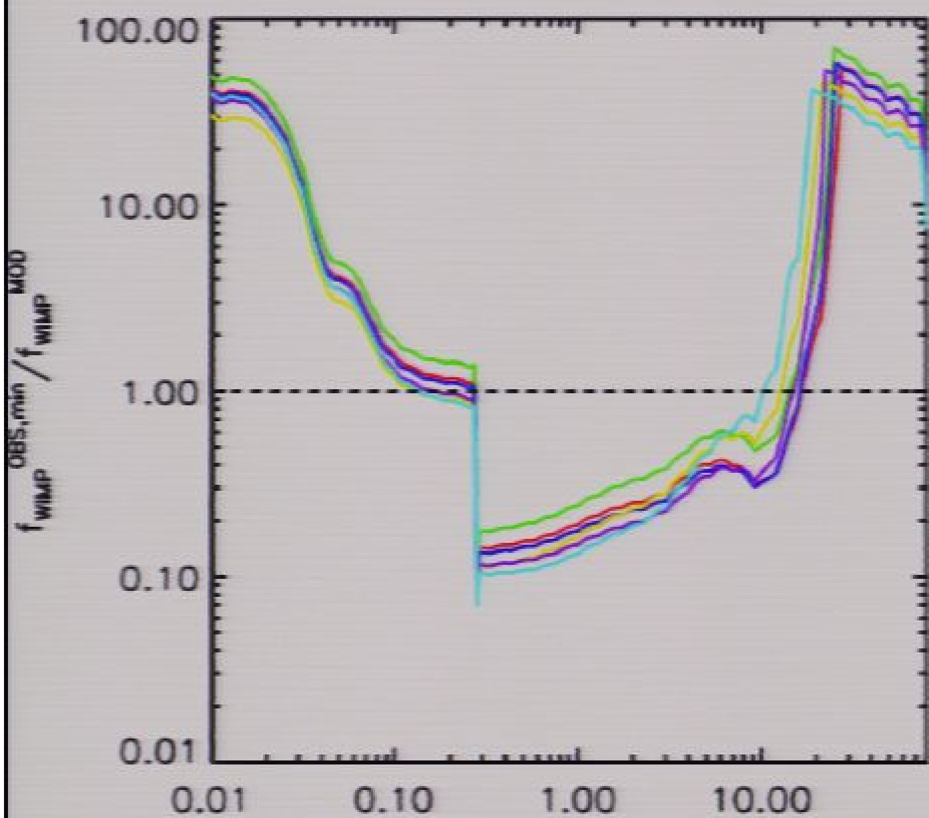

- Minimum contribution from subhalos
- SFG = 53%of EGB(E>1GeV)
- Blazars = 16% of EGB (E>1GeV)

Benchmark no.	Annihilation Channel	m_ϕ (MeV)	m_χ (TeV)	α_c	δ (MeV)	$\frac{S_{max}\langle\sigma v\rangle_0}{3\times10^{-26}\,cm^3\,s^{-1}}$
1	1:1:2 $e^\pm : \mu^\pm : \pi^\pm$	900	1.68	0.04067	0.15	530
2	1:1:2 $e^\pm : \mu^\pm : \pi^\pm$	900	1.52	0.03725	1.34	360
3	1:1:1 $e^\pm : \mu^\pm : \pi^\pm$	580	1.55	0.03523	1.49	437
4	1:1:1 $e^\pm : \mu^\pm : \pi^\pm$	580	1.20	0.03054	1.00	374
5	1:1 $e^\pm : \mu^\pm$	350	1.33	0.02643	1.10	339
6	$e^\pm$ only	200	1.00	0.01622	0.70	171

$$m_\chi \sim 200\,GeV, \chi\chi \to b\bar{b} \text{ and } \langle\sigma v\rangle \sim 6.2\times10^{-27}\,cm^3 s^{-1}$$